NORTHWESTERN UNIVERSITY

Neurobiological Basis of *in vivo* Cortical Atrophy in

Primary Progressive Aphasia Caused by Alzheimer's Disease

A DISSERTATION

SUBMITTED TO THE GRADUATE SCHOOL

IN PARTIAL FULFILLMENT OF THE REQUIREMENTS

for the degree

DOCTOR OF PHILOSOPHY

Field of Neuroscience

By

Daniel Timothy Ohm

EVANSTON, ILLINOIS

March 2019

—ABSTRACT—

Neurobiological Basis of *in vivo* Cortical Atrophy in

Primary Progressive Aphasia Caused by Alzheimer's Disease

Daniel Timothy Ohm

The brain is known to shrink in normal aging or neurodegenerative disease and yet the neurobiological underpinnings of the cortical atrophy remain elusive. The structural changes that represent cortical atrophy can be measured during life using the reliable and quantitative method known as magnetic resonance imaging (MRI). Primary progressive aphasia (PPA) is a language-based clinical syndrome characterized by focal left-lateralized cortical atrophy caused by multiple proteinopathies including Alzheimer's disease (AD) and transactive DNA-binding protein of 43 kD (TDP) neuropathology. However, like other disorders characterized by cortical atrophy, the neuropathologic inclusions and cellular determinants of the cortical atrophy observed in PPA are not well understood. Previous work from our lab and others showed that neurofibrillary tau tangles (NFTs) and activated microglia (a neuroinflammatory marker) display regional densities that are closely associated with neurodegenerative processes and are consistent with the aphasic profile of individuals with PPA. In PPA participants with AD neuropathology (PPA-AD) that had MRI scans acquired close to death, we hypothesized that NFTs and activated microglia would be the primary neuropathologic contributors to neurodegeneration detected by MRI-based cortical atrophy or smaller densities of neurons.

In a series of three related studies, the goal of the current dissertation was to examine the relationships between neuropathologic and cellular alterations in the postmortem brain, as well as

their individual relationships with *in vivo* cortical atrophy in PPA. In Study 1, the neuropathologic basis of *in vivo* cortical atrophy was investigated in PPA-AD by determining if the magnitudes of regional atrophy were associated with the histopathologic hallmarks of AD neuropathology (NFTs and amyloid-beta plaques [APs]). Consistent with previous findings in PPA-AD and other AD clinical subtypes, only NFTs were found to be selectively associated with the greatest cortical atrophy measured in the left language regions in PPA-AD. In Study 2, activated microglia were exclusively quantified in the white matter in order to characterize the unique distribution of the neuroinflammatory marker and determine its association with cortical atrophy in two PPA pathologic subtypes (PPA-AD and PPA-TDP). The results indicated that while greater densities of activated microglia were related to regions of greater gray matter atrophy in PPA, this relationship was not consistently observed within individual PPA pathologic subtypes. Finally, in Study 3, the cellular determinants of *in vivo* cortical atrophy were examined in PPA-AD. This investigation involved the quantification of microglial subtypes (hypertrophic and ramified) potentially serving different roles in inflammation and disease progression and comparing each subtype to densities of neurons, AD neuropathology, and regional atrophy. Greater cortical atrophy was found to be associated with smaller densities of ramified microglia. Further analysis was carried out on a subset of regions in the PPA-AD cohort to determine how pathologic changes in white matter were related to cellular and neuropathologic changes in the gray matter. The results indicated that not only were NFTs and activated microglia (in gray and white matter) related to each other, each of these pathologic markers displayed a negative relationship with neurons as well.

These multidisciplinary studies provided new insight into the histopathologic basis of *in vivo* cortical atrophy in PPA-AD by showing that NFTs displayed significant relationships with microglial activation, neurodegeneration, and cortical atrophy in PPA-AD. Therefore, similar to

findings in amnestic AD, NFTs and neuroinflammation likely serve significant roles in the neuropathologic change and neurodegenerative processes that lead to the impaired cognition characteristic of the PPA clinical profile.

—ACKNOWLEDGEMENTS—

Thank you to my thesis committee and co-mentors, Drs. Emily Rogalski and Changiz Geula, for your professional and scientific advice throughout the graduate training. I am so appreciative that you took me on as a student and agreed to a co-mentorship to give me a uniquely well-rounded training experience for my PhD. With the collaborative help from you two and the rest of the Mesulam Center, my desire to adopt a multidisciplinary approach to my thesis work was fulfilled. In the process, I will never take for granted that I was given the opportunity to pursue some of my favorite research topics: language (dys)function and neurodegenerative disease.

The multidisciplinary work completed for this dissertation was inherently a team effort with contributions made from neurologists, neuropsychologists, neuroscientists, statisticians, and motivated volunteers and employees at the Mesulam Center. Each provided expertise, technical assistance, or thoughtful conversations that helped shape my research projects and the interpretation of findings. Interacting with such a diverse group of intelligent and dedicated scientists was an invaluable learning experience on collaboration and scientific communication.

I want to express my sincere gratitude to my family and friends, near and far, for their endless love and support. The welcomed distractions, words of encouragement, and commiseration were all instrumental in keeping me motivated to complete the long journey of the

PhD. My parents deserve special mention for prioritizing the successes of their children; in words and actions, I feel that you two taught me the importance of a sound mind in a sound body, encouraged my inquisitive nature and skepticisms, and provided continuous support to help me persevere despite the challenges that arose.

Finally, it is especially important to acknowledge the generous donations provided by the participants and their families, for without them, none of this work would have been possible.

─**TABLE OF CONTENTS**─

—LIST OF TABLES & FIGURES—

—GENERAL INTRODUCTION—

The brain is known to shrink to various degrees in normal aging and neurodegenerative disease. These structural changes in cortex are concerning not only because a healthy organ is not expected to atrophy, but also because the locations and rates of atrophy tend to be linked to specific impairments and progression of cognitive decline. Therefore, what contributes to cortical atrophy and what causes the progressive disease-related shrinkage represent critical topics of investigation in neuroscience and in neurological disorders without treatments or cures.

This dissertation explored the neurobiological basis of anatomical changes in a single clinical dementia syndrome known as primary progressive aphasia (PPA). The reasons for investigating PPA are many but include the fact that PPA represents a unique model to study the neurobiology of language and neurodegeneration. In PPA, language deficits are accompanied by asymmetric and regionally specific patterns of cortical atrophy and neuropathology. Therefore, there are important opportunities to compare the distribution of atrophy and pathology within an individual PPA brain, obviating the need for healthy control brains. Neurodegenerative diseases such as Alzheimer's disease (AD) can cause PPA. Given that AD neuropathology can cause a range of distinct clinical syndromes that includes an aphasic presentation (PPA), the study of PPA caused by AD can expand our understanding of how a common neuropathology is responsible for a clinical spectrum of disorders. The following introduction provides necessary background on cortical atrophy, AD, and PPA, along with the rationale for the multidisciplinary approach carried out in a series of studies designed to uncover the histopathologic and cellular basis of *in vivo* cortical atrophy in PPA.

I. Cortical Atrophy

The cerebral cortex is comprised of billions of cells that situate themselves during early

development into orderly structural patterns referred to as cytoarchitecture. This complex but evident order has prompted dozens of neuroanatomists for over a century to make numerous attempts to subdivide the cortex using methods that include, but are not limited to, gyrification patterns, cellular morphology, neurochemicals and receptors, myelin, connectivity, ontogenetics, and function. With the notion that structure follows function, these efforts continue to try, with mixed success, to reconcile the architectonic and functional boundaries of the cortex **(Amunts and Zilles, 2015)**.

Regardless of the numerous ways to parcellate the brain, there is a cytoarchitectonic consensus that neocortical cells organize into distinct layers and cylinders/columns. In relation to the pial surface, cell layers run parallel while cell columns are perpendicular and thus intersect the layers. Seminal anatomical and electrophysiological studies suggest that these structural modules of cortex are more than just epiphenomena of cortical development, they are specialized functional units as well **(Mountcastle, 1957)**. Columns, for example, have modality-specific inputs as their defining feature that is processed by the internal chain of neurons before systematically projecting outputs to extrinsic targets **(Mountcastle, 1997)**. Similar to columns, cortical layers are known to receive common afferents and project common efferents; however, layers do not appear to exhibit common functional properties in response to parallel electrode penetrations beyond a distance of a few hundred microns **(Mountcastle, 1997)**.

The structural and functional properties of these two fundamental cytoarchitectonic features of the cerebral cortex can be beneficial to conceptualizing what cortical atrophy represents and how patterns of neurodegeneration develop and progress. Consider, for example, that regardless of the method by which cortical atrophy is assessed, there are only three basic measurements: thickness, surface area, or volume. One measurement is not necessarily considered superior over the other until one considers the microstructure of brain anatomy. For instance,

thickness measurements are likely to be more sensitive to selective cell layer loss, while surface area is probably better at detecting changes in columnar organization. As a product of both thickness and surface area, volume will be influenced by any and all cytoarchitectonic changes in dynamic ways.

It is also important to note that the intricate synaptic connections of adjacent neurons in different spatial directions is particularly relevant to theories of disease propagation. More specifically, layer versus column atrophy could lend insight into the increasing evidence for pathologic protein transmission via synaptically connected neurons that begins locally (e.g., within layers) before spreading to neighboring and more distant regions **(Brettschneider *et al.*, 2015)**. The extent to which whole neurons or parts of neurons are shrinking or lost within the cortical layers or columns remain active areas of research that aim to elucidate the cellular basis of cortical atrophy. The atrophy within cortical layers and columns known to occur in a disease context is elaborated in *part IX* below.

This dissertation focused assessments of cortical atrophy to only cortical thickness at the whole hemisphere or regional level. One reason for using cortical thickness measurements was that they can be put in the context of prior investigations that often report cortical thickness or volume changes. However, cortical volumes were excluded from the following investigations considering that in contrast to thickness, volume is a product of both thickness and surface area whereby each parameter has been shown to vary independently and disproportionately to one another in ways that still need further elucidation **(Winkler *et al.*, 2010; Meyer *et al.*, 2013)**. Finally, since neurodegenerative disease such as AD often selectively targets some cortical layers over others **(Hirano and Zimmerman, 1962; Brun and Englund, 1981; Pearson *et al.*, 1985; Lewis *et al.*, 1987; Arnold *et al.*, 1991; Braak and Braak, 1991)**, it was decided that it would also be important to use cortical thickness measurements as they are theoretically more sensitive

at detecting changes in the cell lamina. Therefore, the relationships described in this dissertation using global and regional thickness analyses produced foundational insight into what neurobiological changes underlie cortical atrophy. Future experiments can expand upon these initial findings related to cortical thickness by employing other measurements of atrophy.

Cortical atrophy can be measured in various ways including after death in postmortem tissue or alternatively during life using magnetic resonance imaging (MRI). The *in vivo* MRI is a particularly important approach because of its clinical utility in aiding diagnoses due to its ability of reliably and quantitatively detecting structural changes throughout disease progression **(Frisoni et al., 2010)**. Assessing the morphology of cortical gray matter is performed using T_1-weighted MRI scans together with automated computerized methods such as voxel-based morphometry or cortical surface analyses. While voxel-based morphometry was among the first approaches and still widely used, studies have shown that surface-based analyses may be more sensitive in detecting age- or disease-related gray matter changes compared to voxel-based analyses **(Hutton et al., 2009)**. All quantitative analyses of *in vivo* cortical atrophy reported in this dissertation were carried out using FreeSurfer (v5.1.0, *http://surfer.nmr.mgh.harvard.edu*), a well-validated software suite that constructs inner and outer cortical surface boundaries to detect morphometric properties of neuroanatomy at submillimeter resolution **(Fischl and Dale, 2000)**.

II. Alzheimer's Disease (AD): Pathologic Diagnosis

The neurobiological basis of MRI-based cortical atrophy has been investigated in several types of neurodegenerative diseases and clinical phenotypes, but perhaps none as extensively as individuals diagnosed with "Alzheimer's disease (AD) neuropathologic change". To receive the neuropathologic diagnosis of AD, postmortem brain tissue sampled from specified regions must stain positive for two histopathologic features: amyloid-ß plaques (APs) and neurofibrillary tau tangles (NFTs) **(Hyman et al., 2012; Montine et al., 2012)**.

NFTs are comprised of tau **(Kosik *et al.*, 1986)**, a microtubule-associated protein abundant in the axon where it supports axonal transport by binding and stabilizing the microtubules **(Weingarten *et al.*, 1975)**. In AD, tau is translocated to the somatodendritic compartment and undergoes hyperphosphorylation and misfolding into paired helical filaments that lead to the formation of intraneuronal NFTs and neuropil threads **(Alonso *et al.*, 1994; del C Alonso *et al.*, 1996; Iqbal *et al.*, 2015)**. NFTs have long been known to be heterogeneous aggregates that vary according to their fibrillar composition and molecular staining profiles. The distinguishable morphologic features of NFTs have given rise to a putative chronological evolution of NFTs based on fibrillar structure that includes "pre-NFTs" (lacking fibrils that imply pre-maturity) and typical NFTs (bearing fibrils and therefore mature) **(Uchihara, 2014)**. The insoluble mature NFTs can become extraneuronal ghost NFTs when NFT-bearing neurons die, but the extent to which this occurs remains to be clarified. NFTs are a critical component of the pathologic diagnosis of AD given the evidence for NFTs propagating in a spatiotemporal fashion that correlates with neurodegeneration and clinical severity **(Braak and Braak, 1991; Arriagada *et al.*, 1992; Bierer *et al.*, 1995; Braak and Braak, 1995; Gomez-Isla *et al.*, 1997; Giannakopoulos *et al.*, 2003)**.

APs are comprised of amyloid-ß protein **(Glenner and Wong, 1984)**, a peptide of 40 or 42 amino acids that is derived from the amyloid precursor protein after its sequential cleavage by ß- and δ-secretases **(Kang *et al.*, 1987; Vassar *et al.*, 1999)**. In AD, the larger amyloid-ß peptide of 42 amino acids appears to be the more pathologic protein **(Younkin, 1998)**, known for its formation of intermediate soluble oligomers before becoming insoluble ß-pleated sheet fibrils that form a variety of extracellular deposits that are commonly classified into two groups: diffuse or dense-core APs **(Serrano-Pozo *et al.*, 2011a)**. Diffuse APs tend to be amorphous and non-neuritic (lacking tau-positivity), with little association with neurodegenerative processes and thus is not part of the pathologic diagnosis of AD **(Masliah *et al.*, 1990; Hyman *et al.*, 2012)**. Dense-core

APs, also known as neuritic APs, exhibit a central compact core surrounded by a halo of dystrophic neurites that are often tau-positive and an important consideration in the AD pathologic diagnosis given their co-localization with glial activation, synapse loss, and neuronal degeneration **(Itagaki et al., 1989; Masliah et al., 1994; Urbanc et al., 2002)**.

AD neuropathologic change involves other features such as neuronal loss and gliosis, but only the location and frequency of amyloid-ß deposits, neuritic dense-core APs, and NFTs contribute to the consensus criteria and formal pathologic diagnosis.

III. AD: Clinical Diagnosis and Clinical Variants

"AD neuropathologic change" is the most common cause of "dementia of the Alzheimer-type" (DAT), a clinical diagnosis made during life and independent of the pathologic diagnosis **(McKhann et al., 2011)**. DAT is a syndrome characterized by impairments typically in learning and recall of recently learned information; this amnestic presentation can occur in isolation or in combination with other less prominent deficits in non-amnestic domains that include language, executive, or visuospatial function **(McKhann et al., 2011)**. DAT is also known as "typical AD dementia" because it is now recognized that AD neuropathologic change can cause a spectrum of distinct clinical syndromes. The clinical AD phenotypes include the most common amnestic presentation (typical AD) and non-amnestic presentations (atypical AD) **(Galton et al., 2000; Kramer and Miller, 2000; Alladi et al., 2007; Warren et al., 2012)**. The three principal non-amnestic syndromes that constitute atypical AD are distinguishable by the earliest most impaired cognitive domain: visuospatial dysfunction in "posterior cortical atrophy" **(Hof et al., 1989; Crutch et al., 2017)**, language dysfunction in "primary progressive aphasia (PPA)" **(Mesulam, 1982; Mesulam et al., 2014b; Rogalski et al., 2016)**, and behavioral/executive/attentional dysfunction in the "behavioral/dysexecutive/frontal" variant of AD **(Johnson et al., 1999; Ossenkoppele et al., 2015b)**. Less common clinical syndromes have been considered to be part

of the atypical AD variants. One example is the asymmetric ideomortor/ideational apraxias and akinetic rigidities characteristic of "corticobasal syndrome" **(Armstrong *et al.*, 2013)**. Sill other AD variants may exist based on age of onset; while "early-onset AD" represents individuals with typical amnestic presentations that begin before age 65 and have a rapid progression that leads to death in a few years, "late-onset AD" describes individuals with slow rates of disease progression lasting a decade or more **(Frisoni *et al.*, 2007; Warren *et al.*, 2012)**.

The clinical AD variants leave much to be understood regarding how a common neuropathologic etiology can cause separate clinical syndromes. In pursuit of answering that question and others as they relate to selective vulnerability, PPA has emerged as a fruitful subject for research. The past two decades of research have produced significant advancements in the characterization of PPA and its subclassifications based on clinical and neuropathologic features reviewed in further detail in the following two sections.

IV. Primary Progressive Aphasia (PPA): Clinical Diagnosis and Clinical Subtypes

Language is an emergent function of a complex neural network of the human brain; therefore, it is not surprising that heterogenous clinical presentations manifest when the language network is partially and progressively damaged in PPA. In a concerted effort to facilitate consistency in the clinical diagnosis of PPA, experienced clinicians have identified consensus criteria for the classification of PPA and its clinical subtypes based on distinguishable early presentations **(Gorno-Tempini *et al.*, 2011)**. To be given the root diagnosis of PPA, not only does an individual need to present with a language disorder (*aphasia*) that emerges as the earliest and most prominent deficit (*primary*) relative to other neurological impairments in the first 1-2 years of onset, the language dysfunction must worsen over time (*progressive*) due to underlying neurodegenerative disease **(Mesulam, 1982; Mesulam, 2001; Mesulam, 2003)**. The PPA diagnosis cannot be made if the pattern of impairments is due to other medical problems such as a

psychiatric condition, cancer, stroke, or a traumatic event.

After the initial diagnosis, PPA patients can often be classified into a clinical subtype. Three principal subtypes are currently recognized: 'agrammatic/non-fluent', 'logopenic', and 'semantic' **(Gorno-Tempini *et al.*, 2011)**. Each PPA clinical subtype can be distinguished by varying intactness of language comprehension, grammaticality, and speech. In brief, agrammatic PPA (PPA-G) presents with abnormal syntax, fluency, and commonly apraxia of speech. Logopenic PPA (PPA-L) presents with word-finding pauses, circumlocutions, phonemic paraphasias, and often poor repetition. Unlike PPA-G and PPA-L, semantic PPA (PPA-S) is characterized by significant deficits in single word comprehension that is associated with anomia and impaired word-retrieval. Mixed PPA often shares features with PPA-G and PPA-L such that grammar and comprehension deficits are observed with similar severity at time of evaluation. However, these subtypes may need modifications given that when some patients can present with symptoms that do not cleanly fit a subtype's criteria, they are rendered unclassifiable, or in other patients their symptoms match criteria for multiple subtypes and are therefore designated 'mixed' **(Mesulam *et al.*, 2014a)**.

V. PPA: Associated Pathologic Diagnoses

PPA is caused by a number of different neurodegenerative diseases that can only be confirmed in the postmortem brain and most often include frontotemporal lobar degeneration (FTLD) or AD neuropathology. The AD pathologic diagnosis and characteristics of AD neuropathology were described earlier in ***part II***. Consensus criteria has been established for making the pathologic diagnosis of FTLD, which actually represents a grouping of diseases that can be divided into two main proteinopathies based on the nature of the proteinaceous inclusions: "tauopathies" (FTLD-tau) and "ubiquitinopathies" (FTLD-U) **(Cairns *et al.*, 2007)**. FTLD-tau has inclusions immunolabeled with antibodies to tau and the most common primary diagnoses

include the following: Pick disease, corticobasal degeneration, and progressive supranuclear palsy. FTLD-U has inclusions labeled with antibodies to ubiquitin or p62. The most common ubiquitin-positive neuropathology is the transactive DNA-binding protein of 43 kDa (TDP-43) **(Cairns *et al.*, 2007; Bigio, 2013)**. For the purposes of this dissertation, only the AD and FTLD-TDP pathologic diagnoses are described in detail because the PPA participants that were examined in each investigation happen to only have either AD or FTLD-TDP as their primary pathologic diagnosis.

TDP-43 is a DNA- and RNA-binding nuclear protein that can become a pathologic inclusion once it is hyperphosphorylated and usually ubiquitinated **(Mackenzie and Neumann, 2017)**, resulting in an insoluble aggregate mislocalized in the nucleus or cytoplasm **(Neumann *et al.*, 2006; Cohen *et al.*, 2011)**. It turns out that the resultant intracellular TDP-43 inclusions exhibit morphologic heterogeneity. At present, TDP inclusions are morphologically characterized as either dystrophic neurites, neuronal cytoplasmic inclusions, or neuronal intranuclear inclusions **(Mackenzie *et al.*, 2011)**. Furthermore, these distinct inclusions form patterns of accumulation within the gray and white matter that is of anatomical, and likely clinical, significance. As a result, FTLD-TDP has been subdivided into 4 pathologic subtypes (types A, B, C, D), where each pathologic subtype is distinguishable based on the cortical layer one or more TDP deposits predominate, the type of inclusion deposited, and the frequency relative to other TDP inclusions **(Mackenzie *et al.*, 2011)**. A 5th subtype (type E) has been recently proposed to categorize TDP aggregates that do not follow the original A, B, C, or D types **(Lee *et al.*, 2017)**. Many of the FTLD-TDP subtypes have associations with specific genetic mutations and clinical phenotypes such as PPA, but more clinicopathologic studies are needed to fully parse these relationships.

In the pursuit to find the neuropathologic basis of the clinical syndrome that is PPA, clinicopathologic studies have shown that the three main subtypes of PPA tend to each have a

pathologic diagnosis that they are most often associated with: PPA-G and FTLD-tau, PPA-L and AD, and PPA-S and FTLD-TDP. However, these associations are far from consistent. In fact, available evidence points to the conclusion that there is no one-to-one relationship between the clinical phenotype and the underlying molecular pathology **(Hodges *et al.*, 2004; Kertesz *et al.*, 2005; Forman *et al.*, 2006; Mesulam *et al.*, 2008; Deramecourt *et al.*, 2009; Grossman, 2010; Harris *et al.*, 2013; Mesulam *et al.*, 2014b)**. Put another way, a single molecular pathology can cause more than one type of clinical syndrome and that is because it seems to matter more *where* the neuropathology is deposited anatomically than which *type* of neuropathology has accumulated.

VI. PPA: A Model for Selective Vulnerability and the Determinants of Cortical Atrophy

PPA is particularly suitable for advancing our understanding of the underpinnings of selective vulnerability and the neurobiological substrates of structural and cognitive changes. Firstly, PPA is relatively rare and understudied compared to other clinical dementias **(Knopman and Roberts, 2011; Grossman, 2014)**. Secondly, PPA is characterized by focal and asymmetric degenerative patterns that can be leveraged to better understand disease mechanisms **(Gorno-Tempini and Miller, 2013; Mesulam *et al.*, 2014a)**. More specifically, the anatomy of cognitive and cortical changes in PPA provide a unique opportunity to tease apart the neuropathologic and cellular determinants of clinically compromised versus relatively spared regions within the same brains. This means that many relationships can be established independent of a control group and the resultant findings shed insight into the selective vulnerability of cortical regions responsible for the PPA clinical phenotype. Finally, as the aphasic variant when AD is the primary postmortem diagnosis, the study of PPA-AD can provide valuable information about the similarities and disparities between it and the rest of the clinical AD spectrum.

VII. Possible Neuropathologic Contributors to Cortical Atrophy

The neuropathologic contributors to cortical atrophy have been extensively examined in

DAT-AD. The cortical atrophy patterns characteristic of DAT-AD can often be differentiated from the atrophy patterns associated with other clinical disorders and AD variants such as PPA-AD **(Ossenkoppele *et al.*, 2015a)**. In DAT-AD, both hemispheres show significant cortical atrophy in almost every lobe of the brain, with the most prominent and earliest cortical atrophy typically in the medial temporal lobe and temporoparietal junction **(Frisoni *et al.*, 2007; Möller *et al.*, 2013)**. Cortical atrophy has also been shown to progressively spread in a spatiotemporal pattern that mirrors the NFT progression and Braak NFT stage in DAT-AD **(Thompson *et al.*, 2003; Vemuri *et al.*, 2008; Whitwell *et al.*, 2008; Whitwell *et al.*, 2012)**. While both NFTs and APs appear to contribute to neurodegenerative processes in DAT-AD, NFTs may be the stronger pathologic correlate of antemortem cortical atrophy **(Dallaire-Théroux *et al.*, 2017)**. In addition to cortical atrophy, neocortical and hippocampal NFTs have also been linked to the severity and progression of cognitive decline in DAT-AD **(Arriagada *et al.*, 1992; Bierer *et al.*, 1995)**. Taken together, these findings strongly indicate that in comparison to APs, the location and extent of NFTs more consistently correspond to the anatomy of cortical atrophy and cognitive decline characteristic of DAT-AD.

The neuropathologic basis of cortical atrophy remains unclear in the clinical AD variants such as PPA-AD. MRI has revealed focal and asymmetric cortical atrophy concentrated to language regions of the language dominant hemisphere in PPA **(Rogalski *et al.*, 2011a; Rogalski *et al.*, 2014; Rogalski *et al.*, 2016)**. Similar to the underpinnings of memory impairments and medial temporal lobe atrophy typical of DAT-AD, recent studies suggest that the language deficits and atrophy of language cortices characteristic of PPA-AD are associated with the accumulation of NFTs **(Gefen *et al.*, 2012; Josephs *et al.*, 2013)**. These early findings in PPA-AD, in combination with DAT-AD investigations, provide converging evidence that NFTs may be a common and major contributor to cortical atrophy across the distinct clinical variants of AD.

VIII. Possible Neuroinflammatory Contributors to Cortical Atrophy

Regardless of the underlying molecular pathology, there appears to be an invariable glial-mediated neuroinflammatory response in neurodegenerative diseases. The examination of cells and mediators that drive neuroinflammation is a burgeoning area of research given that neuroinflammation may play an important role in the pathogenesis and severity of diseases like AD **(McGeer and McGeer, 2001)**. Both reactive astrocytes and activated microglia produce inflammatory responses **(Serrano-Pozo *et al.*, 2011b; Serrano-Pozo *et al.*, 2013b)**, but microglia deserve special consideration as the resident immune cells of the brain. Most neuroinflammation is often attributed to reactive microglia, first described long ago by del Rio-Hortega and shortly later by Penfield to be an abundant population of macrophages of the central nervous system **(Penfield, 1925; Del Rio-Hortega, 2012; Sierra *et al.*, 2016)**. Microglia are the first line of defense to brain lesions, and their sensitivity and responsiveness to changes in the brain are critical to maintaining homeostasis and normal brain health. However, microglia also appear to have maladaptive properties that feed the debate on how they may contribute to neurodegenerative disease **(Kreutzberg, 1996; Mosser and Edwards, 2008; Perry *et al.*, 2010; Streit *et al.*, 2014; Svahn *et al.*, 2014; Salter and Stevens, 2017)**.

The precise roles of microglia in health and disease are still under investigation. Microglia are heterogeneous in function and appearance, with some morphologic phenotypes more closely linked to neurodegenerative processes compared to others. Resting "ramified" microglia appear relatively smaller, with long, thin branches that are motile and likely survey for pathophysiological changes in preparation to convert to the activated state **(Perry *et al.*, 2010)**. Classically "activated" microglia are often considered the typical macrophages that appear hypertrophic with thicker and shorter processes. Activated microglia may serve roles in wound healing, host defense, and regulatory processes **(Mosser and Edwards, 2008)**. When activated, microglia undergo a change

in morphology and an upregulation of cell-surface receptors and cytoplasmic proteins that can be readily targeted by immunohistochemical techniques to reveal their presence and distribution. In the activated state, microglia have the capacity to secrete harmful cytotoxic mediators including cytokines, reactive oxygen species, and other factors that stimulate inflammatory processes linked to neuronal damage **(McGeer and McGeer, 2001)**. Other phenotypes likely exist in the microglial spectrum **(Mosser and Edwards, 2008; Streit and Xue, 2009; Bachstetter *et al.*, 2015)**, and their extent in gray versus white matter have not been quantitatively evaluated. Therefore, the differentiation and regional accumulation of microglia in gray versus white matter are critical to the investigation of how activated microglia, a potential neuroinflammatory marker and indicator of pathology, may be contributing to selective neurodegeneration measured during life (e.g., cortical atrophy).

The majority of microglia-centered studies have come from examinations of individuals diagnosed with DAT-AD. Activated microglia appear in close proximity to APs and NFTs in AD **(McGeer *et al.*, 1987; Styren *et al.*, 1990; Serrano-Pozo *et al.*, 2011b)**, and there is evidence for glial-mediated inflammation that could be an initially protective response to accumulating AD neuropathology that becomes neurotoxic once chronically activated due to the initial pathologic threat failing to be eliminated **(McGeer and McGeer, 2001; Solito and Sastre, 2012)**. The inflammatory processes and co-localization of microglia with other pathologic inclusions have implicated microglia in the progression of multiple diseases. For example, activated microglia accumulate near demyelinating pathology in multiple sclerosis **(Singh *et al.*, 2013)**, Pick bodies in frontotemporal dementia (FTD) patients with underlying FTLD-tau **(Schofield *et al.*, 2003; Lant *et al.*, 2014)**, and TDP-43 inclusions in FTD and PPA patients with underlying FTLD-TDP **(Lant *et al.*, 2014; Kim *et al.*, 2016)**.

The distribution of neuroinflammatory markers and how they may contribute to

neurodegenerative processes in non-amnestic variants of AD such as PPA-AD are not well understood. A recent study of atypical AD patients with predominately aphasic presentations demonstrated that relative to the temporal cortex, the parietal cortex had a greater concentration of phosphorylated tau immunoreactivity and neuroinflammatory markers including activated microglia that was not observed in typical amnestic AD patients **(Boon *et al.*, 2018)**. These distinguishable patterns of activated microglia between amnestic and non-amnestic AD phenotypes is reminiscent of the emerging evidence for divergent patterns of NFTs found in DAT-AD (symmetric distributions) versus PPA-AD (asymmetric distributions) **(Gefen *et al.*, 2012; Josephs *et al.*, 2013)**. It remains to be determined why NFTs do not conform to typical Braak staging in non-amnestic variants of AD, but neuroinflammation might play a role. Quantitative investigations in PPA-AD would be beneficial in determining the extent of microglial activation in gray matter and white matter and how microglia distributions relate to patterns of neurodegenerative processes such as cortical atrophy.

IX. Possible Cellular Determinants of Cortical Atrophy

Neurodegeneration likely represents most of cortical atrophy; as the word neurodegeneration suggests, cells such as neurons are degenerate and probably die in the face of neuropathologic stressors. However, in contrast to the neuropathologic studies that have evaluated relationships between AD neuropathology and antemortem cortical atrophy, far less is understood about the postmortem cellular markers that contribute to cortical atrophy. It has been known for decades that neuronal loss occurs on a regional and laminar basis that parallels histopathologic burden in DAT-AD **(Hirano and Zimmerman, 1962; Brun and Englund, 1981; Coleman and Flood, 1987; Arnold *et al.*, 1991; Gomez-Isla *et al.*, 1997; Arendt *et al.*, 1998)**. In addition to selective cell layer loss, minicolumns have been shown to thin in AD and aging **(Chance *et al.*, 2011)**. Further analyses of individual neurons have shown that neurodegeneration is also due to a

reduction in cell size and loss of integral parts of neurons (i.e., axons, dendrites, and spines), with pyramidal projection neurons being uniquely susceptible to neurofibrillary degeneration and synapse density representing the strongest correlate of cognitive impairments in DAT-AD **(Coleman and Flood, 1987; DeKosky and Scheff, 1990; Terry *et al.*, 1991; Braak *et al.*, 2000; Uylings and de Brabander, 2002; Masliah *et al.*, 2006)**. Far less experimentation has been completed in non-amnestic dementias such as FTD and PPA, but similar findings have been reported. For example, neuronal loss and gliosis has been observed in a regional-, laminar-, and stage-dependent manner in individuals diagnosed with FTLD-tau or FTLD-TDP **(Kersaitis *et al.*, 2004; Yousef *et al.*, 2017)**. In summary, compared to normal controls and age-related changes, many lines of evidence suggest that a multitude of neuronal changes (that are cell-type and anatomically specific) collectively contribute to neurodegeneration in diseases such as AD **(Morrison and Hof, 1997)**.

Another important cell type to consider is glia. The relationship with between glia and cortical atrophy is paradoxical: glia are space-filling cells that also have the capacity to exacerbate neurodegenerative processes and thus cortical atrophy. Glia are a prominent constituent of the cortex given that the latest quantitative estimates indicate that the adult human brain has an approximately 1:1 ratio of glia-to-neurons **(Azevedo *et al.*, 2009)**. Therefore, glial changes should also be an important cellular substrate of cortical atrophy. In various pathologic contexts, it is currently unclear how glia contribute to neurodegeneration and cortical atrophy considering that glia (and microglia in particular) exhibit a prolific response to disease that makes them simultaneously neuroprotective, neuroinflammatory, and prone to senescence and dysfunction **(Block *et al.*, 2007; Mosser and Edwards, 2008; Perry *et al.*, 2010; Svahn *et al.*, 2014)**. In AD, neuropathologic inclusions do not form inside glia and yet, scores of microglia react to accumulating neuropathology by way of hypertrophy, moving to inclusion sites, and by

proliferating **(Solito and Sastre, 2012; Gomez-Nicola *et al.*, 2013; Serrano-Pozo *et al.*, 2013a)**. These particular microglial changes might actually negate the effects of cortical atrophy driven by neuronal loss or shrinkage, resulting in microglial activation having a negative or lack of relationship with cortical atrophy that has been reported previously **(Serrano-Pozo *et al.*, 2011b)**. Conversely, gliosis is known to be a typical feature of regions undergoing neurodegeneration and neuropathologic change. Therefore, heightened microglial activation in regions with greater neuropathologic change in combination with microglia having the capacity to mediate neurotoxic effects that exacerbate neurodegenerative processes could mean microglial activation might have positive relationships with measures of cortical atrophy **(Femminella *et al.*, 2016; Kreisl, 2017)**. Consistent with findings in DAT-AD, densities of astroctyes and activated microglia appear to be related to disease severity and neurodegenerative processes in FTD and **PPA (Schofield *et al.*, 2003; Broe *et al.*, 2004; Lant *et al.*, 2014; Kim *et al.*, 2018)**.

Despite the logical notion that neuronal changes underlie cortical atrophy, very little neurobiological evidence exists as to what MRI-based cortical atrophy is detecting in terms of cellular changes in disease. One study found that MRI-based hippocampal volume correlated with the number of neurons counted in the subsector CA1 of the hippocampus in DAT-AD and vascular dementia **(Zarow *et al.*, 2005)**. However, similar to previous reports that quantitated neuronal changes in DAT-AD, the findings are difficult to generalize because data was often restricted to a small and singular region, usually the selectively vulnerable hippocampus or entorhinal cortex. The neuronal and glial changes that constitute neurodegeneration and contribute to cortical atrophy need to be confirmed at a multi-regional level in the clinical AD phenotypes including PPA-AD.

X. Objectives of Present Studies and Expected Outcomes

The main goal of this dissertation was to explore the histopathologic basis of *in vivo* cortical atrophy in a clinical population diagnosed with PPA and AD neuropathologic change. To

maximize the certainty of what neurobiological changes underlie cortical atrophy, PPA participants were included only if their last MRI scan was close to death (<2.5 years). It was expected that the findings of these investigations would help identify mechanisms of neurodegeneration and uncover what structural MRI is detecting in clinical and research settings.

Three studies were designed to examine the relationships between neuropathology, cells, and cortical atrophy in the same corresponding regions. Stereology was used to quantify densities of neuropathology and cells in the gray matter given the method's reputation as the gold standard for unbiased and quantitative estimates of postmortem markers **(Schmitz and Hof, 2005)**. The high packing density of activated microglia in white matter precluded a reliable stereologic analysis and thus optical density analyses were adopted as a quantitative alternative. Neuroimaging analyses employing surface-based methods were used to measure cortical thickness atrophy.

In Study 1, the neuropathologic basis of *in vivo* cortical atrophy was examined in PPA-AD with the hypothesis that NFTs would be a stronger predictor of cortical atrophy than APs. While processing PPA-AD tissue for cellular markers including a neuroinflammatory marker for microglia, it became evident that microglial activation was often more pronounced in the white matter compared to gray matter across PPA pathologic subtypes in ways not previously reported. Consequently, Study 2 was launched to perform a novel examination aimed at characterizing the distribution of white matter activated microglia and determining their relationship with gray matter atrophy in PPA-AD and PPA-TDP participants. It was expected that greater densities of microglial activation would be found in more atrophic regions. Finally, the focus for Study 3 shifted back to gray matter to explore the cellular basis of *in vivo* cortical atrophy, in addition to integrating findings from Studies 1 and 2 to determine how neurons and microglial subtypes were related to AD neuropathology and white matter activated microglia. The central hypothesis of this third

investigation was that smaller densities of neurons would be related to greater densities of NFTs and hypertrophic microglia as well as greater cortical atrophy. In addition, it was hypothesized that hypertrophic microglia would be related to NFTs, APs, and white matter activated microglia, while microglial phenotypes would display different relationships with cortical atrophy.

Given the lack of effective interventions to prevent or slow diseases such as AD, clinical strategies may need to develop therapeutics that target new pathologic or inflammatory pathways. While MRI methods are becoming better at detecting and tracking these changes over time in living patients, these related processes remain incompletely understood in the human brain. Quantitative postmortem examinations of how AD neuropathology and neuroinflammation (microglial function) relate to neurodegenerative processes measured by MRI should help fill in critical gaps in knowledge. These multidisciplinary experiments are part of an ongoing effort to identify neuropathologic culprits and susceptibility markers of degeneration that lead to debilitating disorders such as PPA.

—STUDY 1—

Neuropathologic Basis of *In Vivo* Cortical Atrophy in PPA-AD

ABSTRACT

The neuropathologic basis of *in vivo* cortical atrophy in neurodegenerative diseases that cause dementia remains poorly understood. Primary progressive aphasia (PPA) is a language-based dementia syndrome characterized by asymmetric cortical atrophy and associated with multiple proteinopathies, including the neurofibrillary tangles (NFTs) and amyloid-ß plaques (APs) of Alzheimer's disease (AD). A systematic and quantitative investigation of the relationships between NFTs, APs, and *in vivo* cortical atrophy in PPA-AD is lacking. In this study, regional cortical thickness in five PPA-AD participants who had magnetic resonance imaging (MRI) within 7-30 months of death was compared to an age-matched control group. NFTs and dense-core APs were quantified in postmortem brain sections using the Thioflavin-S stain and stereology. *In vivo* and postmortem data were collected within 14 anatomically corresponding regions that included five language and two non-language regions in the left hemisphere along with their contralateral homologues. Linear mixed models accounting for repeated measures and stratified by hemisphere and type of region (language vs. non-language) were used to determine the hemispheric and language selectivity of pathologic changes as well as the relationships between cortical atrophy and AD neuropathology. Consistent with the aphasic profile of PPA, left language regions displayed more cortical atrophy ($p=0.01$) and NFT densities ($p=0.02$) compared to right language homologues. Left language regions also showed more cortical atrophy ($p<0.01$) and NFT densities ($p=0.02$) than left non-language regions. A subset of data was analyzed to determine the predilection of NFTs and APs for neocortical regions compared to entorhinal cortex

in the left hemisphere, which showed that the three most atrophied language regions had significantly greater NFT (*p*=0.04) and AP densities (*p*<0.01) than the entorhinal cortex in the left hemisphere. These results provide quantitative evidence that NFT accumulation in PPA selectively targets the language network and may not follow the Braak staging of neurofibrillary degeneration described in the more typical amnestic dementia of AD. NFT densities were also positively associated with cortical atrophy within the left hemisphere language regions (*p*<0.01) and their right language homologues (*p*<0.01) whereas the AP densities were not. Given previous findings from typical amnestic AD, the current study of PPA-AD provides converging evidence that NFTs are the principal determinants of atrophy and clinical phenotypes associated with AD.

INTRODUCTION

Magnetic resonance imaging (MRI) is a reliable and quantitative method for detecting structural changes in the brain during life. The basis of these anatomical changes is not well understood at the neurobiological level, especially in neurodegenerative diseases that cause cortical atrophy and dementia. The neuropathologic contributors to MRI-based cortical atrophy have been extensively examined in individuals clinically diagnosed during life with an amnestic dementia of the Alzheimer-type (DAT) and pathologically diagnosed postmortem with Alzheimer's disease (DAT-AD). The amyloid-ß plaques (APs) and neurofibrillary tau tangles (NFTs) are the primary histopathologic hallmarks of AD neuropathology. While both appear to contribute to neurodegenerative processes in DAT-AD, NFTs may be the stronger pathologic correlate of antemortem cortical atrophy **(Dallaire-Théroux *et al.*, 2017)**. In addition to cortical atrophy, neocortical and hippocampal NFTs have also been linked to the severity and progression of cognitive decline in DAT-AD **(Arriagada *et al.*, 1992; Bierer *et al.*, 1995)**. Taken together, these findings strongly indicate that in comparison to APs, the location and extent of NFTs more consistently correspond to the anatomy of cortical atrophy and cognitive decline characteristic of

DAT-AD. However, the neuropathologic basis of cortical atrophy remains unclear outside of those with DAT-AD. AD neuropathology is known to cause distinct types of non-amnestic dementia **(Kramer and Miller, 2000; Alladi *et al.*, 2007; Mesulam *et al.*, 2008; Gefen *et al.*, 2012; Warren *et al.*, 2012; Mesulam *et al.*, 2014b; Rogalski *et al.*, 2016)** with each clinical syndrome displaying common and variant-specific atrophy patterns **(Ossenkoppele *et al.*, 2015a)**. The purpose of the current study was to determine if NFTs could also be the primary driver of cortical atrophy in a non-amnestic variant of AD known as primary progressive aphasia (PPA).

PPA with AD neuropathology (PPA-AD) is the aphasic variant of AD, a syndrome characterized by a gradual dysfunction of language processing with initial preservation of other cognitive domains such as memory **(Mesulam, 1982; Mesulam, 2003)**. AD is the pathologic diagnosis in approximately 40% of individuals with PPA **(Knibb *et al.*, 2006; Mesulam *et al.*, 2008; Rohrer *et al.*, 2012; Mesulam *et al.*, 2014b)**. MRI has revealed focal and asymmetric cortical atrophy that is concentrated in language regions of the language dominant hemisphere in PPA **(Rogalski *et al.*, 2011a; Rogalski *et al.*, 2014; Rogalski *et al.*, 2016)**. Similar to the underpinnings of memory impairments and medial temporal lobe atrophy typical of DAT-AD, recent studies suggest that the language deficits and atrophy of language cortices characteristic of PPA-AD are associated with NFT densities **(Gefen *et al.*, 2012; Josephs *et al.*, 2013)**. These early findings in PPA-AD, in combination with studies of DAT-AD, provide converging evidence that NFTs are possibly a common and major contributor to cortical atrophy across the distinct clinical variants of AD.

Previous studies examining DAT-AD and PPA-AD participants presented with several shortcomings that may have clouded the reported relationships between AD neuropathology and *in vivo* atrophy. For example, many of these investigations included wide interval ranges (intervals = ~1-8 years) between the final MRI scan and death **(Jack *et al.*, 2002; Silbert *et al.*, 2003;**

Csernansky *et al.*, 2004; Jagust *et al.*, 2008; Josephs *et al.*, 2008; Vemuri *et al.*, 2008; Whitwell *et al.*, 2008; Burton *et al.*, 2009; Burton *et al.*, 2012; Erten-Lyons *et al.*, 2013; Josephs *et al.*, 2013; Kaur *et al.*, 2014; Dallaire-Théroux *et al.*, 2017), a potential problem since rates of atrophy and neuropathologic accumulations have yet to be clarified and atrophy likely worsened over the longer intervals. Measurements of atrophy were often confined to the hippocampus **(Jack *et al.*, 2002; Silbert *et al.*, 2003; Csernansky *et al.*, 2004; Jagust *et al.*, 2008; Vemuri *et al.*, 2008; Burton *et al.*, 2009; Burton *et al.*, 2012; Erten-Lyons *et al.*, 2013; Josephs *et al.*, 2013; Kaur *et al.*, 2014)**, whole brain volume **(Silbert *et al.*, 2003; Csernansky *et al.*, 2004; Josephs *et al.*, 2008; Erten-Lyons *et al.*, 2013; Kaur *et al.*, 2014)**, or ventricular volumes **(Silbert *et al.*, 2003; Josephs *et al.*, 2008; Erten-Lyons *et al.*, 2013; Kaur *et al.*, 2014)**, making it difficult to generalize the neuropathologic-anatomic relationships across more of the brain. Select studies have conducted larger analyses within 3-4 regions **(Burton *et al.*, 2012; Josephs *et al.*, 2013)**, but their neuropathologic data were only collected unilaterally, a limitation also shared by studies of fewer regions **(Jack *et al.*, 2002; Josephs *et al.*, 2008; Vemuri *et al.*, 2008; Whitwell *et al.*, 2008; Burton *et al.*, 2009)**. Bilateral examinations of multiple regions remain uncommon yet are critical to elucidating the relationship between neuropathology and atrophy, especially in clinical syndromes such as PPA that present with such stark hemispheric asymmetries.

NFTs and APs vary greatly across anatomical regions, gyral depth, and cortical layers in AD brains **(Hirano and Zimmerman, 1962; Brun and Englund, 1981; Pearson *et al.*, 1985; Lewis *et al.*, 1987; Arnold *et al.*, 1991; Braak and Braak, 1991; Arendt *et al.*, 2016)**. However, previous DAT-AD and PPA studies infrequently obtained representative quantitative estimates of histopathologic markers. Qualitative evaluations of postmortem neuropathology and MRI that were collected with vague anatomical correspondence have likely led to inaccurate interpretations of neuropathologic-anatomic relationships. For example, atrophy has been assessed visually

(Whitwell *et al.*, 2008; Burton *et al.*, 2009), and neuropathologic accumulation has been determined by ranking **(Jack *et al.*, 2002; Csernansky *et al.*, 2004; Jagust *et al.*, 2008; Josephs *et al.*, 2013),** Braak stage **(Silbert *et al.*, 2003; Csernansky *et al.*, 2004; Jagust *et al.*, 2008; Josephs *et al.*, 2008; Vemuri *et al.*, 2008; Whitwell *et al.*, 2008; Erten-Lyons *et al.*, 2013)** or other semi-quantitative methods **(Csernansky *et al.*, 2004; Josephs *et al.*, 2008; Josephs *et al.*, 2013)** using only a few, if not single, postmortem sections.

The current study sought to address these methodological limitations by using stereologic quantitation of AD neuropathology and surface-based measurements of *in vivo* cortical atrophy in a well-characterized cohort of PPA-AD participants with MRI scans relatively close to death (7-30 months). Due to asymmetric and region-specific atrophy, PPA represents an ideal dementia model for bilateral, multi-regional investigations that are not commonly conducted in other neurodegenerative diseases. The focal degenerative patterns observed in PPA brains provided a unique opportunity to tease apart the relative contributions that pathologic lesions make to compromised versus relatively spared regions within the same brains (e.g., left versus right hemisphere; language versus non-language regions). FreeSurfer neuroimaging software was utilized for the dual purpose of measuring cortical atrophy and providing a reliable methodology for delineating 14 bilateral regions involved in the cognitive domains of language, memory, and vision. Postmortem coronal sections were matched to *in vivo* coronal MRI visualized in each FreeSurfer-derived region, ensuring anatomical correspondence between atrophy measurements and stereologic quantification of NFTs and APs.

The primary aim of this investigation was to determine if densities of AD neuropathology predicted *in vivo* cortical atrophy in PPA-AD. A secondary aim was to assess the selective vulnerability of the language network in PPA-AD by confirming that AD neuropathology and cortical atrophy were asymmetric and had a predilection for language regions in comparison to

non-language regions. Considering previous findings in PPA-AD and DAT-AD, we expected larger densities of NFTs, not APs, to be associated with greater cortical atrophy in language regions of the language-dominant hemisphere in PPA-AD.

METHODS

Participants

The current study included five right-handed PPA participants with AD as the primary neuropathologic diagnosis, each of whom had obtained at least one structural MRI scan acquired close to death. Each PPA patient was enrolled through the PPA Research Program at the Mesulam Cognitive Neurology and Alzheimer's Disease Center at the Northwestern University Feinberg School of Medicine. The diagnosis of PPA and subtypes was based on previously described diagnostic guidelines which includes at least a two year history of progressive, isolated impairments of speech or language functions **(Mesulam, 1982; Mesulam, 2001; Gorno-Tempini *et al.*, 2011)**. Two PPA participants were clinically diagnosed with the logopenic variant (PPA-L), one with the agrammatic variant (PPA-G), and two were unclassifiable by extant criteria (PPA-U). All five PPA participants received a postmortem diagnosis of "high" AD neuropathologic change based on published consensus criteria **(Hyman *et al.*, 2012; Montine *et al.*, 2012).** A cognitively healthy control group consisting of 35 participants of similar age and education were included in the neuroimaging analysis. The Northwestern University Internal Review Board approved this study and all participants gave informed consent to their involvement and brain donations. Clinical history and characteristics of each PPA case are presented in **Table 1.1** and **1.2,** respectively.

MRI acquisition

Structural MRI scans were acquired from all PPA and healthy control participants on a 3T Siemens TIM Trio scanner using a 12-channel birdcage head coil at the Northwestern University

Center for Translational Imaging. A T$_1$-weighted 3D MPRAGE sequence included the following:

repetition time = 2300 ms, echo time = 2.91 ms, inversion time = 900 ms, field of view = 256 mm,

flip angle = 9°, 1 mm^3 voxel resolution collected over 176 sagittal slices. The mean interval of

time between the last scan and death (SDI) was 1.96±0.8 years; range 0.61-2.54 years (**Table 1.2**).

Table 1.1 **Clinical presentations of PPA-AD participants.**

Participant	Clinical History
1	The patient presented at age 58 with a 2-year history of problems in word finding, spelling, and handling numbers. His speech contained multiple word-finding pauses with simplifications and circumlocutions but without paraphasias. Grammar production in both speech and writing, repetition, and naming were preserved. Activities of daily living were intact. He received a diagnosis of logopenic PPA and enrolled in research. Two years later the patient returned for a research visit and underwent an MRI scan. At that time, his aphasia severity prevented completion of much of the testing battery. His informant endorsed moderate impairment in activities of daily living, severe anxiety, and severe depression. He died 7 months later at age 62.
2	The patient initially presented at age 57 with a 2-year history of significant word finding difficulties and mild executive dysfunction. At the time of research enrollment, at age 59, his aphasia severity and executive dysfunction precluded a reliable subtype diagnosis. The patient returned for a research MRI scan two years later. At that time, activities of daily living were severely impaired and his informant endorsed moderate behavioral disturbances including disinhibition, depression, and aberrant motor activities. He died about 2 years later at age 64.
3	The patient presented at age 69 with a 2-year history of word finding deficits, stuttering, decline in motivation, and difficulty following conversations. Dysfluency without agrammatism, with intact repetition, naming, and single word comprehension led to a diagnosis of logopenic PPA. At that time the patient enrolled in research and was followed annually. At his last visit at age 74, he underwent MRI scanning and a brief neuropsychological examination. Despite severe dysfluency and naming deficits, the patient had relatively intact single word comprehension and nonverbal working memory. His informant endorsed moderately impaired activities of daily living and moderate apathy. He died 2 years later at age 76.

4	The patient presented at age 57 with a 5-6-year history of word finding impairments, difficulty reading and writing, and possible slowing of information processing. Speech was agrammatic and dysfluent, repetition and naming were severely impaired, and he was unable to write. Comprehension of single words were relatively intact except for unusual words such as "illumination". At the time of research enrollment and MRI scan at age 58, his aphasia severity level precluded a subtype diagnosis. He died 2.5 years later at age 61.
5	The patient presented at age 74 with a 2-3-year history of word finding problems. He reported an increase in the use of fillers, the misuse of pronouns, and trouble handling numbers and reading. Speech was circumlocutory with phonemic paraphasias and word finding pauses, but without agrammatism or dysarthria. Writing, however, was agrammatic. Single word comprehension and repetition were preserved. He enrolled in the research program with a diagnosis of agrammatic PPA and was scanned at the age of 76. He died 2.5 years later at age 78.

Table 1.2 Characteristics of PPA-AD participants.

PPA-AD Case #	PPA Clinical Subtype	Education (Years)	Age at Onset (Years)	Age at Scan (Years)	Age at Death (Years)	Symptom Duration (Years)	Scan/Death Interval (Years)	Postmortem Interval (Hours)	Fixative	*APOE* Status
1	L	16	56	61	62	4.7	0.61	6	F	*3,3*
2	U	12	55	62	64	7.9	2.14	14	F	*3,3*
3	L	15	67	74	76	8.6	2.00	8	P	*3,4*
4	U	14	51	59	61	9.4	2.54	19	P	*3,4*
5	G	18	72	76	78	6.2	2.54	28	P	*3,4*

L = logopenic; G = agrammatic; U = unclassifiable due to severity of impairments; P = paraformaldehyde; F = formalin; *APOE* = apolipoprotein E

MRI processing

Structural MRI were pre-processed using FreeSurfer (v5.1.0, *http://surfer.nmr.mgh.harvard.edu*), a well-validated software suite capable of detecting morphometric properties of neuroanatomy at submillimeter resolution **(Fischl and Dale, 2000)**. Topological surface errors were removed with manual iterative corrections based on established guidelines **(Ségonne *et al.*, 2007)**. Cortical thickness was calculated by measuring the distance between surface representations of the white-gray boundary and pial-CSF boundary **(Dale *et al.*, 1999)**. The asymmetry and regional severity of cortical atrophy was determined using whole-brain and regional analyses in the five PPA participants in comparison to 35 previously described healthy controls **(Rogalski *et al.*, 2014)**. The whole brain vertex-wise assessment of cortical atrophy involved the generation of a cortical surface heat map at the PPA group level to visualize areas of peak cortical thinning in comparison to the control group (**Fig. 1.1a**). The region of interest (ROI) analysis included measuring the cortical size for each ROI using mean cortical thickness and converting the thickness values to z-scores derived from regional thickness measurements collected from the healthy control group.

Regions of interest

A total of fourteen *a priori* ROIs were examined in each PPA case, seven per hemisphere (**Fig. 1.1b**). ROIs involved multiple cognitive domains, including language ROIs implicated in the PPA clinical profile, and non-language ROIs representing relatively spared cognitive functions (primary sensory and memory areas) over most of the disease duration. Within the left language-dominant hemisphere, five ROIs were language related and two were non-language related. The contralateral homologue of each ROI was used to investigate hemispheric asymmetry. The bilateral 'language ROIs' consisted of the inferior frontal gyrus (IFG), anterior superior temporal gyrus (aSTG), posterior superior temporal gyrus (pSTG), anterior inferior parietal lobule (aIPL),

and posterior inferior parietal lobule (pIPL). The bilateral 'non-language ROIs' were the memory related entorhinal cortex (EC) and the primary visual cortex (V1). While the EC is known to be highly vulnerable to AD neuropathology and atrophy early in DAT-AD **(Braak and Braak, 1991; Gomez-Isla *et al.*, 1996; Schmitz *et al.*, 2016)**, this region has not been thoroughly investigated in PPA, a dementia in which memory is not the salient deficit early in the disease course. The extent to which neuropathology and atrophy impact memory regions like the EC in PPA-AD will provide novel information regarding this region's integrity in the context of the heavily compromised language regions. In contrast, primary sensory regions such as V1 are typically less vulnerable to AD neuropathology and atrophy in most clinical presentations of AD (i.e., common exceptions include posterior cortical atrophy and early onset DAT-AD) **(Pearson *et al.*, 1985; Lewis *et al.*, 1987; Hof *et al.*, 1993; Uylings and de Brabander, 2002; Broe *et al.*, 2003; Ossenkoppele *et al.*, 2015a)**. V1 has also received little experimental attention in PPA, but it was anticipated to display little to no neuropathology and atrophy in PPA-AD.

Each *a priori* ROI was initially delineated in the native space of each subject using the Desikan-Killiany atlas **(Desikan *et al.*, 2006)** available in FreeSurfer, which reliably subdivides the human cortex into gyral-based ROIs **(Fischl *et al.*, 2004)**. FreeSurfer tools were utilized to make small modifications to three atlas-generated regions to construct the IFG, aSTG, and pSTG. The IFG region required the merging of the 'pars opercularis' and 'pars triangularis' regions, while a precise division of the 'superior temporal gyrus' along its longest axis created three equal parts, including an anterior segment (aSTG) and a posterior segment (pSTG), (**Fig. 1.1b**).

Tissue processing

Brains were cut into ~1-2 cm coronal blocks and fixed in either 10% formalin for 2 weeks or 4% paraformaldehyde for 30-36 hours at 4ºC, and then submerged into an increasing concentration gradient of sucrose (10-40%) for cryoprotection (**Table 1.2**). Coronal blocks were

cut into 40 μm-thick coronal sections and collected in a 1:24 series. Depending on the size of the ROI, 5-16 sections per ROI were analyzed to ensure representative sampling. In one series of tissue, APs and NFTs were visualized with the Thioflavin-S stain (1%), which recognizes ß-pleated sheet protein conformations associated with mature AD neuropathology. Thioflavin-S-positive NFTs (fluorescent cytoplasmic fibrils that resembled the size and shape of somas) and dense-core APs (extracellular coronas of dystrophic neurites that surrounded a central mass of brighter fluorescence) were selectively quantified (**Fig. 1.3**). These particular NFTs and APs (as opposed to pre-NFTs and diffuse APs) represent the pathologic hallmarks of AD and bear close relationships to neurodegenerative processes that likely underlie cortical atrophy **(Masliah *et al.*, 1994; Bobinski *et al.*, 1996; Gomez-Isla *et al.*, 1997; Urbanc *et al.*, 2002; Giannakopoulos *et al.*, 2003)**. A series of adjacent tissue sections was processed immunohistochemically for neuronal nuclear protein (NeuN, mouse monoclonal; EMD Millipore; 1/2000), which selectively stains neuronal somas and thus the full extent of gray matter, permitting reliable anatomic identification and correspondence to Thioflavin-S-positive sections.

Stereologic quantification and anatomic correspondence

Given that the major aim of the study was to relate *in vivo* cortical atrophy to postmortem AD neuropathology, it was critical that both datasets were reliably acquired from the same anatomical regions. A precise correspondence was achieved between brain regions during life and after death by initially visualizing each FreeSurfer-generated ROI on high resolution coronal slices in Freeview, FreeSurfer's visualization tool. Next, coronal slices in Freeview were matched to every available coronal section of postmortem tissue immunohistochemically stained with NeuN to guide the boundaries drawn on the postmortem tissue. The NeuN-positive tissue then directed the consistent placement of regional boundaries in the parallel series of Thioflavin-S-positive tissue, restricting stereological quantitation of AD markers to the same anatomical regions where

cortical atrophy was measured during life.

NFTs and dense-core APs were quantified at a final magnification of 60x across all cortical layers of each ROI using stereological analysis performed on a workstation equipped with a Nikon Eclipse E800 microscope, motorized stage, and stereology software (StereoInvestigator v11.07, MBF Bioscience). The optical fractionator probe was used to estimate the populations of NFTs and APs from all available sections per ROI, with sampling grid dimensions that varied by anatomical region to produce a coefficient of error ≤ 0.15 (**Schmitz & Hof 2005**). The size of the counting frame was kept at 125 μm^2, and a disector height of 16 μm with guard zones of 2 μm were set in order to ensure that quantification only occurred in the area of the tissue in which there was optimal staining and to prevent biases related to sectioning artifacts. Section thickness was measured at each counting site to calculate an average section thickness used in estimating populations of NFTs and APs. Densities of NFTs and APs were used for statistical analyses. Densities of NFTs and APs per mm^3 were calculated by taking the estimated population using number weighted section thickness and dividing by the planimetry volume in each ROI.

Statistical analyses

FreeSurfer software was used to generate the cortical thinning heat maps of each hemisphere by contrasting the cortical thickness of the PPA brains against the healthy control group. A general linear model on every vertex along the cortical surface calculated the differences in cortical thickness between groups. Areas of peak cortical thinning (i.e., atrophy) were detected and visualized after applying a stringent false discovery rate (FDR) threshold of 0.0001 to adjust for multiple comparisons **(Genovese *et al.*, 2002)**.

Averaged cortical thicknesses from each ROI in each participant were converted to standardized z scores (representing the magnitude of cortical atrophy in each ROI) using the mean and standard deviation from age-matched healthy controls:

$$z = (\mu_{\text{ healthy controls}} - [\text{averaged cortical thickness}])/ \sigma_{\text{ healthy controls}}$$

All analyses were conducted using linear mixed models accounting for repeated measures. To assess if cortical atrophy displayed hemispheric asymmetry in each regional domain (language and non-language), the relationship between atrophy and hemisphere was evaluated after stratifying by the type of region. To evaluate if atrophy was different between language and non-language regions, the association between atrophy and type of region was determined in only the left hemisphere. To assess the hemispheric asymmetry of NFT and AP densities in each regional domain, the following relationships were evaluated after stratifying by the type of region: NFT density and hemisphere, and APs and hemisphere. To examine the language region selectivity of AD neuropathology, the associations that NFT and AP densities each have with type of region were carried out in only the left hemisphere. These two models were then repeated but excluded V1, IFG, and aSTG in order to determine the predilection of NFT and AP densities for the most atrophied neocortical regions (pSTG, aIPL, pIPL) relative to the entorhinal cortex. In addition, models were performed to evaluate the relationship between NFT and AP densities in left language regions and in contralateral language homologues. Lastly, models were performed to evaluate the relationships that cortical atrophy had with NFT and AP densities in left language regions and in contralateral language homologues. Adjusters varied by model: when cortical atrophy was compared to NFT and AP densities, models were adjusted for age at death and SDI; when cortical atrophy was related to hemisphere or type of region, models were adjusted for age at scan and SDI; when NFT or AP densities were the outcomes, models were adjusted for age at death and postmortem interval. Significance was set to $p<0.05$ for all comparisons using SAS software v9.4; SAS Institute.
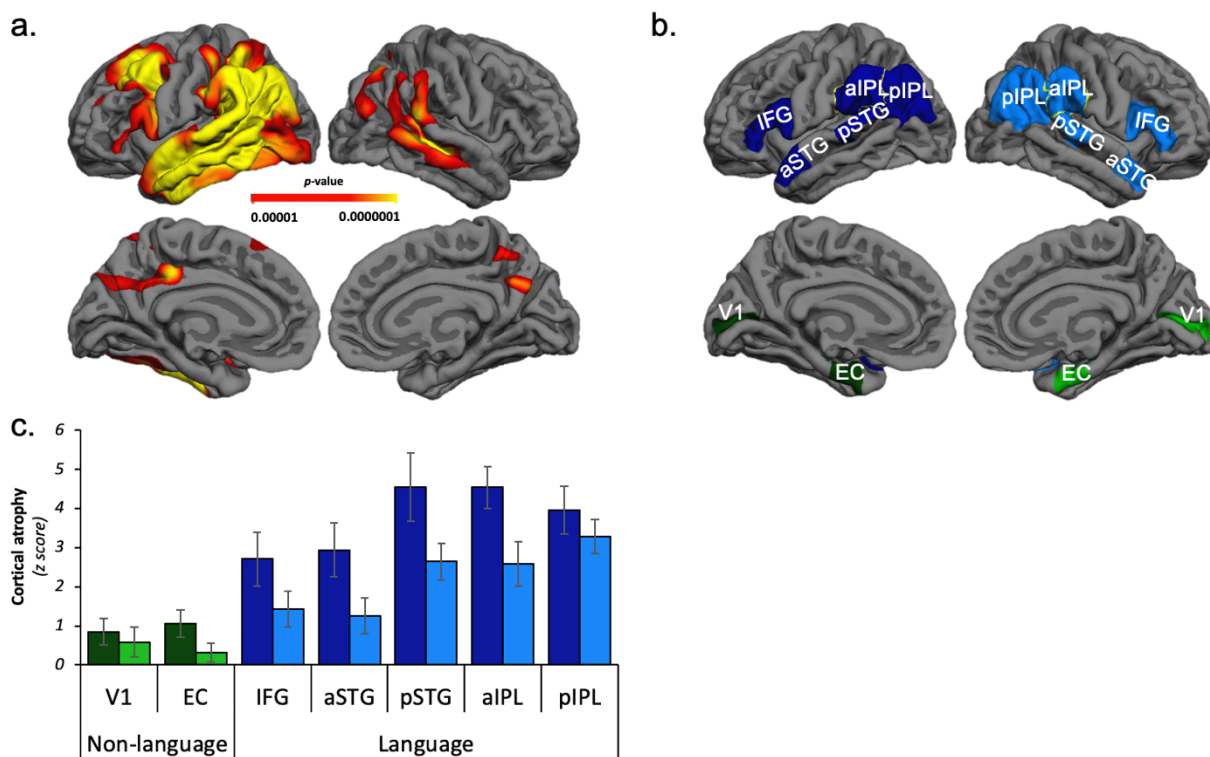
Figure 1.1 *In vivo* **cortical atrophy was asymmetric and selectively greater in language ROIs in PPA-AD.**
a) Heat map identifying peak sites of cortical atrophy in the PPA-AD group relative to the healthy control group on lateral and medial reconstructions of a template cortical surface in FreeSurfer. Cortical thinning was more prominent in the left hemisphere language network, especially the temporal and parietal lobes. FDR correction set to 0.0001. **b)** Left language ROIs (dark blue), right language homologues (blue), left non-language ROIs (dark green), right non-language ROIs (green) displayed bilaterally on lateral and medial reconstructions of a template cortical surface in FreeSurfer. Inferior frontal gyrus (IFG), anterior superior temporal gyrus (aSTG), posterior superior temporal gyrus (pSTG), anterior inferior parietal lobule (aIPL), posterior inferior parietal lobule (pIPL), entorhinal cortex (EC), primary visual cortex (V1). **c)** The PPA-AD group had significantly more cortical atrophy in the left language regions compared to right language homologues (*p*=0.01), but asymmetry was not observed within the non-language regions. Cortical atrophy was significantly greater in the language regions compared to the non-language regions in the left hemisphere (*p*<0.01). Left language ROIs = dark blue bars; right language homologues = blue bars; left non-language ROIs = dark green bars; right non-language ROIs = green bars.

RESULTS

Hemispheric and language region selectivity of cortical atrophy

Cortical atrophy measured at the whole-brain level or by ROI were consistent with the patterns of atrophy previously reported from PPA-AD or PPA with suspected AD neuropathology

(Gefen *et al.*, 2012; Mesulam *et al.*, 2014b; Rogalski *et al.*, 2016). A stringent FDR of 0.0001 was used to identify peak cortical thinning using a vertex-wise thickness analyses across the whole brain of the PPA-AD group (**Fig. 1.1a**). As expected, cortical atrophy was left-lateralized including the entire lateral temporal lobe, posterior aspects of the frontal lobe excluding the motor cortex, and most of the parietal lobe with sparing of the superior parts of the superior parietal lobule and precuneus. Bilateral cortical thinning was restricted to the inferior precuneus and the temporoparietal junction extending into the superior temporal sulcus. There was no significant cortical thinning observed in most medial regions or most of the occipital lobe, including the bilateral non-language regions EC and V1 at the whole-brain group level.

ROI analyses of cortical atrophy determined differences between hemispheres and between language and non-language domains. Left language regions displayed greater cortical atrophy compared to right language homologues ($p=0.01$), but no asymmetry was observed in the non-language regions (**Fig. 1.1c**). In the left hemisphere, cortical atrophy was significantly greater in the language regions compared to the non-language regions ($p<0.01$; **Fig. 1.1c**). The greatest cortical atrophy was observed in the regions comprising the left temporoparietal junction (pSTG, aIPL, and pIPL).

Hemispheric and language region selectivity of AD neuropathology

NFT densities were greater in the left language regions compared to the right language homologues ($p=0.02$), but not in the bilateral non-language regions (**Fig. 1.2a, Fig. 1.3**). AP densities did not show significant asymmetry when models were stratified to the language and non-language regions (**Fig. 1.2b, Fig. 1.3**). NFT densities were significantly greater in language regions compared to non-language regions within the left hemisphere ($p=0.02$; **Fig. 1.2a, Fig. 1.3**). Left language regions showed a non-significant trend for having greater AP densities than left non-language regions ($p=0.05$).
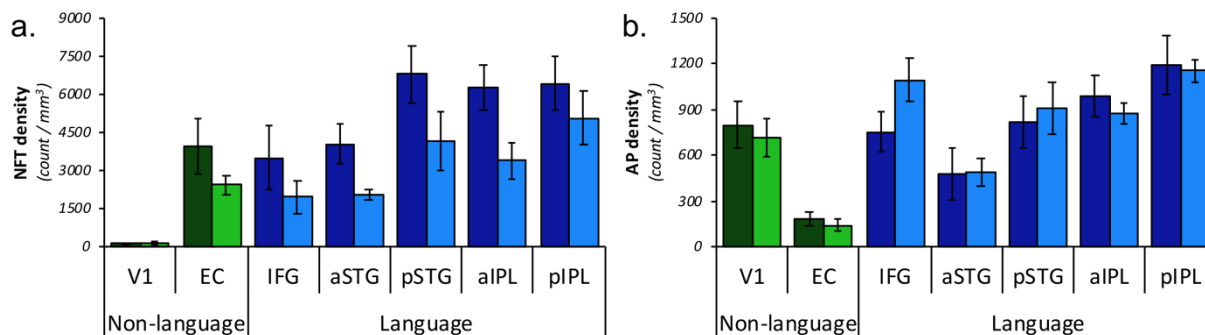
Figure 1.2 Only NFT densities displayed hemispheric asymmetry and language region selectivity in PPA-AD.
a) NFT densities were greater in the left language regions compared to their right hemisphere homologues (p=0.02); non-language regions did not harbor asymmetric densities of NFTs. NFT densities were significantly greater in language regions compared to non-language regions within the left hemisphere (p=0.02). **b)** AP densities displayed a non-significant trend for language selectivity (p=0.05) and did not show significant asymmetry.
Left language ROIs = dark blue bars; right language homologues = blue bars; left non-language ROIs = dark green bars; right non-language ROIs = green bars.

To test whether NFT and AP accumulation had a predilection for the most atrophied language regions compared to the EC (an early site of structural and AD neuropathologic change in DAT-AD), a subset of data was analyzed in the left hemisphere that excluded V1, IFG, and aSTG. These analyses showed that the three most atrophied language regions (i.e., pSTG, aIPL, pIPL) had greater mean densities of NFTs (p=0.04) and APs (p<0.01) compared to the EC.

Relationships between NFTs, APs, and cortical atrophy

NFT densities were not associated with AP densities in the language regions or in right language homologues. Cortical atrophy had a positive relationship with NFT densities in the left language regions (p<0.01; **Fig. 1.4a**) and their contralateral homologues (p<0.01). Cortical atrophy was not associated with AP densities in the language regions or in right language homologues (**Fig. 1.4b**).
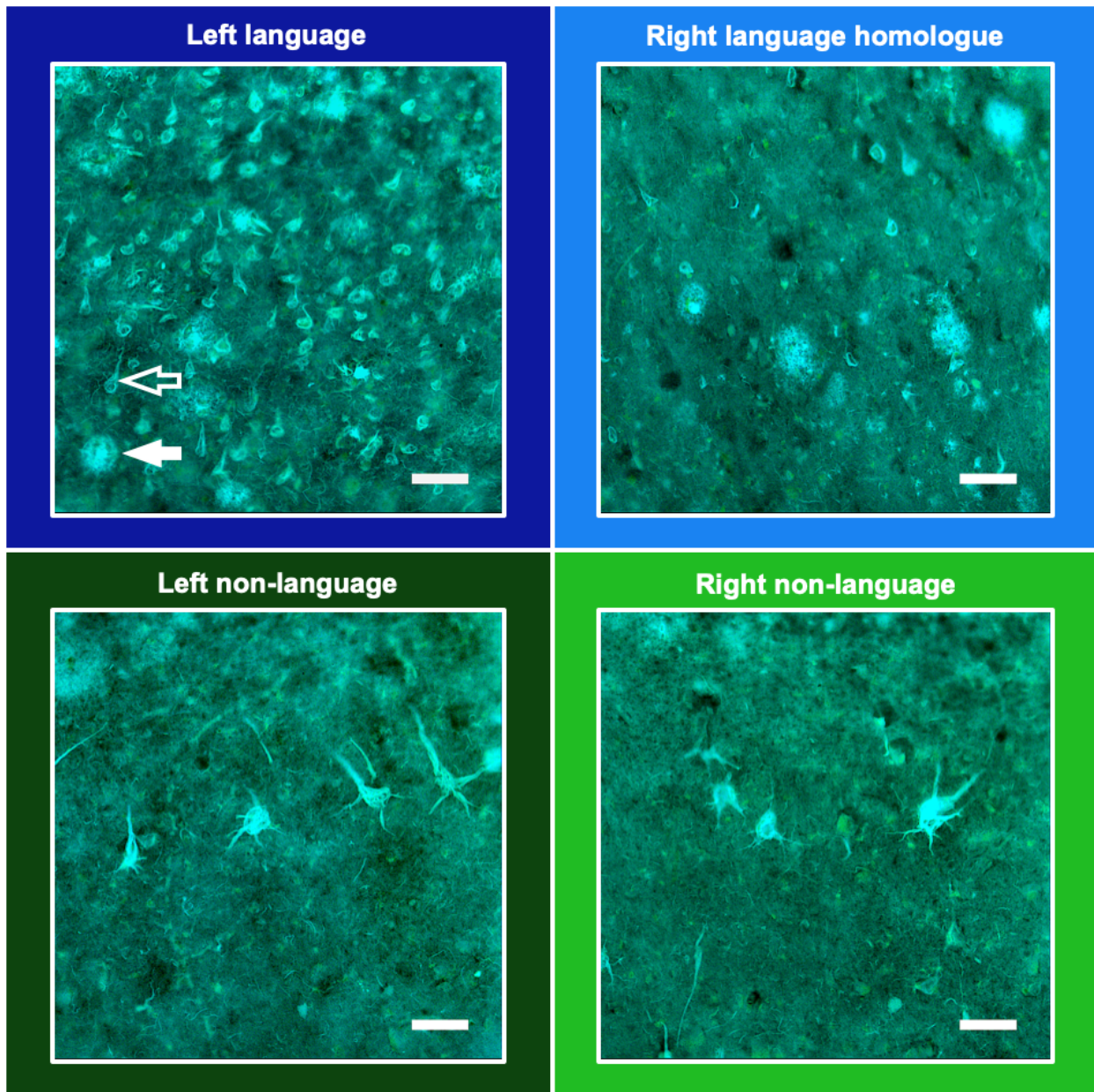
Figure 1.3 Representative photomicrographs of the differential distributions of APs and NFTs across hemispheres and regions in PPA-AD.

NFTs accumulated more in language ROIs of the language dominant (left) hemisphere. APs had similar accumulations across hemispheres regardless of ROI. Top row is the aIPL, a language ROI; bottom row is the EC, a non-language ROI. Images acquired at a magnification of 20x. Scale bars set to 50 μm. The closed arrow denotes an AP; the open arrow denotes an NFT.
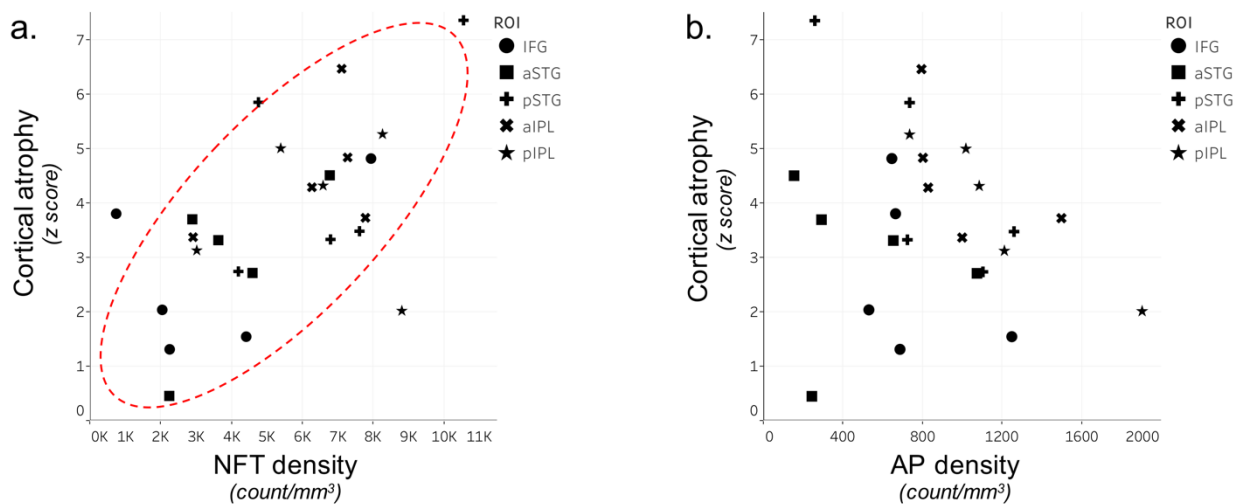
Figure 1.4 *In vivo* **cortical atrophy was related to NFTs, but not APs, in PPA-AD.**
a) Cortical atrophy showed a positive relationship with NFT densities within the left language regions ($p<0.01$).
b) Cortical atrophy was not related to AP densities in the regions examined.

DISCUSSION

Cortical atrophy might be an intermediate feature of disease progression, emerging after a substantial accumulation of neuropathology, but preceding or concurrent to prominent clinical deficits **(Jack *et al.*, 2010; Jack Jr *et al.*, 2013)**. NFTs appear to be the stronger correlate of cortical atrophy in DAT-AD **(Dallaire-Théroux *et al.*, 2017)**, but it is not clear if this relationship is present in non-amnestic presentations of AD. The current study sought to determine the relationships between *in vivo* cortical atrophy, AP densities, and NFT densities in PPA-AD. Based on a quantitative analysis of MRI scans relatively close to death and stereologic estimations of AD neuropathology lacking in previous studies of PPA-AD or DAT-AD, we found that NFTs, not APs, showed a distribution reflective of the asymmetric aphasic profile that was also significantly associated with cortical atrophy. We show for the first time that NFTs were commensurate with cortical atrophy inside and outside the language network of PPA-AD (**Fig. 1.4a**), which is consistent with the NFT and atrophy relationship measured by tau-PET (positron emission tomography) in individuals with PPA **(Ossenkoppele *et al.*, 2016; Xia *et al.*, 2017; Josephs *et al.*,**

2018; Nasrallah *et al.*, 2018b). Moreover, the asymmetry of only NFTs agrees with previous clinicopathologic relationships reported by our group and others which have shown that NFTs have an anatomical distribution that is mostly concordant with the atrophy and clinical symptoms characteristic of the PPA phenotype **(Gefen *et al.*, 2012; Josephs *et al.*, 2013)**.

While the clinical syndromes of DAT and PPA might share the same underlying AD neuropathology, the mechanisms involved and the sequence of events leading to atrophy and clinical impairment might differ. Given that regions with more neuropathology may represent earlier sites of disease manifestation and neurodegeneration, our findings in PPA-AD suggest that the distribution of NFTs violates the Braak staging of neurofibrillary accumulation typically observed in DAT-AD. More specifically, we quantitatively showed in PPA-AD that mean NFT densities were significantly greater in three neocortical language regions of the left temporoparietal junction compared to the entorhinal cortex **(Fig. 1.2a)**. Evidence for limbic-to-neocortical Braak staging of NFTs comes from cross-sectional postmortem examinations made in different clinical stages of DAT-AD. The earliest known sites of NFT formation in DAT-AD are in allocortical areas such as the entorhinal cortex **(Braak and Braak, 1991)**, basal forebrain **(Sassin *et al.*, 2000; Mesulam, 2004; Geula *et al.*, 2008)**, or brainstem nuclei **(Rub *et al.*, 2000; Parvizi *et al.*, 2001; Grudzien *et al.*, 2007; Grinberg *et al.*, 2009)**. In contrast, APs may follow a neocortical-to-limbic propagation in DAT-AD with an origin in the isocortex of frontal, parietal, or temporal lobes **(Arriagada *et al.*, 1992; Thal *et al.*, 2002)**.

There is emerging evidence that neocortical areas may be the earliest sites of neuropathology and neurodegeneration in non-amnestic variants of AD such as PPA-AD **(Phillips *et al.*, 2017)**. The preponderance of AD neuropathology to left language regions in our PPA-AD cohort supports the possibility of a neocortical pathogenesis, and is consistent with longitudinal studies showing that the language network exhibits the earliest and most severe atrophy in PPA

(Rogalski *et al.*, 2011a; Rogalski *et al.*, 2014). Therefore, it could be the case that neuropathology began in the most vulnerable language regions that define the PPA phenotype, compromising their integrity before propagating to neighboring regions based on patterns of connectivity and susceptibility **(Braak and Braak, 1996; Mesulam, 1999; de Calignon *et al.*, 2012; Liu *et al.*, 2012; Brettschneider *et al.*, 2015)**. This theoretical trans-synaptic spread across neocortical-to-limbic regions could explain the unique distribution of AD neuropathology and cortical atrophy we observed in our PPA-AD cohort, as well as the progression of impairments from language to non-language cognitive domains across successive stages of disease course. Longitudinal PET studies and postmortem examinations of individuals with PPA at earlier preclinical stages can help elucidate the neuropathologic origin and stereotypical propagation hypothesized in PPA.

Cortical atrophy differentiated language from non-language regions in the left hemisphere which was most consistent with the distribution of NFT densities. However, both NFT and AP densities were significantly greater in the left temporoparietal junction compared to the left EC. The concentration of both AD neuropathologic markers to these select language regions is not yet clear, but a synergistic interaction may have driven their prominence. For example, it has been hypothesized in DAT-AD **(Han and Shi, 2016)** that an Aß-Tau interactive model might better predict neuropathologic change and cognitive deficits compared to the serial amyloid-cascade model **(Hardy and Higgins, 1992)** or dual-pathway models **(Small and Duff, 2008)** put forth previously for typical AD. Our observations in PPA-AD suggest that the language network is distinctly vulnerable to structural and AD neuropathologic changes and may have been the site of a possible feedback loop promoting the greatest neurodegeneration. Still, it is important to note that in the present study in PPA-AD, NFT and AP densities were not related to each other in the language regions and NFT densities greatly outnumbered AP densities in all neocortical and entorhinal regions except the visual cortex. In fact, the NFT-to-AP ratio was almost two-fold

higher in the left language regions compared to their contralateral homologues. Thus, the dissimilar densities and distributions of NFTs and APs across the cortex may also reflect independent pathogenic mechanisms by which each pathology makes different contributions to neurodegenerative processes in PPA-AD.

While language regions displayed elevated densities of APs and more so NFTs, the relatively less vulnerable non-language regions in PPA-AD displayed unique patterns that were not observed in language regions. For example, V1 was the least atrophic and contained the smallest densities of NFTs, but its AP densities were comparable to AP densities in almost all language regions (**Fig. 1.2a**). In contrast, entorhinal cortex contained the smallest densities of APs, but NFT densities were comparable to NFT densities in the anterior language regions (i.e., IFG, aSTG; **Fig. 1.2a**). These observations indicate that V1 had a greater AP-to-NFT ratio while the entorhinal cortex had a greater NFT-to-AP ratio. The clinical significance of these opposing patterns in non-language regions remains unclear in our PPA-AD cohort. All PPA-AD participants had intact vision that permitted the completion of the neuropsychological battery and none reported visual impairments beyond the need for corrective lenses. In relation to entorhinal cortex integrity, some memory impairments eventually surfaced in a few PPA cases, but spatial navigation was not formally assessed after diagnosis. Nevertheless, all PPA-AD participants had primary deficits disproportionately greater in the language domain, which was concordant with NFT and atrophy severity.

Concomitant factors may have influenced the relationship between AD neuropathology and cortical atrophy. We have recently shown that the same PPA-AD cohort included in this study had significant microglial activation in the white matter that was associated with gray matter atrophy **(Ohm *et al.*, 2018)**. In addition to glial-mediated inflammation, upstream intermediates of NFTs and APs may have caused, at least in part, the neurodegenerative patterns. There is

evidence that soluble precursors of insoluble NFTs (tau oligomers) and APs (amyloid-ß oligomers) track disease progression **(Koss *et al.*, 2016)** and have neurotoxic, and potentially synergistic capacities that operate independent of their downstream counterparts (i.e., NFTs and APs) **(Bloom, 2014)**. Consistent with most observations made in DAT-AD **(Dallaire-Théroux *et al.*, 2017)**, the distributions of dense-core APs did not mirror the neurodegenerative processes in PPA-AD. Since it has been shown that APs do not parallel disease progression in DAT-AD **(Arriagada *et al.*, 1992),** one potential reason for this discordance could be that the accumulation or clearing of APs occur at rates dissimilar to the rate of atrophy in the time elapsed between the final MRI scan and death. Determining if and how these factors affect gray matter composition and structure should be pursued in future investigations.

The participants that met inclusion criteria for this study resulted in a small cohort that were only male. The investigation of a larger population with balanced sexes is warranted to ensure that the findings of the current study are replicable. However, the small number of PPA-AD participants permitted an extensive and quantitative analysis of postmortem tissue that could be systematically compared to MRI scans close to death. Genetic, developmental, or other acquired risk factors might confer region-specific vulnerabilities to disease in PPA **(Rogalski *et al.*, 2013)**. While the current PPA-AD cohort had no known genetic risk factors, 3 participants had a personal (cases 3 & 5) and/or family (cases 2, 3, & 5) history of learning disability. Additionally, 2 participants had a family history of either AD (case 5) or Parkinson's disease (case 1).

In summary, the current investigation demonstrated that AD neuropathology had a predilection for left language regions that incurred the most atrophy in PPA-AD. Only NFTs accumulated in accordance with both the hemispheric and language selectivity characteristic of PPA-AD and were significantly related to cortical atrophy in most cortical regions examined.

Since NFTs appear to be more closely associated with reductions in gray matter across the clinical spectrum of AD, it is likely that NFTs play a prominent role in the neuronal loss and/or shrinkage underlying cortical atrophy. Future studies are necessary to identify the cellular changes associated with cortical atrophy and AD neuropathology in PPA.

Prominent Microglial Activation in Cortical White Matter is Selectively Associated with Cortical Atrophy in PPA

ABSTRACT

Primary progressive aphasia (PPA) is a clinical syndrome characterized by selective language impairments associated with focal cortical atrophy favoring the language dominant hemisphere. PPA is associated with Alzheimer's disease (AD), frontotemporal lobar degeneration (FTLD), and significant accumulation of activated microglia. Activated microglia can initiate an inflammatory cascade that may contribute to neurodegeneration, but their quantitative distribution in cortical white matter and their relationship with cortical atrophy are unknown. We investigated white matter activated microglia and their association with gray matter atrophy in 10 PPA cases with either AD or FTLD-TDP pathology. Activated microglia were quantified with optical density measures of HLA-DR immunoreactivity in two regions with peak cortical atrophy, and one non-atrophied region within the language dominant hemisphere of each PPA case. Non-atrophied contralateral homologues of the language dominant regions were examined for hemispheric asymmetry. Qualitatively, greater densities of activated microglia were observed in cortical white matter when compared to gray matter. Quantitative analyses revealed significantly greater densities of activated microglia in the white matter of atrophied regions compared to non-atrophied regions in the language dominant hemisphere ($p<0.05$). Atrophied regions of the language dominant hemisphere also showed significantly more activated microglia compared to contralateral homologues ($p<0.05$). White matter activated microglia accumulate more in atrophied regions in the language dominant hemisphere of PPA. While microglial activation may

constitute a response to neurodegenerative processes in white matter, the resultant inflammatory processes may also exacerbate disease progression and contribute to cortical atrophy.

INTRODUCTION

Primary progressive aphasia (PPA) is a clinical dementia syndrome characterized by selective and gradual dissolution of language function, with preservation of other cognitive domains in the initial stages of disease progression **(Mesulam, 1982)**. Consistent with this clinical phenotype, brains of PPA patients display focal and asymmetric cortical atrophy **(Rogalski *et al.*, 2014)** in language regions of the language dominant hemisphere (typically left), as determined by structural magnetic resonance imaging (MRI) scans. Diverse neuropathologic changes occur in the gray matter of PPA brains, but the neuropathologic mechanisms of cortical atrophy remain poorly understood.

PPA is associated with Alzheimer's disease (AD) and frontotemporal lobar degeneration (FTLD). FTLD includes non-Alzheimer's tauopathies (FTLD-tau) and transactive response DNA-binding protein of 43-kD (TDP-43) proteinopathies (FTLD-TDP) **(Mesulam *et al.*, 2014b)**. Regardless of the underlying molecular pathology, there is extensive activation of microglia in PPA, which may serve as a potential inflammatory marker for pathology and disease severity that also plays a role in neurodegenerative processes **(Perry *et al.*, 2010)**. We have previously shown that activated microglia accumulate in gray matter of PPA brains **(Kim *et al.*, 2016)**, but their density and distribution in white matter, and their relationship to neurodegenerative processes such as cortical gray matter atrophy are unknown in PPA.

The precise roles of microglia in health and disease are still under investigation. Microglia are the resident macrophages of the brain that engage in immune surveillance to maintain homeostasis. They exist in a continuum of shapes and sizes, ranging from '*ramified*' microglia which tend to be small, thin, and highly branched, to '*activated*' microglia which appear larger

due to their hypertrophy and shorter, thicker processes **(Perry *et al.*, 2010)**. The morphologic heterogeneity of microglia is believed to reflect a spectrum of functions. While ramified microglia appear motile and survey the local environment for danger, activated microglia may serve roles in wound healing, host defense, and regulatory processes **(Mosser and Edwards, 2008)**. When activated, microglia undergo a change in morphology and an upregulation of cell-surface receptors and cytoplasmic proteins that can be readily targeted by immunohistochemical techniques to reveal their presence and distribution. In the activated state, microglia have the capacity to secrete harmful cytotoxic mediators including cytokines, reactive oxygen species, and other factors that stimulate inflammatory processes linked to neuronal damage **(McGeer and McGeer, 2001)**. Activated microglia also appear in close proximity to pathologic insults such as amyloid-β plaques and neurofibrillary tangles in AD **(McGeer *et al.*, 1987; Styren *et al.*, 1990; Serrano-Pozo *et al.*, 2011b)**, demyelinating pathology in multiple sclerosis **(Singh *et al.*, 2013)**, Pick bodies in frontotemporal dementia (FTD) patients with underlying FTLD-tau **(Schofield *et al.*, 2003; Lant *et al.*, 2014)**, and TDP-43 inclusions in FTD and PPA patients with underlying FTLD-TDP **(Lant *et al.*, 2014; Kim *et al.*, 2016)**. Together, inflammatory processes and co-localization with pathologic proteins have implicated activated microglia in disease pathogenesis.

The experimental study of microglial activation in white matter has been sparse in diseases such as AD and FTLD. One report showed that activated microglia increased linearly with age in the white matter of the superior frontal gyrus, with no obvious difference between AD patients and non-AD elderly controls **(Rogers *et al.*, 1988)**. Similar observations were reported in the white matter of hippocampus and superior frontal gyrus, with comparable patterns of activated microglia between AD patients and non-demented elderly controls **(Styren *et al.*, 1990)**. Other studies have reported high densities of activated microglia in the white matter of the hippocampus **(McGeer *et al.*, 1987)** and entorhinal cortex in AD brains **(Xiang *et al.*, 2006; Bachstetter *et al.*, 2015)**, and

prominent microglial activation in white matter when compared to gray matter in the frontal cortex and superior temporal gyrus in FTLD-tau and FTLD-TDP brains **(Schofield *et al.*, 2003)**. These findings suggest that microglial activation corresponds to pathologic changes in gray and white matter across disease phenotypes. However, the limited number of regions examined, and the relatively qualitative nature of these studies, make it difficult to determine the extent of activated microglia in human white matter and its potential regional selectivity.

The purpose of this study was to characterize the regional distribution and hemispheric asymmetry of activated microglia in cortical white matter of the brains of PPA patients with AD or TDP-43 pathology, and to determine their relationship with regional cortical gray matter atrophy. As a marker for neuroinflammation and possibly a correlate of neurodegeneration, we hypothesized that activated microglia accumulate more in white matter of cortical regions with prominent gray matter atrophy.

METHODS

Participants

Ten recent PPA cases with AD or FTLD-TDP pathology and available structural MRI scans were included in the study. Eight out of 10 PPA cases were enrolled through the PPA Research Program at the Cognitive Neurology and Alzheimer's Disease Center at Northwestern University Feinberg School of Medicine. Two PPA cases (#6 and #7) were not enrolled in the PPA Research Program, but were clinically evaluated at our Center. The diagnosis of PPA was based on at least a two year history of progressive, isolated impairments of speech or language functions; clinical subtypes (logopenic, agrammatic, and semantic) were classified based on previously described diagnostic guidelines **(Mesulam, 1982; Mesulam, 2001; Gorno-Tempini *et al.*, 2011)**. Case characteristics are included in **Table 2.1**.

Assessments of cortical atrophy and regions of interest

The location and extent of cortical atrophy were determined by postmortem assessments and corroborated with *in vivo* structural MRI data (**Fig. 2.1**). Photographs of intact, postmortem brains were collected from each PPA case and visually inspected to determine regions of principal atrophy and areas with undetectable atrophy. Six regions were selected and subsequently examined in each PPA case, three per hemisphere (**Table 2.2**). The three regions within the language dominant hemisphere included two regions with peak cortical atrophy, and one non-atrophied region. Non-atrophied contralateral homologues of each region were assessed to determine if activated microglia displayed asymmetric densities between hemispheres.

Structural MRI data were acquired on a 3T scanner from 35 previously described (**Rogalski et al., 2014**) healthy controls and 8/10 PPA participants. The remaining two PPA cases had clinical MRI scans acquired on a 1.5T scanner. FreeSurfer software (v5.1.0, http://surfer.nmr.mgh.harvard.edu) was used to analyze the 3T structural MRI in 7/10 PPA cases (#1-5, 9, 10). FreeSurfer generated cortical surface heat maps (false discovery rate correction set to 0.05 (**Genovese et al., 2002**) on the native space for each PPA case to detect areas of peak cortical thinning (i.e., gray matter cortical atrophy) in comparison to the control group. The cortical surface heat maps were visually inspected to validate the regions of peak cortical atrophy (areas in yellow, **Fig. 2.1**) identified from postmortem assessments. Movement artifacts precluded a reliable FreeSurfer analysis of structural MRI collected from case #8, prompting a visual inspection of atrophy from coronal MRI slices. Similarly, clinical MRI scans were visually inspected to corroborate postmortem identification of atrophy for PPA case #6 and 7. The mean interval between MRI and death was 2.77 ± 1.5 years; range 0.6-6 years (**Table 2.1**).

Table 2.1 Characteristics of PPA-AD and PPA-TDP participants.

PPA Case #	Pathologic Diagnosis	Clinical Subtype	Sex	Handedness	Education (Y)	Age at Death (Y)	Symptom Duration (Y)	Scan/ Death Interval (Y)	Post-mortem Interval (H)	Fixative
1	AD	L	Male	Right	16	61	4.7	0.6	6	F
2	AD	U	Male	Right	12	63	7.9	2.1	14	F
3	AD	L	Male	Right	15	75	8.6	2.0	8	P
4	AD	U	Male	Right	14	61	9.4	2.5	19	P
5	AD	G	Male	Right	18	78	6.2	2.5	28	P
6	TDP, Type B	L→G	Male	Right	13-15	59	2	1.7	12	F
7	TDP, Type A	L	Male	Left	18	65	8	6	6	F
8	TDP, Type B	Gsp	Male	Right	18	55	4.4	2.6	29	F
9	TDP, Type A	Gsp	Male	Right	16	70	4.6	3.1	4	F
10	TDP, Type A	M	Female	Right	11	74	6.7	4.6	10	F

AD = Alzheimer's disease; TDP = transactive DNA-binding protein; L = logopenic; G = agrammatic; Gsp = agrammatic with motor speech deficits; M = mix of agrammatic and semantic deficits; U = unclassifiable due to severity of impairments; Y = years; H = hours; P = paraformaldehyde; F = formalin.
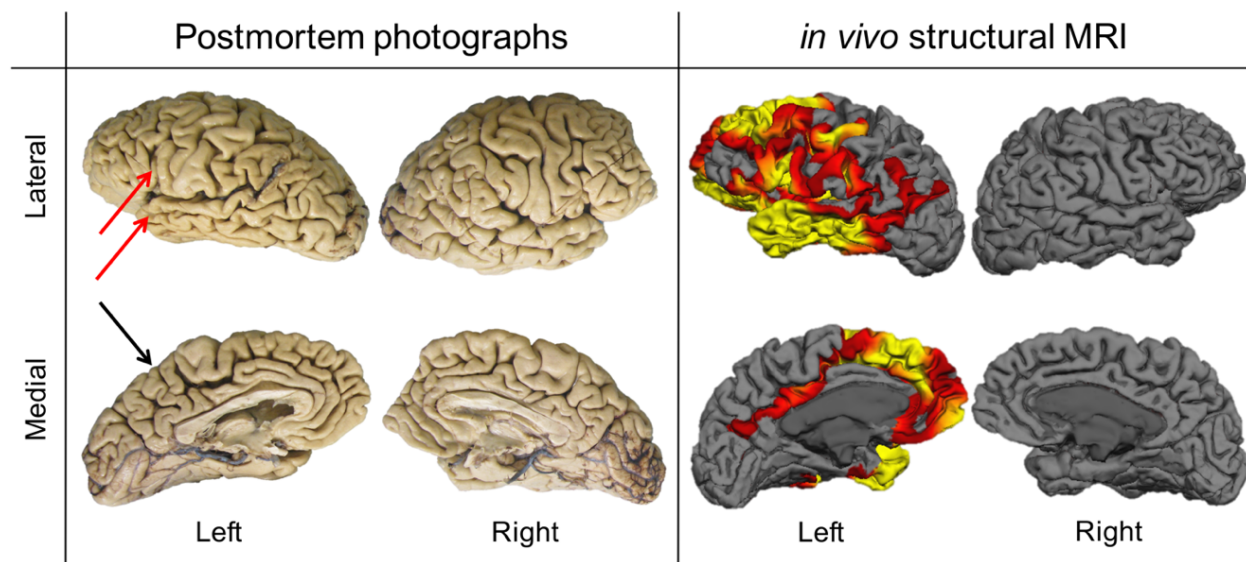
Figure 2.1 Cortical atrophy is focal and asymmetric in PPA.

The location and extent of cortical atrophy were determined by postmortem assessments and corroborated with *in vivo* structural MRI data acquired close to death. Gross pictures of the postmortem brain and MRI are shown from PPA-TDP case #10 as an example. Regions of interest were selected based on areas with peak cortical atrophy (red arrows; IFG and aSTG) and areas with undetectable cortical atrophy (black arrow; PrC). Red and yellow (yellow > red) represent significant cortical thinning (i.e., atrophy).

Table 2.2 Bilateral regions assessed per PPA case.

PPA neuropathologic subtype	AD					TDP				
PPA case #	1	2	3	4[a]	5	6	7	8	9	10
Non-atrophied regions	V1	V1	V1	--	V1	aIPL	pIPL	aIPL	aIPL	PrC
Atrophied regions	aIPL	IFG	pSTG	--	aSTG	IFG	IFG	IFG	IFG	IFG
	pIPL	aSTG	aIPL	--	pSTG	aMTG	aSTG	aSTG	aMTG	aSTG

Primary visual cortex (V1); inferior frontal gyrus (IFG); anterior inferior parietal lobule (aIPL); posterior inferior parietal lobule (pIPL); anterior superior temporal gyrus (aSTG); posterior superior temporal gyrus (pSTG); anterior middle temporal gyrus (aMTG); precuneus (PrC)

[a]PPA-AD case #4 was excluded from quantitative analyses due to lack of consensus between postmortem and MRI assessments of peak cortical atrophy (see Results).

Tissue processing

Brains were fixed in either 10% formalin (F) or 4% paraformaldehyde (P) for 30-36 hours at 4°C, and then submerged into increasing gradients of sucrose (10-40%) for cryoprotection (**Table 2.1**). A 1-in-24 series of 40 μm-thick coronal sections was collected from each region (six sections per region). Tissue was processed immunohistochemically without antigen retrieval using the avidin-biotin peroxidase complex method employing the Vectastain Elite Kit and 3,3'-diaminobenzidine as the chromogen. Activated microglia were visualized immunohistochemically using an antibody against the human leukocyte antigen-D related (HLA-DR) protein (mouse monoclonal; Dako; 1/1000) (**Fig. 2.2, Fig. 2.3a**) and an antibody against CD68 (mouse monoclonal; Dako; 1/500) (**Fig. 2.3b**). HLA-DR is a cell surface glycoprotein present in microglia in class II of the major histocompatibility complex that mediates the presentation of foreign antigens in normal and diseased brains (**De Tribolet *et al.*, 1984; McGeer *et al.*, 1988; Gehrmann *et al.*, 1993**). CD68 is a macrophage-specific lysosomal-associated protein that labels microglia in resting and activated states (**da Silva and Gordon, 1999; Lant *et al.*, 2014; Bachstetter *et al.*, 2015; Taipa *et al.*, 2017a**).

For anatomic specification in each case, a series of sections was processed with the cresyl violet Nissl stain or immunohistochemically for neuronal nuclear protein (NeuN, mouse monoclonal; EMD Millipore; 1/2000).

Assessments of activated microglia

HLA-DR-immunoreactive microglia were assessed qualitatively and measured quantitatively in each PPA case. The current study restricted quantitative analyses to HLA-DR staining, but CD68-immunoreactive microglia were also assessed qualitatively in a subset of PPA-AD and PPA-TDP cases to determine if another, less specific marker of activated microglia displayed similar patterns to HLA-DR staining. The qualitative assessment encompassed regions

of interest and neighboring areas (gray matter and white matter) to document the full extent and distribution of activated microglia. The quantitative measurement included quantification of HLA-DR-immunoreactive microglia in the cortical white matter toward the gyral crown of each region using photomicrographs acquired at 4x magnification. The cortical white matter was sampled once in every gyrus that comprised a region (1-4 photomicrographs per coronal section; 6-19 photomicrographs per region) to ensure that a representative sampling of the anatomy was acquired for analyses. The number of gyri in each region varied based on anatomical location regardless of degree of atrophy. For example, frontal and parietal regions typically had more than one gyrus compared to temporal regions which typically had one gyrus. Therefore, more photomicrographs were acquired in regions with more gyri, while still maintaining a similar mean number of photomicrographs sampled per region, regardless of whether it was an atrophied (10 ± 4.7 photomicrographs) or a non-atrophied (9 ± 3.9 photomicrographs) region. Irrespective of region, photomicrographs rarely contained gray matter, but when they did contain a small area of gray matter, the image was cropped to ensure that the quantification of activated microglia was limited to the white matter only. Photomicrographs containing only white matter were imported into ImageJ software (version 1.51) to measure the optical density (OD) of HLA-DR immunoreactivity. OD was calculated using the following formula:

$$OD = \log (\text{maximum light intensity/mean light intensity})$$

where maximum intensity is 255 for 8-bit images. OD was averaged across photomicrographs and used as a single data point in each region. The OD values acquired from the two atrophied regions were averaged to obtain one OD value used in analyses. Images displaying greater concentration and/or size of HLA-DR-immunoreactive microglia equated to lower light transmission, resulting in higher OD values.

The acquisition and subsequent postprocessing of photomicrographs were conducted by

two independent investigators (D.T.O. and G.K., respectively). Photomicrographs were collected systematically from an investigator with strong anatomical knowledge (D.T.O.) to ensure sampling was drawn from appropriate anatomical locations consistently and accurately before the images were cropped and analyzed by a second investigator (G.K.) blinded to the atrophy patterns specific to that region or PPA case.

Statistical analyses

Each PPA participant with available quantitative MRI close to death was statistically compared to a control group of 35 healthy participants using spherical surface maps of the whole brain. A general linear model on every vertex along the cortical surface was used to calculate the significant differences in cortical thickness between groups.

Mean optical densities of activated microglia passed normality for all groups compared. Paired t-tests were used to determine differences in mean optical densities of activated microglia between atrophied and non-atrophied regions within the language dominant hemisphere. To assess asymmetry, paired t-tests determined the difference in mean optical density between hemispheres within atrophied and non-atrophied regions. Two-tailed Pearson correlation determined the relationship between age and mean optical densities of activated microglia. Significance was set to $p<0.05$ for all comparisons. All statistical analyses of optical densities were performed using GraphPad Prism (version 7.0 for Mac, GraphPad Software, La Jolla California USA, www.graphpad.com).

RESULTS

Clinical and neuropathologic findings

Ten PPA cases were confirmed to have either AD pathology (PPA-AD; n=5) or FTLD-TDP pathology (PPA-TDP; n=5) at death based on published consensus criteria **(Cairns et al., 2007; Mackenzie et al., 2011; Hyman et al., 2012; Montine et al., 2012)**. Each PPA-AD case

was diagnosed with "high" AD neuropathologic change. Two PPA-TDP cases (#6 and 8) had FTLD-TDP type B pathology, and three PPA-TDP cases (#7, 9, and 10) had FTLD-TDP type A pathology. While additional pathologic features (e.g., cerebrovascular disease, arteriosclerosis) were present in most cases, they were minor and secondary to the primary pathologic diagnoses (i.e., AD and FTLD-TDP). Myelin rarefaction of the subcortical white matter varied in severity (i.e., mild to moderate) and was asymmetric in select PPA cases.

Of the five PPA-AD participants, two were clinically diagnosed with the logopenic variant (PPA-L), one with the agrammatic variant (PPA-G), and two were unclassifiable (PPA-U) due to the severity of their condition at the time of examination (see **Table 2.1**). In the PPA-TDP cohort, two were agrammatic with a speech disorder (PPA-Gsp), one had a mixture of agrammatism and comprehension deficits (PPA-M), one was logopenic, and one was logopenic before progressing to agrammatic (L→G; see **Table 2.1**). The 35 healthy participants did not differ in education or age compared to the PPA participants with available quantitative MRI. The PPA-AD and PPA-TDP groups did not differ in sex, education, age at death, disease duration, or postmortem interval (PMI). While 9/10 PPA participants were right-handed with likely left hemisphere language dominance, PPA-TDP case #7, which was previously described **(Mesulam *et al.*, 2005)**, was left-handed and displayed right hemisphere language dominance based on a language task that produced fMRI activations in right perisylvian cortical regions.

Gray matter cortical atrophy

Each PPA case was evaluated individually to determine areas of greatest atrophy and undetectable atrophy. General patterns of cortical atrophy were observed: PPA-AD typically displayed the greatest atrophy in lateral temporal and parietal lobes, while PPA-TDP showed the most atrophy in the frontal and lateral anterior temporal lobes.

Peak atrophy sites varied by individual and by pathologic diagnosis but were most

consistently found in language regions of the language dominant hemisphere (**Fig. 2.1**). The language dominant hemisphere contained the atrophied regions in all PPA cases, and the non-atrophied region included primary visual cortex in PPA-AD and areas of the parietal lobe in PPA-TDP (**Table 2.2**). The contralateral homologues to all regions examined in the language dominant hemisphere had undetectable cortical atrophy (non-atrophied). Postmortem assessments of PPA case #4 revealed symmetric and mild cortical atrophy throughout the cerebrum, and asymmetric atrophy in the temporal lobe (pSTG) where it was moderate on the left and mild on the right. However, the MRI cortical thinning map for case #4 could not confirm this pattern of atrophy as it revealed no significant cortical thinning bilaterally.

Qualitative patterns of activated microglia in cortical white matter versus gray matter

HLA-DR staining was consistently present in white and gray matter of all PPA cases, but the intensity of staining in white matter varied greatly between regions and within brain sections (**Fig. 2.2**). Qualitative observations of the postmortem tissue revealed HLA-DR staining dark enough for the naked eye to readily discern the gray/white matter junction and regional asymmetries. Relative to the gray matter, the white matter tended to have a more homogeneous distribution of activated microglia, but topographic patterns were observed in relation to the gyral crown and fundus. Staining was often more prominent toward the gyral crown and in the short association U-fibers found in the white matter directly adjacent to the gray matter (**Fig. 2.2, red insets**). High power magnification of the more prominent staining reflected a greater density of activated microglia, larger hypertrophic microglia, and often a combination of the two (**Fig. 2.2, black insets**). The higher densities of activated microglia were occasionally due to round clusters of larger, overlapping hypertrophic microglia that ranged in diameter between 30-100 µm (**Fig. 2.3**). Activated microglia typically displayed the hypertrophic morphology in the white matter, while the gray matter showed a greater spectrum of morphologies that were distributed unevenly

across the cortical layers (**Fig. 2.2**). Microglia of the ramified type were virtually absent in the white matter in all regions examined. When large clusters of activated microglia were present, they were observed more often in the U-fiber tracts (**Fig. 2.2, red insets**). In direct contrast to the atrophied regions in the language dominant hemisphere, non-atrophied regions displayed sparse and lightly stained activated microglia in the white matter bilaterally such that the boundary between white and gray matter could only be determined at high magnification.

CD68 staining largely reflected the HLA-DR staining patterns observed in the gray matter and white matter across PPA-AD and PPA-TDP. Qualitative comparisons clearly demonstrated greater densities of CD68-immunoreactive microglia in the white matter of atrophied regions in the language dominant hemisphere when compared to non-atrophied regions (**Fig. 2.3b**). Additionally, CD68-immunoreactive microglia showed asymmetry such that regions contralateral to the language dominant hemisphere displayed less staining. In contrast to HLA-DR staining, however, CD68-immunoreactive microglia had less robust staining that was mostly restricted to the somas and relatively absent in the dendritic processes. CD68-immunoreactive microglia were less dense throughout all regions of interest in comparison to HLA-DR staining. Nevertheless, the overall staining patterns for CD68 were strikingly similar to HLA-DR and consistent with our hypothesis that more activated microglia in white matter are associated with regions of greater atrophy.

Neuropathologic subtypes of PPA displayed notable differences in HLA-DR staining. Staining was often more prominent in the white matter of PPA-TDP compared to PPA-AD (**Fig. 2.2**). While PPA-TDP displayed more activated microglia in anterior regions of the frontal and temporal white matter, PPA-AD showed more activated microglia in posterior regions of the temporal and parietal white matter. Despite less intense staining of the white matter in PPA-AD, the delineation between white and gray matter was accentuated by a relative absence of staining
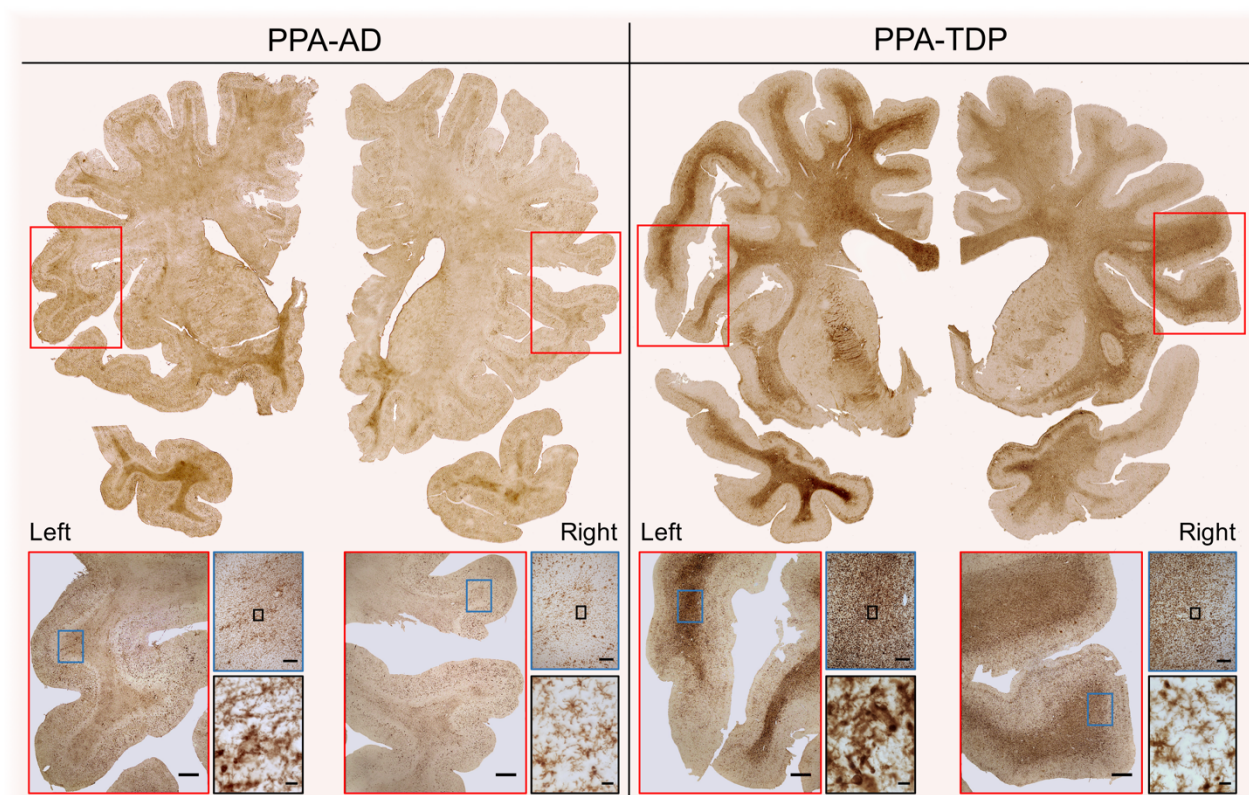
Figure 2.2 Activated microglia accumulate with regional and hemispheric selectivity in PPA.
Representative HLA-DR staining in bilateral whole-hemisphere sections from PPA-AD case #3 and PPA-TDP case #8, including photomicrographs taken at 0.5x (red), 4x (blue), and 60x (black) magnifications. Across PPA neuropathologic subtypes, HLA-DR staining often appeared greater in white matter compared to gray matter, and high magnification revealed that the intensity of the staining was due to larger, denser populations of activated microglia. Scale bars = 2mm, 200μm, 20μm for 0.5x, 4x, 60x magnifications, respectively.

in cortical layer VI across all brain regions in PPA-AD (**Fig. 2.2, PPA-AD—red insets**). High magnification of layer VI revealed that the reduced staining was due to several factors including a lower density of activated microglia, relatively lighter stained activated microglia, little to no clusters of activated microglia, and a greater proportion of ramified microglia (**Fig. 2.2; PPA-AD—blue insets**). In contrast, brain regions in PPA-TDP displayed more homogeneous staining across the cortical layers (**Fig. 2.2, PPA-TDP—red insets**). The densities of activated microglia were also more homogenous in the cortical white matter in PPA-TDP, but many regions displayed

darker staining in the short association U-fibers of white matter due to clusters and/or larger, more densely packed activated microglia.

The PPA-TDP subgroup was comprised of FTLD-TDP Type A (n=3) and Type B (n=2) pathologic diagnoses (**Table 2.1**) that appeared to reflect small differences in activated microglia densities. While visual inspection of the patterns of HLA-DR-immunoreactivity showed a similar range in intensity within the small cohort, Type B cases tended to have a 1.3—2.3x greater mean optical density of activated microglia compared to Type A cases across the regions examined. Despite these differences, asymmetric densities of activated microglia were consistently found in the atrophied regions regardless of FTLD-TDP type.

Quantification of HLA-DR staining in cortical white matter regions

Analysis within the language dominant hemisphere

The densities of activated microglia were examined in the greatest atrophied regions within the language dominant hemisphere and compared to a non-atrophied region within the same language dominant hemisphere. Analyses of activated microglia were carried out in 9 PPA cases; PPA case #4 was excluded due to the relative absence of detectable cortical atrophy and lack of corroboration between postmortem and MRI assessments.

Within the language dominant hemisphere of all PPA cases combined, the mean optical density of activated microglia was greater in atrophied regions compared to non-atrophied regions ($p<0.05$; **Fig. 2.4**). An analysis of each PPA neuropathologic subtype revealed a non-significant trend for a greater mean optical density of activated microglia in the atrophied regions compared to the non-atrophied regions in PPA-AD ($p=0.075$). The difference between atrophied and non-atrophied regions was not statistically different in PPA-TDP ($p=0.113$). Despite these results, individual differences were notable. In one case (PPA-TDP case #7), the mean optical density of activated microglia was 5.5x greater in the language dominant atrophied region compared to the

non-atrophied region. On average, the mean optical densities in the atrophied regions were almost 3x greater than that in the non-atrophied regions of 7/9 PPA cases (three PPA-AD; four PPA-TDP). The remaining 2/9 PPA cases (PPA-AD case #1; PPA-TDP case #6) displayed similar optical densities in the atrophied and non-atrophied regions of the language dominant hemisphere.

Analysis of asymmetry

The contralateral homologues of the atrophied and non-atrophied regions in the language dominant hemisphere were also examined in this study to establish whether activated microglia accumulate asymmetrically. An asymmetric distribution of activated microglia was only anticipated in the language dominant atrophied regions given the asymmetric cortical atrophy and the prominent language deficits characteristic of PPA.
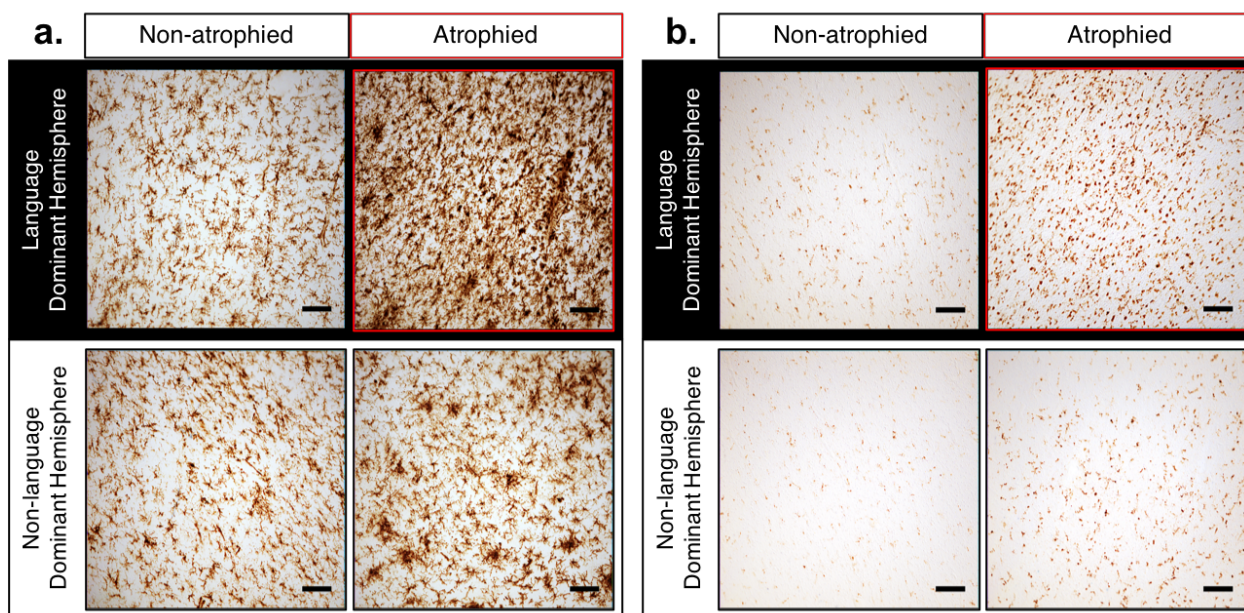
Figure 2.3 Activated microglia display more prominent staining in atrophied regions that often favor the language dominant hemisphere in PPA.

3a) Photomicrographs of representative HLA-DR staining in an atrophied region (pSTG) and a non-atrophied region (V1) within the language dominant hemisphere, along with their non-atrophied contralateral homologues from PPA-AD case #3. **3b)** Photomicrographs of representative CD68 staining in an atrophied region (IFG) and a non-atrophied region (aIPL) within the language dominant hemisphere, along with their non-atrophied contralateral homologues from PPA-TDP case #8. Atrophied regions have a red border; non-atrophied regions have a black border. Photomicrographs acquired at 10x magnification. Scale bars = 100μm

When PPA cases were combined, atrophied regions in the language dominant hemisphere showed a significantly greater mean optical density of activated microglia than their contralateral counterparts ($p<0.05$; **Fig. 2.4**). A non-significant trend for greater mean optical density in the language dominant atrophied regions was observed in PPA-AD ($p=0.082$) and PPA-TDP ($p=0.088$). As expected, non-atrophied regions of all PPA cases combined did not display asymmetric differences in mean optical densities ($p=0.307$; **Fig. 2.4**). This pattern was preserved when examining the PPA-AD ($p=0.574$) and PPA-TDP cohorts ($p=0.226$) separately. In addition, optical densities of activated microglia did not correlate with variables such as age or PMI.
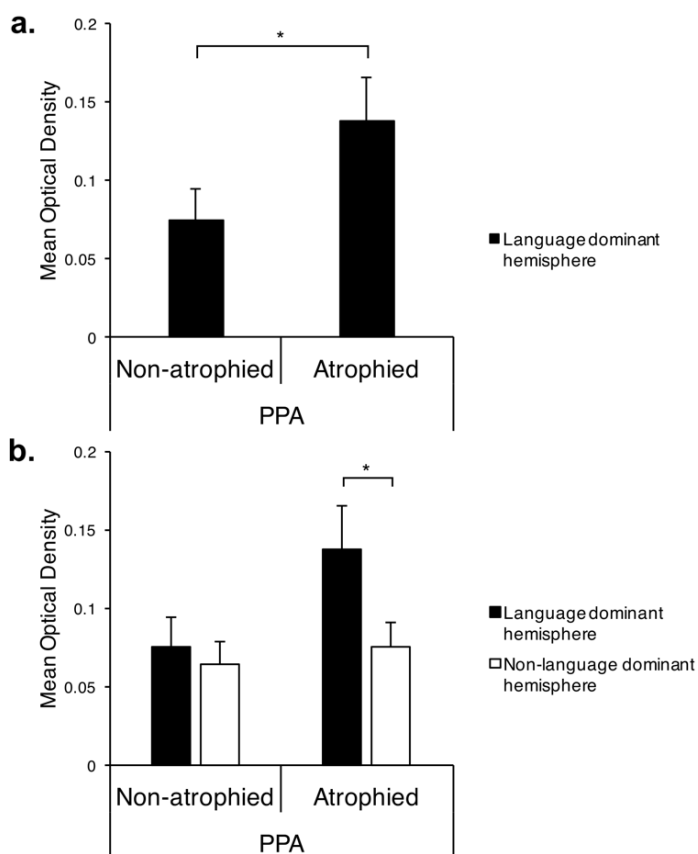
Figure 2.4 Activated microglia show a predilection for atrophied regions and the language dominant hemisphere in PPA.

4a) A *t*-test showed that the mean optical density of activated microglia is greater in atrophied regions compared to non-atrophied regions within the language dominant hemisphere of all PPA cases combined. *$p<0.05$

4b) In the assessment of hemispheric asymmetry, a *t*-test indicated that atrophied regions in the language dominant hemisphere have a greater mean optical density of activated microglia than their contralateral homologues. *$p<0.05$

DISCUSSION

The present study investigated the density and distribution of activated microglia in the white matter of PPA participants, and their relationship to gray matter cortical atrophy. Consistent

with our hypothesis, there were more white matter activated microglia in atrophied regions than non-atrophied regions within the language dominant hemisphere. Activated microglia were also more pronounced in atrophied regions of the language dominant hemisphere in comparison to the contralateral hemisphere. Little is known about the distribution and magnitude of white matter microglial activation in neurodegenerative diseases such as AD or FTLD. Our findings suggest that white matter activated microglia accumulate with regional and hemispheric selectivity, which corresponds to patterns of gray matter neurodegeneration in PPA with AD or FTLD pathology.

The predilection of HLA-DR-immunoreactive microglia to regions of peak cortical atrophy suggests that activated microglia could be contributing to neurodegenerative processes by possibly secreting cytotoxic molecules that can exacerbate the inflammatory response. At the same time, it is well known that activated microglia can also provide protective benefits. The diverse roles of activated microglia make it difficult to tease apart the functional consequences of the prominent microglial activation observed in the current study, and this topic warrants further exploration. Nevertheless, our findings indicate that white matter activated microglia have a close relationship with gray matter neurodegeneration not previously reported.

Age, fixation, PMI, and clinical factors such as pre-agonal conditions could influence the HLA-DR-immunoreactivity of microglia present in the white matter **(Mattiace *et al.*, 1990)** . In our well-characterized cohort of PPA cases, we did not find any link between HLA-DR antigenicity and these potential confounding variables. HLA-DR-immunoreactivity produced a range of staining intensity that did not vary systematically across the PPA cases examined. More specifically, cases with PMI >6 hrs (n=6) presented HLA-DR staining comparable to the cases with PMI <6 hrs (n=3), leading to the conclusion that the PMI did not influence the HLA-DR antigenicity in our cohort. In addition, the type of fixative did not noticeably impact the HLA-DR-immunoreactivity since the PPA cases with paraformaldehyde fixation (n=2) showed a range

of HLA-DR staining intensity that paralleled the staining intensities found in the PPA cases with formalin fixation (n=7). Neither age nor PMI correlated with optical densities of activated microglia. However, given that microglial activation may scale with age **(Rogers *et al.*, 1988)**, it is possible that age-related factors could have contributed, at least in part, to the activated microglia observed in non-atrophied regions. The only factors we found that influenced the pattern of HLA-DR-immunoreactivity in our cohort are reported as the main findings in this study—gray matter cortical atrophy and underlying neuropathology.

The white matter tended to have a greater accumulation of activated microglia in PPA-TDP in comparison to PPA-AD. A recent report on CD68-positive activated microglia in patients with FTLD-TDP compared to typical AD and controls showed that the frontal white matter was the only cortical region that differentiated the two pathologic groups, with greater microglial scores in FTLD than AD **(Taipa *et al.*, 2017a)**. Similarly, findings from a study of patients with underlying FTLD or AD pathology reported that there was greater microglial activation in the frontal white matter of FTLD brains compared to AD brains, while temporal gray matter showed more microglial activation in AD than FTLD **(Lant *et al.*, 2014)**. Our qualitative assessment also found anatomic selectivity in the accumulation of activated microglia. More specifically, the frontal white matter showed greater microglial activation in PPA-TDP than PPA-AD, and the parietal white matter tended to display greater microglial activation in PPA-AD than PPA-TDP.

It is not currently known what could be contributing to the prominent microglial activation in the white matter of patients with PPA. Even though AD and TDP-43 pathology mostly accumulate in the gray matter, TDP-43-positive inclusions have been found in white matter glia **(Armstrong, 2017)** and may specifically deposit in oligodendrocytes of patients with FTD **(Neumann *et al.*, 2007)**. All five PPA-TDP cases examined in this study displayed sparse TDP inclusions in the white matter of the brain regions examined. In addition, 4/5 PPA-TDP cases had

mild to moderate myelin rarefaction of the white matter that was occasionally more severe in regions where more atrophy was detected in the language dominant hemisphere. Although the present PPA-TDP cohort did not have progranulin gene (*GRN*) mutations, it has been shown that the haploinsufficiency caused by *GRN* mutations results in significantly elevated serum levels of the proinflammatory cytokine interleukin 6 compared to patients without the *GRN* mutation (**Bossù *et al.*, 2011**). In addition, the progranulin (PGRN) protein associated with *GRN* mutations is known to be involved in immunity and has anti-inflammatory properties such that when there is a PGRN deficiency, neuroinflammation is enhanced through microglial activation (**Martens *et al.*, 2012**). A higher rate of autoimmunity has been linked to greater neuroinflammation in FTD, semantic variant PPA, and *GRN* mutation carriers (**Miller *et al.*, 2013; Miller *et al.*, 2016; Lall and Baloh, 2017**) , but this association is not well understood in PPA patients with underlying FTLD-TDP or AD pathology.

Despite a close link with neuroinflammation (**McGeer and McGeer, 2001; Block and Hong, 2005; Perry *et al.*, 2010; Serrano-Pozo *et al.*, 2011b**), AD pathology does not accumulate in the white matter of PPA-AD where the activated microglia are densest. However, soluble amyloid-beta has been shown to accumulate in greater concentrations in the white matter versus gray matter in clinically typical AD (**Collins-Praino *et al.*, 2014**) . Furthermore, postmortem examinations of amnestic AD patients have revealed multiple forms of white matter change, including reductions in axons (**Englund and Brun, 1990**) and myelin (**Sjöbeck *et al.*, 2005**), and increases in glial levels that scale with white matter disease (**Sjöbeck and Englund, 2003**). Similar to the PPA-TDP cases, most of the PPA-AD cases included in this study had mild to moderate myelin rarefaction of the subcortical white matter. It is also important to note that in PPA, language network connectivity has been shown to be compromised in early stages of the syndrome before significant cortical atrophy, implying reductions in synaptic activity or axonal

degeneration could be early root causes of language impairments **(Bonakdarpour *et al.*, 2017)**. Additional studies that measure the changes in myelin, axons, and other glial populations will help determine the potential causes of microglial activation in the white matter, and how the microglial response is related to the gray matter atrophy observed in PPA.

Recent advances in *in vivo* neuroimaging techniques have contributed to new insights into white matter degeneration in PPA. For example, proton magnetic resonance spectroscopy has demonstrated that abnormalities occur in the arcuate fasciculus in PPA **(Catani *et al.*, 2003)**. Diffusion tensor imaging (DTI) studies have linked white matter changes to language impairments specific to the clinical subtypes of PPA **(Powers *et al.*, 2013; D'Anna *et al.*, 2016)**. However, the extent to which gray and white matter degeneration occur in parallel or sequentially is not yet known in PPA. Importantly, longitudinal MRI studies have shown that white matter atrophy can be severe in PPA **(Brambati *et al.*, 2015)**, and white matter changes can progress more rapidly than gray matter atrophy in as little as one year **(Lam *et al.*, 2014)**. Other DTI investigations have reported that white matter abnormalities in PPA can be more extensive than the changes in gray matter **(Agosta *et al.*, 2013; Mahoney *et al.*, 2013)**. In addition, several DTI studies have indicated that patients with typical AD or PPA display reductions in white matter structural integrity that precede or are independent of gray matter cortical atrophy and clinical symptoms **(Stricker *et al.*, 2009; Migliaccio *et al.*, 2012; Sachdev *et al.*, 2013; Frings *et al.*, 2014)**. Discordant degeneration between white and gray matter has also been shown in a study of typical amnestic AD patients where gray and white matter changes did not always overlap anatomically **(Caso *et al.*, 2015)**. It remains to be determined if factors such as neuroinflammation or prion-like propagation contribute to these patterns of degeneration. Interestingly, the PPA case excluded from our study due to undetectable atrophy still had prominent white matter activated microglia that unexpectedly appeared greater in regions of the non-language dominant hemisphere. Future longitudinal studies

coupled with positron emission tomography ligands specific to neuroinflammatory markers will be critical for uncovering the relationships between atrophy, inflammation, and pathology in the gray and white matter.

While the PPA profile might suggest that all language regions would be the most atrophied regions associated with the greatest densities of activated microglia, this was not the case. For example, some language regions such as the IPL in PPA-TDP cases were often not atrophied and harbored very low densities of activated microglia. These patterns of staining and atrophy are noteworthy because they provide evidence that activated microglia do not necessarily have a predilection to all language regions. Instead, they suggest that activated microglia are more closely related to cortical atrophy as we originally hypothesized, which in PPA is usually concentrated to the language network, but not necessarily all language regions. It is also a reminder that the determinants of selective vulnerability in neurodegenerative diseases remain mostly unknown. Elucidating these factors will be important for identifying therapeutic targets for neurodegenerative diseases.

The abnormal proteinopathies of AD (amyloid-beta [plaques] and tau [neurofibrillary tangles]) and FTLD-TDP (truncated and translocated TDP-43) are associated with focal neurodegenerative changes in specific clinical syndromes such as amnestic AD, FTD, and PPA. Except for neurofibrillary tangles, the relationship between the proteinopathy and neurodegeneration (i.e., regional atrophy) is poorly understood. We showed that microglial activation was more prominent in the white matter, although the burden of abnormal disease-specific markers in both AD and FTLD-TDP is more prominent in the gray matter. There was also regional selectivity that mirrored the anatomy of atrophy and the corresponding clinical syndrome. For example, activated microglia accumulated more in regions of greater cortical atrophy and were more numerous in the language dominant hemisphere in PPA. Given this

correspondence between white matter activated microglia and cortical atrophy, this study raises the intriguing possibility that microglia-initiated inflammatory processes may influence the distribution of neurodegeneration. Microglial activation could also constitute a response to the neurodegeneration, but could further exacerbate the disease process through local inflammatory reactions.

<div align="center">

—STUDY 3—

Relationships Between Neurofibrillary Tangles, Activated Microglia, and Neurons

in PPA-AD

</div>

ABSTRACT

Neurofibrillary tangles (NFTs) and amyloid-ß plaques are the pathologic hallmarks of Alzheimer's disease (AD) that cause cellular changes including neurodegeneration and neuroinflammation mediated by activated microglia. Microglia exhibit heterogeneous functions and appearances, with hypertrophic microglia displaying a closer association with AD neuropathology and inflammation compared to ramified microglia. However, changes in microglia and neurons have not been quantitatively examined in the non-amnestic atypical clinical variants of AD. The aphasic variant of AD is known as primary progressive aphasia (PPA-AD), a clinical dementia syndrome characterized by language impairments that corresponds to focal cortical atrophy and a predominance of NFTs in the language dominant hemisphere. The current study conducted a large stereologic investigation of language and non-language regions bilaterally to determine if the patterns of AD neuropathology unique to PPA-AD were related to densities of neurons and microglia. We report that NFT densities were positively associated with densities of activated (hypertrophic) microglia and negatively associated with densities of neurons. In addition to finding a negative relationship between hypertrophic microglia and ramified microglia, there was a double dissociation between microglia subtypes and neurons: densities of hypertrophic microglia were negatively related to densities of neurons, while densities of ramified microglia were positively related to densities of neurons. Our findings indicate that there is a large microglial response in PPA-AD consisting of activated hypertrophic microglia that are strongly associated

with NFT accumulation and smaller neuronal densities. Therefore, the neurotoxicity associated with NFTs and activated microglia might be collectively contributing to patterns of neurodegeneration characteristic of PPA-AD.

INTRODUCTION

Neurodegenerative diseases such as Alzheimer's disease (AD) are associated with irreversible cortical atrophy and cognitive decline. The extracellular amyloid-ß plaques (APs) and intracellular neurofibrillary tau tangles (NFTs) that comprise the pathologic hallmarks of AD are thought to drive the cellular changes that underlie atrophy and dementia severity. In individuals with typical amnestic AD, glia are activated in response to AD neuropathology and microglia in particular can promote a neuroinflammatory response that may play an important role in AD pathogenesis and severity **(McGeer *et al.*, 1987; Rogers *et al.*, 1988; McGeer and McGeer, 2001; Serrano-Pozo *et al.*, 2011b)**. Neuronal changes associated with AD neuropathology include reductions in axonal density **(Englund and Brun, 1990; Sjöbeck *et al.*, 2005)**, dendrites **(Coleman and Flood, 1987; Arendt *et al.*, 1998)**, and synapses **(Terry *et al.*, 1991; Scheff and Price, 2006; Arendt, 2009)**. Neurons also die by the end stage of disease and their loss correlates with NFT number **(Gomez-Isla *et al.*, 1997)**, but the extent of reported neuronal loss has been inconsistent. Neuronal degeneration may also be a major substrate of *in vivo* cortical atrophy, but the relationship between neurons and atrophy are not well understood outside of small regions such as the hippocampus in AD **(Zarow *et al.*, 2005)**. Furthermore, little is known about the distributions and relationships between AD neuropathology and cellular changes in atypical clinical variants of AD **(Alladi *et al.*, 2007; Mesulam *et al.*, 2008; Gefen *et al.*, 2012; Warren *et al.*, 2012; Mesulam *et al.*, 2014b; Rogalski *et al.*, 2016)**. The purpose of the present study was to clarify the relationships between AD neuropathology, activated microglia, neuronal density, and cortical atrophy in the aphasic variant of AD.

Primary progressive aphasia (PPA) caused by AD neuropathology (PPA-AD) is the aphasic variant of AD **(Knibb *et al.*, 2006; Mesulam *et al.*, 2008; Rohrer *et al.*, 2012; Mesulam *et al.*, 2014b; Rogalski *et al.*, 2016)**. PPA is characterized by an asymmetric pattern of focal cortical atrophy in the language dominant hemisphere **(Mesulam, 1982; Rogalski *et al.*, 2011b; Rogalski *et al.*, 2014; Rogalski *et al.*, 2019)**. Unlike the symmetric distributions of APs and NFTs typically observed in amnestic AD **(Moossy *et al.*, 1988)**, NFTs have higher densities in left language regions, displaying concordance with the cortical atrophy patterns and aphasic phenotype of PPA **(Gefen *et al.*, 2012; Josephs *et al.*, 2013)(Ohm *et al.*, under review)**. Furthermore, NFTs have been shown to be a major neuropathologic determinant of *in vivo* cortical atrophy in the amnestic and aphasic presentations of AD **(Dallaire-Théroux *et al.*, 2017)(Ohm *et al.*, under review)**. The atypical deposition of AD neuropathology in PPA raises the question of whether neurons and activated glia display similar regional patterns that correspond to the NFT burden and cortical atrophy unique to PPA-AD.

Microglia are largely responsible for the neuroinflammation associated with AD **(McGeer *et al.*, 1987; Rogers *et al.*, 1988; McGeer and McGeer, 2001; Serrano-Pozo *et al.*, 2011b)**. However, microglia are heterogeneous in function and appearance, with some morphologic phenotypes more closely linked to neurodegenerative processes compared to others. The classic activated microglia are considered the inflammatory brain macrophages that appear hypertrophic with thick and short processes and co-localize with AD neuropathology **(Itagaki *et al.*, 1989; Serrano-Pozo *et al.*, 2011b; Serrano-Pozo *et al.*, 2013a)**. In contrast, ramified microglia appear relatively smaller, with long, thin branches that likely survey their surroundings for pathophysiological changes in preparation to convert to the activated state **(Perry *et al.*, 2010)**. Differentiation of these phenotypes and their individual distributions could reveal specific relationships with neurodegenerative processes. Little quantitative information is available on the

status of glia in PPA, but we have shown that regions of greater cortical atrophy display more activated microglia in the gray matter of PPA caused by transactive DNA-binding protein of 43 kDa (TDP) **(Kim *et al.*, 2016; Kim *et al.*, 2018)** and in the white matter of PPA-AD and PPA-TDP brains **(Ohm *et al.*, 2018)**. No study has identified or quantified different microglial phenotypes in PPA to determine their regional distributions and relationships with other pathologic and cellular changes.

The primary aim of the current study of PPA-AD was to acquire stereologic densities of neurons and microglial phenotypes in the gray matter to determine how they relate to each other and to AD neuropathology (quantified previously in the same regions and PPA-AD cohort **(Ohm *et al.*, under review)**. In a subset of regions with either high or low atrophy in PPA-AD, optical densities of white matter activated microglia measured previously **(Ohm *et al.*, 2018)** were compared in the present study to the pathologic and cellular markers in the gray matter. To better understand the cellular basis of *in vivo* cortical atrophy in PPA-AD, all densities of neurons and microglia were compared to measurements of atrophy in matching regions. Regions of interest included language and non-language domains in the left, language-dominant hemisphere in addition to their contralateral homologues in PPA-AD. Since hypertrophic microglia (HM) are the microglial phenotype more frequently implicated in neuroinflammation and disease compared to ramified microglia (RM), it was expected that more HM would be associated with more AD neuropathology, more atrophy, more white matter activated microglia, and fewer neurons. Fewer neurons were also anticipated in regions with greater atrophy and more neuropathologic burden.

METHODS

Participants

The current study enrolled participants through the PPA Research Program at the Mesulam Center for Cognitive Neurology and Alzheimer's Disease at the Northwestern University Feinberg

School of Medicine. The participants were 5 right-handed individuals who received clinical diagnoses of PPA **(Mesulam, 1982; Mesulam, 2001; Gorno-Tempini *et al.*, 2011)** and pathologic diagnoses of AD **(Hyman *et al.*, 2012; Montine *et al.*, 2012)**. These PPA-AD participants were described previously **(Ohm *et al.*, 2018)(Ohm *et al.*, under review)**. In brief, two PPA participants were clinically diagnosed with the logopenic variant of PPA (PPA-L), one with the agrammatic variant (PPA-G), and two were unclassifiable (PPA-U). Importantly, each PPA participant had acquired a structural MRI scan within 2.5 years of death that was used to measure cortical atrophy relative to a cognitively healthy control group consisting of 35 participants of similar age and education. The Northwestern University Institutional Review Board approved this study and all participants gave consent to their involvement and brain donations. Characteristics of each PPA participant are summarized in **Table 1.2**.

MRI acquisition

All PPA and healthy control participants had structural MRI scans acquired on a 3T Siemens TIM Trio scanner using a 12-channel birdcage head coil at the Northwestern University Center for Translational Imaging. A T_1-weighted 3D MPRAGE sequence included the following: repetition time = 2300 ms, echo time = 2.91 ms, inversion time = 900 ms, field of view = 256 mm, flip angle = 9°, 1 mm^3 voxel resolution collected over 176 sagittal slices. The scan-to-death mean interval (SDI) was 1.96 ± 0.8 years; range 0.61—2.54 years (**Table 1.2**).

MRI processing and regions of interest

The processing of structural MRI was described previously **(Ohm *et al.*, under review)**. In brief, the last MRI scan before death of each participant was pre-processed using FreeSurfer (v5.1.0, *http://surfer.nmr.mgh.harvard.edu*) and topological surface errors were manually corrected according to established guidelines **(Fischl and Dale, 2000; Ségonne *et al.*, 2007)**. FreeSurfer was used to measure the mean cortical thickness in identical regions of interest (ROIs)

created and used previously **(Ohm *et al.*, under review)**. Fourteen ROIs were investigated in each PPA participant, 7 per hemisphere (**Fig. 3.1**). The left language-dominant hemisphere contained 5 language-related and 2 non-language ROIs. The right hemisphere contained the 7 homologues of the left hemisphere ROIs. The 'language ROIs' consisted of the inferior frontal gyrus (IFG), anterior superior temporal gyrus (aSTG), posterior superior temporal gyrus (pSTG), anterior inferior parietal lobule (aIPL), and posterior inferior parietal lobule (pIPL). The bilateral 'non-language ROIs' were the memory-related entorhinal cortex (EC) and the primary visual cortex (V1).
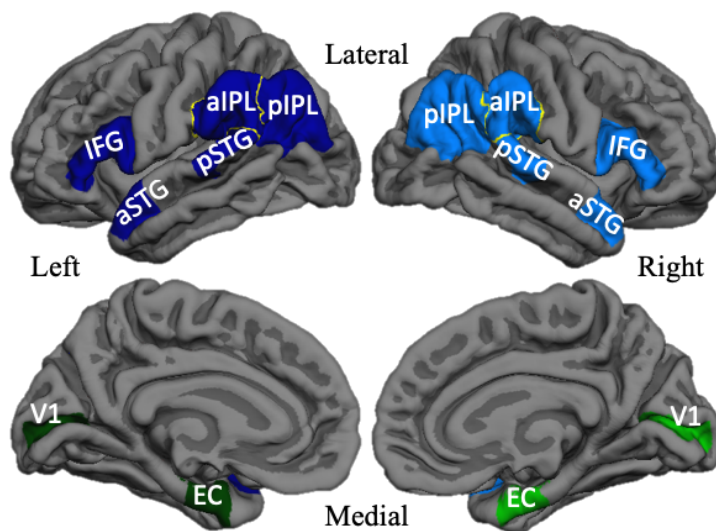
Figure 3.1 Regions of interest in PPA-AD. Left language ROIs (dark blue), right language homologues (blue), left non-language ROIs (dark green), right non-language ROIs (green) displayed bilaterally on lateral and medial reconstructions of a template cortical surface in FreeSurfer. Inferior frontal gyrus (IFG), anterior superior temporal gyrus (aSTG), posterior superior temporal gyrus (pSTG), anterior inferior parietal lobule (aIPL), posterior inferior parietal lobule (pIPL), entorhinal cortex (EC), primary visual cortex (V1).

Tissue processing

Brains of each PPA-AD participant were processed as previously described for staining of AD neuropathology and neurons **(Ohm *et al.*, under review)** or microglia **(Ohm *et al.*, 2018)**. Brains were cut into ~1-2 cm coronal blocks and fixed in either 10% formalin for 2 weeks or 4% paraformaldehyde for 30-36 hours at 4ºC, and then submerged into an increasing concentration gradient of sucrose (10-40%) for cryoprotection (**Table 1.2**). A 1:24 series of 40 μm-thick coronal sections was collected for all PPA-AD participants. Each ROI contained 5-15 sections depending on its anterior-posterior extent. Three series of adjacent sections were processed for all markers

of interest: AD neuropathology was visualized with the Thioflavin-S stain (1%), while microglia and neurons were visualized immunohistochemically without antigen retrieval using the avidin-biotin peroxidase complex method employing the Vectastain Elite Kit and 3,3-diaminobenzidine as the chromogen. The microglial phenotypes of interest to the current investigation (i.e., HM and RM, **Fig. 3.4a**) were consistently detected using an antibody against the human leucocyte antigen-D related (HLA-DR) protein (mouse monoclonal; Dako; 1/1000) **(McGeer *et al.*, 1987)**. Neurons were visualized using an antibody against neuronal nuclear protein (NeuN, mouse monoclonal; EMD Millipore; 1/2000) **(Wolf *et al.*, 1996)**. The left/right hemispheric pair of each region was always stained together in the same immunohistochemical run for each marker of interest.

ROI correspondence

Anatomical correspondence of data acquired during life and after death was achieved using methods described previously **(Ohm *et al.*, under review)**. In brief, all series of postmortem tissue were collected from *a priori* ROIs initially generated in FreeSurfer and visualized in Freeview. Postmortem regional boundaries were previously delineated on NeuN-positive tissue that matched FreeSurfer generated boundaries on every section. Since the NeuN-positive tissue was a parallel series to the HLA-DR and Thioflavin-S-positive tissue, it provided the means to transfer the same regional boundaries onto adjacent sections stained for HLA-DR or Thioflavin-S. This ensured that all postmortem data corresponded to each other and to measures of *in vivo* cortical atrophy.

White matter activated microglia were quantified previously **(Ohm *et al.*, 2018)** in a subset of the 14 ROIs used for stereologic cortical atrophy investigations in the present study. The subset included 2 language and 2 non-language ROIs in the language dominant hemisphere and their contralateral homologues for a total of 8 ROIs examined per PPA participant (**Table 3.1**). The non-language ROIs were always V1 and EC, two regions shown to have less AD neuropathology compared to language ROIs in PPA-AD **(Gefen *et al.*, 2012)(Ohm *et al.*, under review)**.

Language ROIs varied by participant given that they were chosen previously based on peak cortical atrophy in each PPA participant **(Ohm *et al.*, 2018)**. The current investigation performed stereology on the same 5-6 coronal sections per ROI where white matter activated microglia optical densities were acquired.

Table 3.1 **Subset of regions used in white matter activated microglia analysis.**

PPA-AD case #	1	2	3	4	5
Non-language	V1	V1	V1	V1	V1
	EC	EC	EC	EC	EC
Language	aIPL	IFG	pSTG	pSTG	aSTG
	pIPL	aSTG	aIPL	aIPL	pSTG

Stereologic quantification

Stereologic estimates of NFTs and dense-core APs were acquired in a previous investigation (**Ohm *et al.*, under review**). HM, RM, and neurons were quantified at a final magnification of 60x across all cortical layers of each ROI using a stereological analysis performed on a workstation equipped with a Nikon Eclipse E800 microscope, motorized stage, and stereology software (StereoInvestigator v11.07, MBF Bioscience). The optical fractionator probe was used to estimate the populations of each cellular marker from all available sections per ROI, with sampling grid dimensions that varied by anatomical region to produce a coefficient of error ≤ 0.1 **(Schmitz and Hof, 2005)**. The size of the counting frame was kept at 125 μm^2, and a disector height of 16 μm with guard zones of 2 μm were used. Section thickness was measured at each counting site to calculate an average section thickness used in estimating populations of each cellular marker. For each ROI, densities of HM, RM, and neurons per mm^3 were calculated by taking the estimated population using number weighted section thickness and dividing by the planimetry volume.

Statistical analyses

Analyses performed on measurements of *in vivo* cortical atrophy to investigate hemispheric

asymmetry and language region selectivity have been described previously **(Ohm *et al.*, under review)**. In brief, FreeSurfer software was used to measure an average cortical thickness in each ROI. Z scores were calculated to represent the magnitude of cortical atrophy in each ROI relative to a healthy control group using the following equation:

$$z = (\mu \text{ healthy controls} - \text{observed cortical thickness}]/ \sigma \text{ healthy controls})$$

All analyses were conducted using linear mixed models accounting for repeated measures. Given the main focus of the current investigation was to understand how AD neuropathology (NFT, AP) is related to cellular markers (HM, RM, white matter activated microglia, and neuron densities), the first set of models examined the relationships between two postmortem variables at a time. Due to the lack of an established direction specifying which postmortem variable would be the outcome or covariate, we evaluated the relationships in both directions, using a Bonferroni corrected significance level of 0.025. Only one direction was reported, selecting the larger *p* value of the two models. To evaluate the cellular basis of cortical atrophy, models examined the relationship between each cellular marker (densities) and cortical atrophy (z-scores). Models that examined the relationships with white matter activated microglia incorporated a subset of regions **(Table 3.1)**. All of these models were adjusted for hemisphere, type of regional domain (language and non-language regions), and age at death. When cortical atrophy was compared to postmortem marker densities, models were also adjusted for SDI and when postmortem markers were compared to each other, models were adjusted for postmortem interval.

Given our previous findings showing that NFTs and cortical atrophy are significantly greater in the left language regions of this PPA-AD cohort **(Ohm *et al.*, under review)**, additional analyses were carried out on cellular markers (HM, RM, white matter activated microglia, and neurons) to characterize their distributions. To assess if each cellular marker displayed hemispheric asymmetry, the relationship between each cellular marker and hemisphere was

evaluated after stratifying by language or non-language regions. To determine if cellular marker densities were different between language and non-language regions, the association between each cellular marker and type of region (language or non-language) was assessed in only the left hemisphere. These models were adjusted for age at death and postmortem interval. Significance was set to $p<0.05$ for all comparisons unless otherwise stated using SAS software v9.4; SAS Institute.

RESULTS

Qualitative patterns of pathologic and cellular markers in hemispheres, regions, and cortical layers

We previously reported on the language region selectivity of NFTs and dense-core APs and leftward asymmetry of NFTs in PPA-AD **(Ohm *et al.*, under review)** (**Fig. 3.2, bottom panel**). These findings appear unique to PPA-AD in comparison to what is known in amnestic AD and other clinical AD variants. However, the laminar deposition of AD neuropathology in PPA-AD appeared consistent with what has been reported in cortical and limbic regions of amnestic AD **(Hirano and Zimmerman, 1962; Brun and Englund, 1981; Pearson *et al.*, 1985; Lewis *et al.*, 1987; Arnold *et al.*, 1991; Braak and Braak, 1991)**. More specifically, we observed NFTs more frequently in layers II, III, and V throughout language regions of PPA-AD. Dense-core APs typically accumulated in layers II-V without obvious laminar selectivity. Diffuse plaques were more frequent than dense-core APs, but did not display a recognizable pattern between cell layers, language regions, or hemispheres. Across all regions examined, layer I was consistently devoid of dense-core APs and NFTs, and the deepest part of layer VI immediately adjacent to white matter showed infrequent APs and nearly no NFTs. NFTs were exceedingly rare in cortical white matter, but diffuse plaques and dense-core APs were sometimes present in the superficial U-fibers of white matter, an observation reported previously **(Serrano-Pozo *et al.*, 2011a)**.
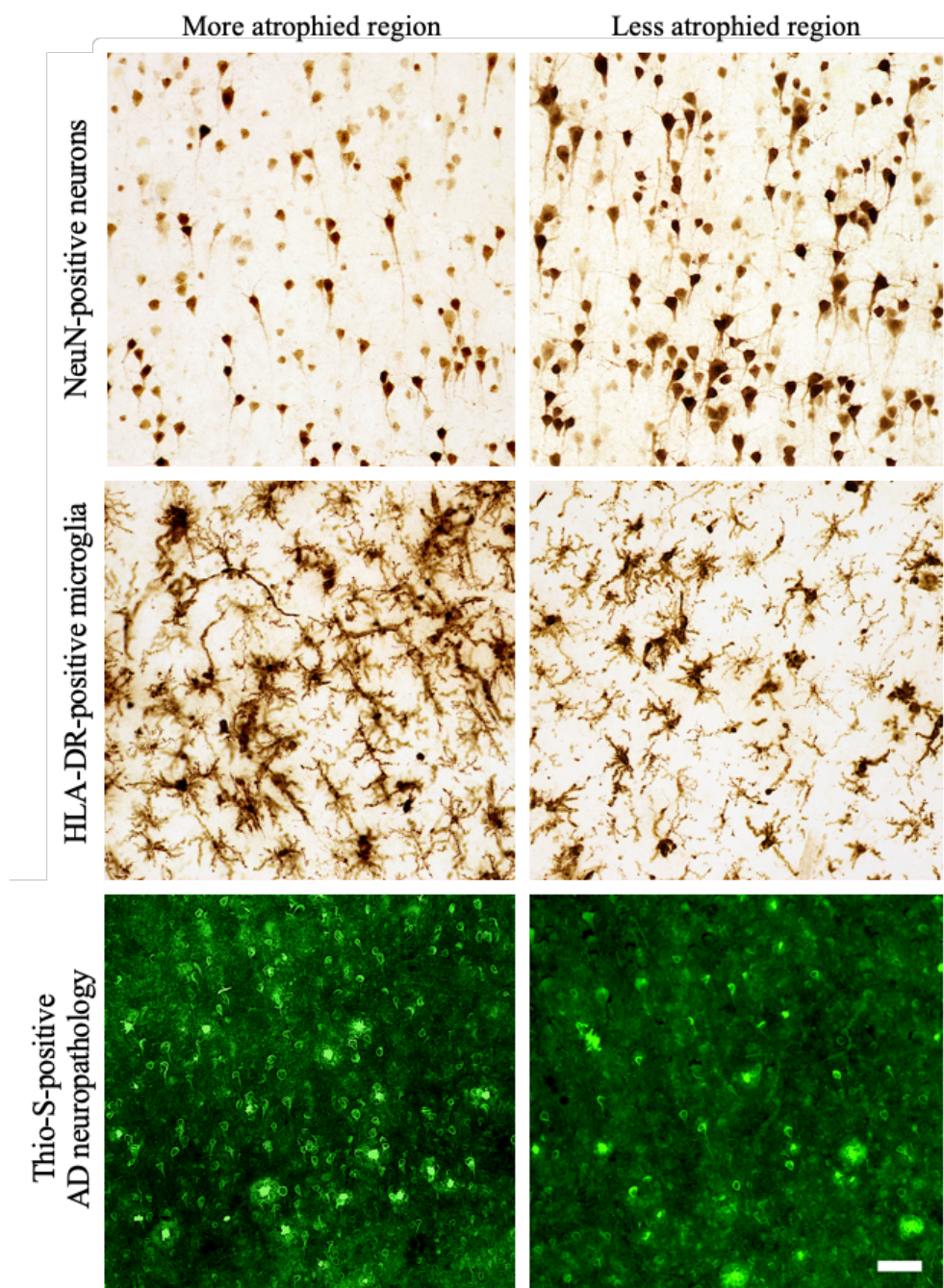
Figure 3.2 Representative photomicrographs of the differential distributions of neurons, activated microglia, and AD neuropathology in layer III of regions with high or low cortical atrophy in a PPA-AD participant. Layer III, a selectively vulnerable cortical layer, typically displayed thinning, fewer neurons, and more NFTs and activated microglia in more atrophied regions compared to less atrophied regions. This pattern was inconsistently seen in other cortical layers and regions within and across PPA-AD participants. Photomicrographs of each marker were acquired at 20x magnification within the gyral crown of aIPL in PPA-AD participant #3. More atrophied region – left aIPL; less atrophied region – right aIPL. Scale bar set to 50 μm.

We have quantitatively described the distributions of HLA-DR-positive microglia in white matter in PPA-AD **(Ohm *et al.*, 2018)**. It is important to note that the activated microglia of the white matter were virtually all of the HM phenotype. Furthermore, greater concentrations of HM were often observed in the association U-fibers of white matter compared to neighboring white matter tracts and layer VI. Within the gray matter, RM were relatively rare in comparison to HM, with no recognizable pattern across cortical layers due to their infrequency. HM often formed large clusters that were widespread across layers II-V, with smaller densities in layer IV and very few if any in layers I and VI in all regions examined (**Fig. 3.2, middle panel**). The accumulation of HM is noteworthy given its similar distribution to the deposition of dense-core APs and NFTs, as well as previously reported topographic patterns of activated microglial clusters/nests in amnestic AD or frontotemporal lobar degeneration **(Brun and Englund, 1981; Lant *et al.*, 2014; Taipa *et al.*, 2017a; Taipa *et al.*, 2017b).**

Concordant with NFT densities and less so AP densities, NeuN-positive neurons were consistently less dense in layers III and V of language regions, with often the least NeuN reactivity in layer III of highly atrophied regions (**Fig. 3.2, top panel**). It is noteworthy that the predominant output of layer III neurons is to neighboring cortical regions where they form the association U-fibers, the same area of white matter where more microglial activation was often observed **(Ohm *et al.*, 2018)**. Reduced NeuN reactivity and/or smaller densities of neurons were occasionally observed toward the gyral fundi relative to the gyral crown. A similar pattern has been previously reported for AD neuropathology in amnestic AD such that more NFTs and APs were observed in the gyral fundi **(Braak and Braak, 1991; Arendt *et al.*, 2016)**. In this PPA-AD cohort, however, neither the distributions nor staining intensities of NFTs, APs, or microglia appeared to reflect the gradation of NeuN reactivity.

In comparison to language regions, non-language regions displayed similar but also

divergent patterns in marker distribution. NFTs were most prominent in layer II and common in layer IV and V of EC, while virtually no NFTs were observed throughout any of the layers of V1. Dense-core APs were common across most layers of V1 and relatively rare in EC, while diffuse plaques were common in EC and scarce in V1. Whereas all 5 PPA-AD participants had EC islands readily discernible by large, NFT-bearing neurons, the islands were inconsistently detected by HM or NeuN-positive neurons. HLA-DR reactivity was generally more pronounced in the upper layers compared to the lower layers of EC. Neuron density appeared greatest in layers II and VI of both EC and V1. In V1, clusters of HM were more concentrated in the stria of Gennari which also displayed stronger HLA-DR reactivity than other cortical layers but less intense than surrounding white matter.

Quantitative distributions of microglial phenotypes and neurons

We have shown that NFT densities mirror the focal and asymmetric cortical atrophy characteristic of PPA **(Ohm *et al.*, under review)**. In this study, further analyses were conducted on cellular markers to evaluate concordance with NFT densities and the aphasic profile of PPA-AD. Densities of HM, RM, and neurons did not display significant hemispheric asymmetry or language region selectivity (**Fig. 3.3**). However, HM showed higher estimated means in the left language regions compared to right homologues that trended toward significance (p=0.08). The expected reverse patterns were observed for RM and neurons such that each showed a lower estimated mean in the left language regions compared to right homologues, but these differences did not reach statistical significance.
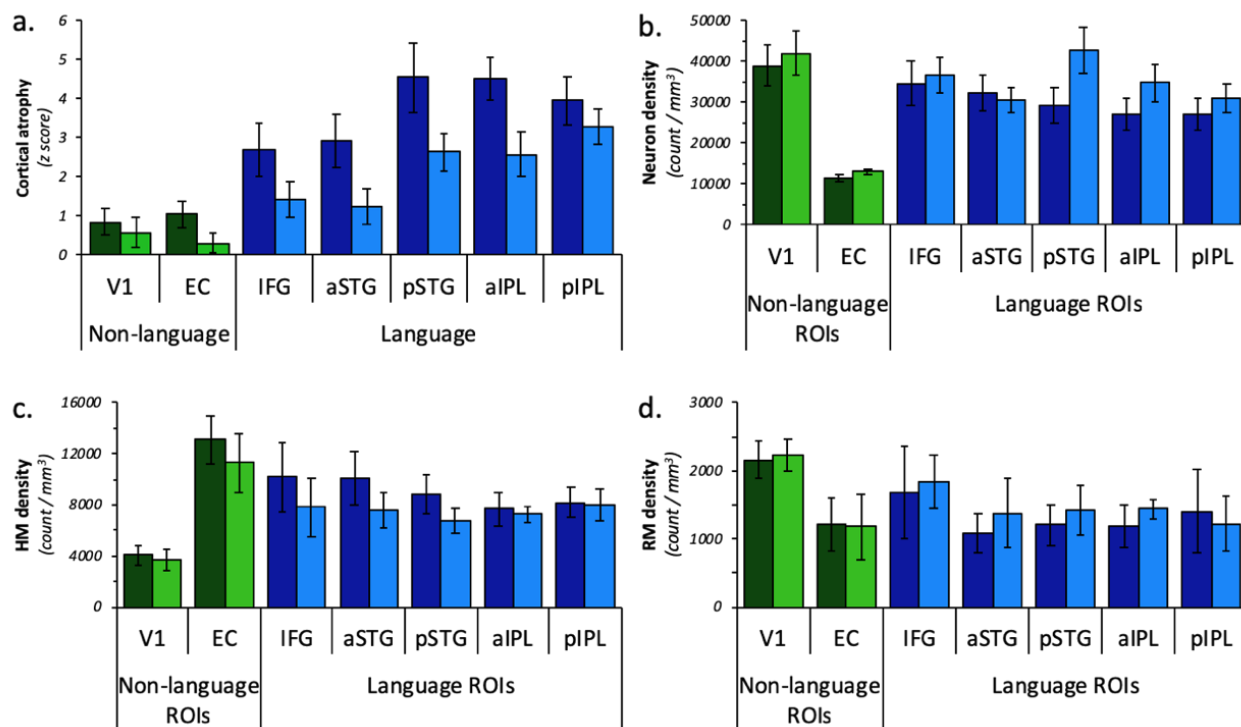
Figure 3.3 Distributions of *in vivo* cortical atrophy, neurons, and microglial phenotypes in PPA-AD.

a) The PPA-AD group had significantly more cortical atrophy in the left language regions compared to right language homologues (p=0.01). Cortical atrophy was also significantly greater in the language regions compared to the non-language regions in the left hemisphere (p<0.01). Densities of neurons **(b)**, hypertrophic microglia (HM; **c**), and ramified microglia (RM; **d**) did not show significant hemispheric asymmetry or language region selectivity.

Left language ROIs = dark blue bars; right language homologues = blue bars; left non-language ROIs = dark green bars; right non-language ROIs = green bars.

Relationships between pathologic and cellular markers

HM densities were inversely related to RM densities (p<0.01; **Fig. 3.4b**). NFT densities were not associated with AP densities, and neither NFTs nor dense-core APs were related to RM densities. NFT densities had a positive relationship with HM densities (p<0.01; **Fig. 3.5a**), and a negative relationship with neuron densities (p=0.01; **Fig. 3.6a**). AP densities displayed a negative relationship with HM densities (p<0.01), and a positive relationship with neuron densities (p<0.01). Neuron densities were positively related to RM densities (p=0.02), and inversely related to HM densities (p<0.01; **Fig. 3.6b**). Mean optical densities of white matter activated microglia showed positive associations with NFT (p<0.01; **Fig. 3.5b**) and HM densities (p<0.01), and

negative associations with AP ($p<0.01$), RM ($p<0.01$), and neuron densities ($p<0.01$; **Fig. 3.6c**).
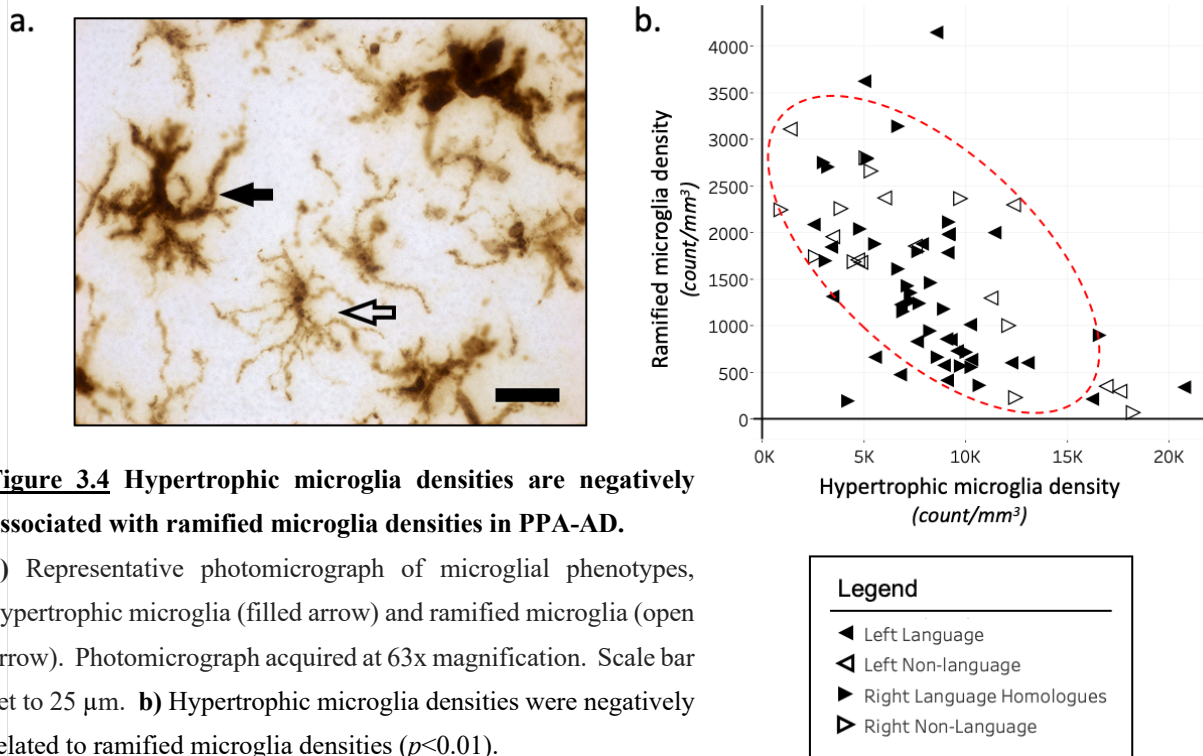
Figure 3.4 Hypertrophic microglia densities are negatively associated with ramified microglia densities in PPA-AD.

a) Representative photomicrograph of microglial phenotypes, hypertrophic microglia (filled arrow) and ramified microglia (open arrow). Photomicrograph acquired at 63x magnification. Scale bar set to 25 μm. **b)** Hypertrophic microglia densities were negatively related to ramified microglia densities ($p<0.01$).
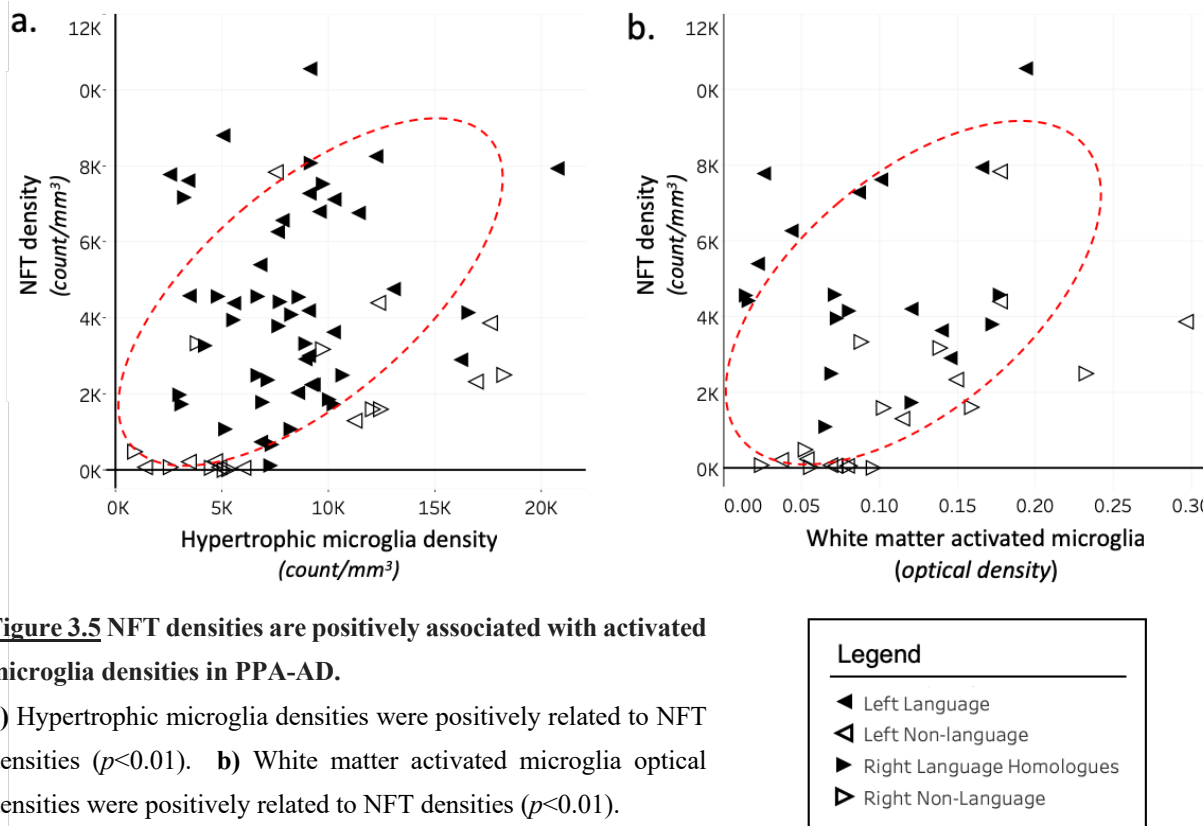
Figure 3.5 NFT densities are positively associated with activated microglia densities in PPA-AD.

a) Hypertrophic microglia densities were positively related to NFT densities ($p<0.01$). **b)** White matter activated microglia optical densities were positively related to NFT densities ($p<0.01$).
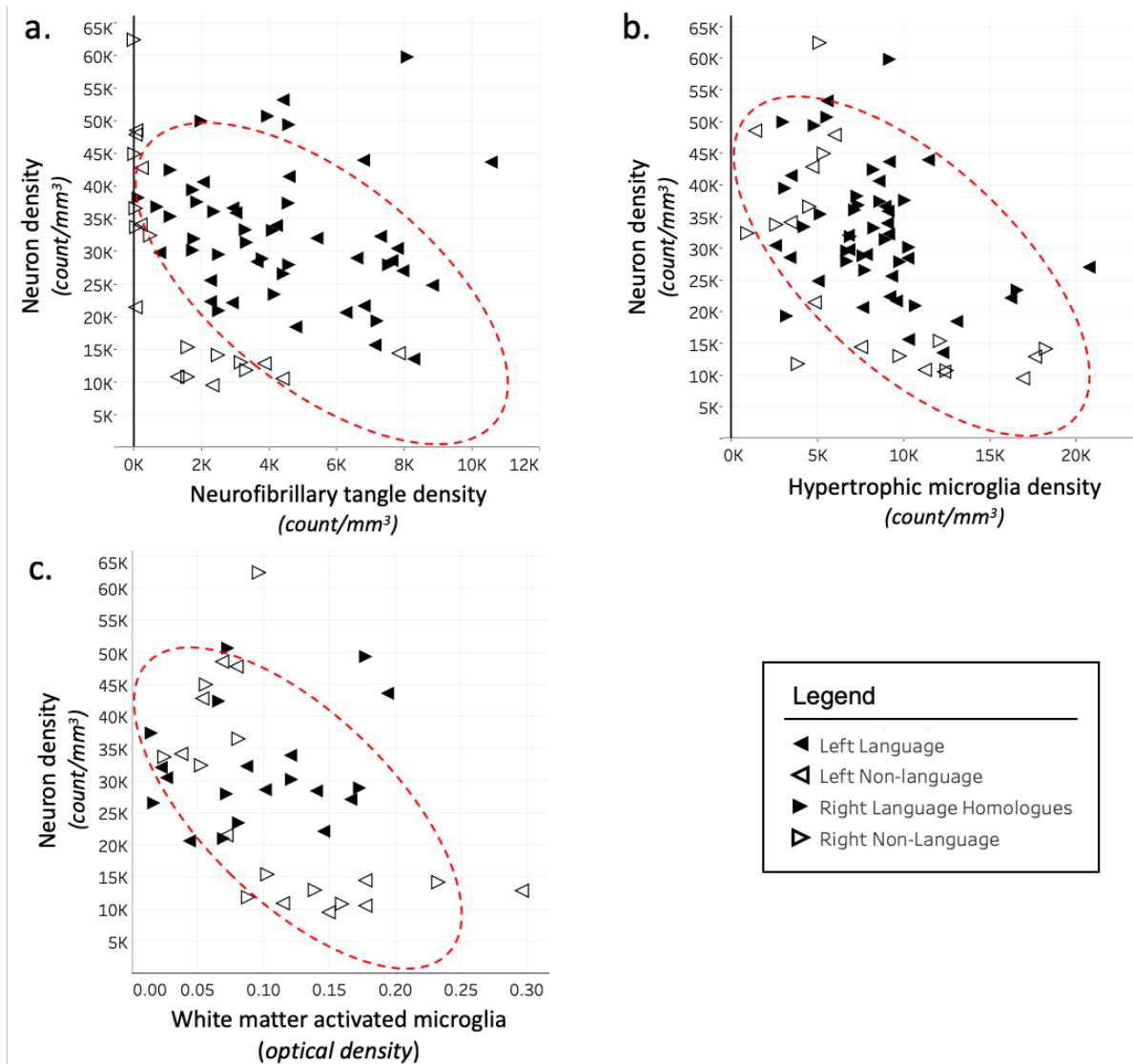
Figure 3.6 Smaller neuron densities are associated with larger densities of NFTs and activated microglia in PPA-AD.

a) Neuron densities were negatively related to NFT densities (*p*=0.01). **b)** Neuron densities were negatively related to hypertrophic microglia densities (*p*<0.01). **c)** Neuron densities were negatively related to white matter activated microglia optical densities (*p*<0.01).

Relationships between *in vivo* cortical atrophy and postmortem cellular markers

We have reported that cortical atrophy is positively related to NFTs, but not dense-core APs **(Ohm *et al.*, under review)**. The current investigation found that cortical atrophy was not significantly associated with any cellular marker in the gray or white matter except RM densities, with which it displayed a negative relationship (*p*=0.03; **Fig. 3.7a**).
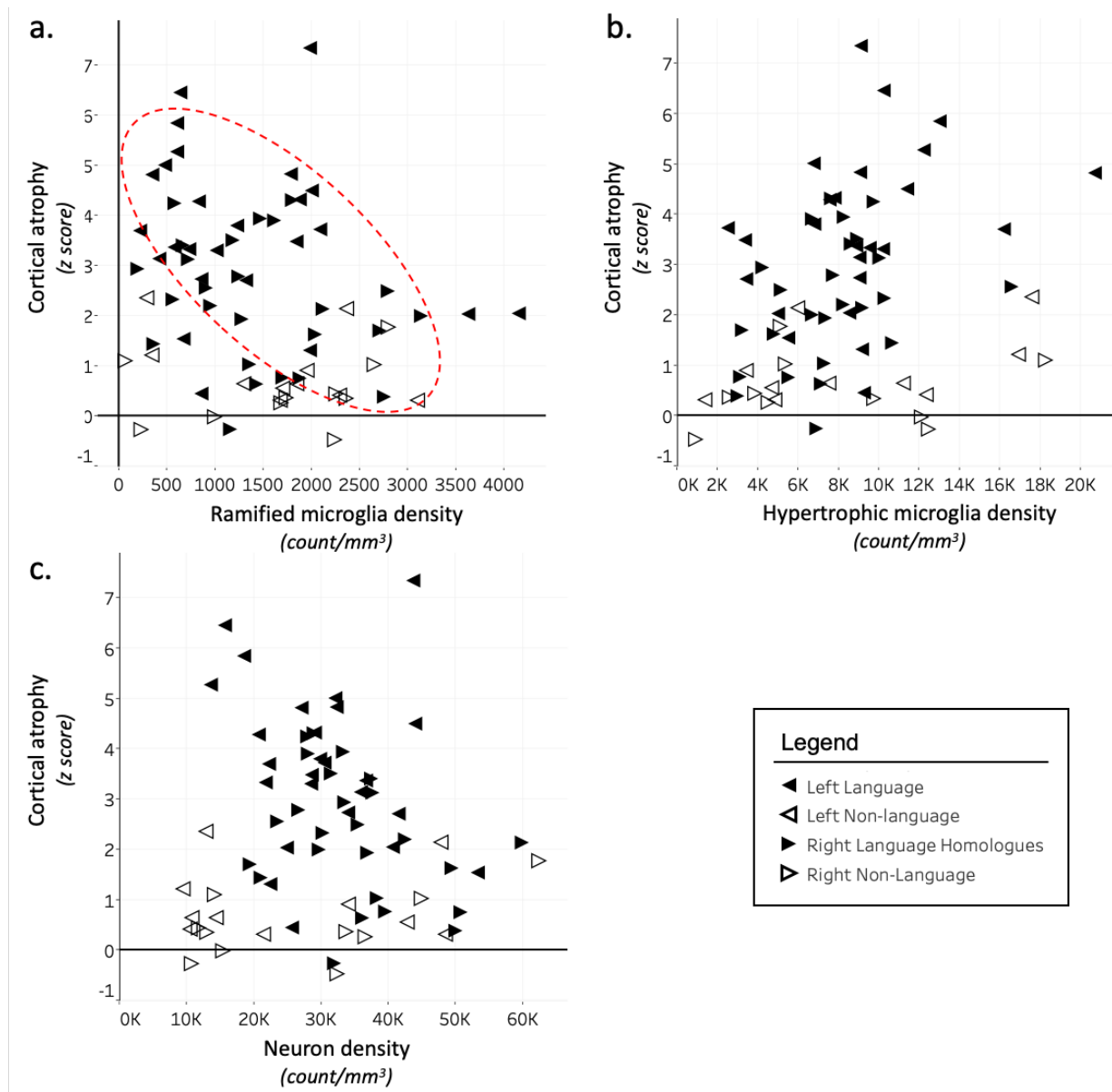
Figure 3.7 *In vivo* **cortical atrophy is negatively associated with ramified microglia densities in PPA-AD.**
a) Cortical atrophy was negatively related to ramified microglia densities (p=0.03), but not related to hypertrophic microglia or neuron densities.

DISCUSSION

The cellular changes that are related to AD neuropathology and likely contribute to cortical atrophy have received sparse attention in PPA-AD. Here, we show that only NFTs displayed positive relationships with activated microglia in the white and gray matter, providing new pathologic evidence for what drives microglial activation in PPA-AD. Second, we found that

neuron densities were smaller in regions with greater neuropathologic change, namely, NFTs and activated microglia. These pathologic and cellular patterns indicate that smaller neuron densities may be a sign of neurodegeneration caused by significant accumulations of NFTs and inflammatory microglia. However, the cellular basis of cortical atrophy remains elusive in PPA-AD considering that neither neurons nor activated microglia were associated with *in vivo* measurements of cortical atrophy. This new postmortem data, in conjunction with our previous report showing NFTs were positively associated with cortical atrophy in PPA-AD **(Ohm *et al.*, under review)**, point to NFTs as a central determinant of microgliosis, smaller neuron densities, and *in vivo* cortical atrophy in PPA-AD.

Status of microglial activation and its relationship to neuropathology and cortical atrophy

The status of activated microglia, a marker of neuroinflammation, and the pathologic changes related to activated microglia have not been quantitatively evaluated in clinical AD variants including PPA-AD. Here we report a double dissociation between microglial phenotypes and neurodegenerative processes in PPA-AD. RM accumulated more in less atrophic regions with more neurons and fewer activated microglia. The negative relationship between RM and cortical atrophy may reflect their purported role as benign sentinels that do not contribute to neurodegenerative processes in PPA-AD until they convert to HM. In contrast to RM, HM displayed positive relationships with NFTs, white matter activated microglia, and a negative relationship with neurons. Therefore, consistent with findings in amnestic AD **(McGeer and McGeer, 2001; Solito and Sastre, 2012)**, neuroinflammation may play a prominent role in disease severity and progression for PPA-AD.

HM were inversely related to RM, possibly due to a widespread activation and conversion of RM to HM in PPA-AD. This is consistent with a previous report in amnestic AD indicating that the majority of the glial response is a phenotypic change as opposed to a proliferation of glia

(Serrano-Pozo *et al.*, 2013a). The current study cannot speculate on the extent of glial proliferation in PPA-AD, but a phenotypic change from RM to HM may have resulted in the disproportionately greater densities of HM than RM observed in almost all ROIs examined in PPA-AD.

While we often observed more activated microglia in regions of greater atrophy and AD neuropathology of PPA-AD, neither HM nor white matter activated microglia were related to *in vivo* cortical atrophy. The lack of relationship between white matter activated microglia and cortical atrophy was consistent with a finding we reported in a previous investigation on PPA. More specifically, we found that atrophied regions did not have a significantly greater optical density of activated microglia compared to non-atrophied regions within pathologic subtypes of PPA, including PPA-AD **(Ohm *et al.*, 2018)**. Sample size and individual variability may have contributed to these findings. However, the hypertrophy and possible proliferation of microglia near pathologic inclusions **(Solito and Sastre, 2012; Gomez-Nicola *et al.*, 2013)** could have expanded the gray matter volume, negating the effects of cortical atrophy driven by neuronal loss or shrinkage, and resulting in a disconnect between the HM and cortical atrophy quantified in this study. Another possibility is that during the short timeframe between last MRI scan and death, the rate of microglial accumulation or phenotypic change could have plateaued or diverged from the rate of atrophy in each hemisphere. In fact, a recent PET study demonstrated that microglia may have an early and late phase of activation over the course of disease progression of AD **(Fan *et al.*, 2017)**. If this is confirmed in PPA-AD, it is possible that earlier stages of microglial activation may arise more focally and in an asymmetric pattern reflective of PPA compared to what was established in this postmortem investigation.

The precise causes of microglial activation in the white matter are not known. Axonal degeneration and myelin loss have been known to occur in amnestic AD **(Englund and Brun,**

1990; Sjöbeck *et al.*, 2005) and similar events may occur in PPA **(Catani *et al.*, 2003; Galantucci *et al.*, 2011; Migliaccio *et al.*, 2012)**. If so, the recruitment of microglia would have been likely as they are the primary phagocytes of the brain that activate and clear the axonal and myelin debris resulting from this degeneration. Wallerian degeneration may have led to these white matter changes in PPA-AD since AD neuropathology almost exclusively accumulates in the gray matter. In parallel, retrograde Wallerian-like degeneration is also conceivable given that tau has an endogenous axonal prominence **(Binder *et al.*, 1985)** and its pathologic hyperphosphorylated state disrupts microtubule stability **(del C Alonso *et al.*, 1996)** that compromises axonal transport and thereby white matter integrity **(Ballatore *et al.*, 2007; Strain *et al.*, 2018)**. Therefore, the positive relationship we observed between NFTs and white matter activated microglia in PPA-AD may reflect a leading neurodegenerative mechanism centered on NFTs and microglia-mediated neuroinflammation. However, amyloid-β oligomers and fibrils cannot be excluded from these pathological events given the evidence for their independent and tau-dependent neurotoxicities **(Lorenzo and Yankner, 1994; Busciglio *et al.*, 1995; Lambert *et al.*, 1998)**. Amyloid-β peptides are also known to cause microglia-mediated inflammation **(Barger and Harmon, 1997)** and have been found in greater concentrations in the white matter compared to gray matter in amnestic AD **(Collins-Praino *et al.*, 2014)**. More research is needed to identify what aspects of white matter are altered and to what extent abnormal tau and amyloid-β promote neuroinflammation in PPA-AD.

Microglia showed different relationships with the hallmarks of AD neuropathology. Although activated microglia are typically associated with dense-core APs in amnestic AD **(Itagaki *et al.*, 1989; Serrano-Pozo *et al.*, 2011b; Serrano-Pozo *et al.*, 2013b)**, we unexpectedly found that HM were negatively related to dense-core APs. Given the growing evidence for microglia heterogeneity **(Böttcher *et al.*, 2019)** and that only HM and RM phenotypes were

quantified in the current study, it will be important to assess how other microglial populations or clusters of activated microglia relate to dense-core APs. The positive association between HM and NFTs is noteworthy given that there is growing evidence for a strong link between NFTs and activated microglia. Models of neuroinflammation and AD have demonstrated that microglia and the inflammatory cytokines they secrete can contribute to tau phosphorylation and propagation of tau pathology **(Li *et al.*, 2003; Ghosh *et al.*, 2013; Asai *et al.*, 2015; Maphis *et al.*, 2015)**. An investigation of frontotemporal dementia patients with underlying frontotemporal lobar degeneration pathology demonstrated that activated microglia co-localized with tau-2 and their densities correlated with tau deposition and neurodegeneration in participants without Pick's disease **(Schofield *et al.*, 2003)**. Moreover, a positron emission tomography (PET) study using the radioligand ^{11}C-PBR28 to measure microglial activation showed that amyloid-negative participants (diagnosed with mild cognitive impairment or amnestic AD) had microglial activation that correlated with tau aggregation **(Dani *et al.*, 2018)**. These findings indicate that independent of AP burden and its neurodegenerative involvement, extracellular tau can activate microglia that may in turn exacerbate tau pathology. Therefore, microglia-mediated neuroinflammation and NFTs may participate in a positive feedback loop that collectively worsen neurodegenerative processes in PPA-AD.

Distributions of cellular markers

Of all the pathologic and cellular markers quantified in this investigation, only NFT densities displayed leftward asymmetry and language selectivity concordant with the cortical atrophy and aphasic profile of PPA. While NFTs and neurons displayed a significant negative relationship suggestive of NFT-driven neurodegeneration, neuron densities did not show asymmetry as expected. One potential reason for these findings is that stereology was carried out on only NeuN-positive neurons. NeuN is known to be specific to neurons, but NeuN reactivity

has also been shown to decline with disease severity suggesting that NeuN might be a better marker of neuronal health compared to neuron loss **(Yousef *et al.*, 2017)**. Therefore, the fairly symmetric patterns of NeuN-positive neuron densities in PPA-AD might represent a general state of poor neuronal health across the cortex by end stage of disease that is not directly reflective of the significant cortical atrophy in PPA.

A strength of the current study was acquiring stereologic densities intrinsic to individual brain regions to establish important pathologic-cellular relationships not previously investigated in PPA-AD. However, neuron densities were not related to *in vivo* cortical atrophy in PPA-AD. Aside from select studies reporting that unilateral CA1 neuron populations correlated with cortical atrophy in amnestic AD **(Kril *et al.*, 2004; Zarow *et al.*, 2005)**, the neuronal basis of *in vivo* cortical atrophy remains mostly unknown in the clinical AD spectrum. To determine if reduction of neurons is a better correlate of regional atrophy in PPA-AD, it will be important for future studies to evaluate a proper control group to acquire estimates of neuron loss in PPA-AD. In addition, other neuronal markers may be more sensitive to neuronal changes and should be explored to expand our understanding of the cellular basis of neurodegeneration. Nevertheless, the current study found utility in the consistency and selectivity of the NeuN marker as it permitted a large stereologic analysis that uncovered new evidence for NFTs and HM having a close and adverse link to NeuN-positivity and/or neuron densities in PPA-AD.

Neurons were quantified across all cell layers in each region, resulting in a neuron density per region that might not have captured more selective neurodegeneration. More specifically, it is possible that focal and asymmetric loss of neurons may be present in specific types of neurons (e.g., pyramidal neurons) in select cortical layers such as layers III and V where more AD neuropathology accumulates. In the current study we observed qualitatively less NeuN-reactivity/neuron densities in layer III where the most NFTs accumulated. These observations, in

combination with our previous report describing greater microglial activation in the U-fiber white matter tracts known to be mostly comprised of layer III cortico-cortical projections **(Ohm *et al.*, 2018)**, may suggest a disproportionate degeneration of layer III in cortical language regions of PPA-AD.

Similar to neuron densities, microglia densities failed to display significant hemispheric or language region selectivity. This was surprising given that HM were positively related to the highly asymmetric NFT deposits and that activated microglia have been shown to be asymmetric in PPA-TDP **(Kim *et al.*, 2018)**. Greater mean densities of HM were observed in left language regions compared to right homologues, but regional asymmetry was subtle and inconsistent in this PPA-AD cohort. In fact, PPA-AD participant #4 paradoxically displayed reversed asymmetry of HM in two temporoparietal language regions that did not correspond to NFTs or atrophy quantified in the same regions of that participant. Other markers of activated microglia have the potential to identify asymmetric patterns **(Hopperton *et al.*, 2018)**, but HLA-DR was an appropriate marker for this investigation due to its strong specificity for activated microglia in neurodegenerative diseases like AD **(McGeer *et al.*, 1987; McGeer *et al.*, 1988)**.

Regional variability

The memory-related EC unexpectedly showed HM densities as great if not greater than language regions and their contralateral homologues. Given that this region did not harbor significant cortical atrophy or AD neuropathology in PPA-AD, it remains unclear what microglia were responding to in the EC. Neuron densities were lowest in EC, which could reflect substantial neuronal loss or the possibility that allocortical regions such as EC have intrinsically smaller densities of neurons compared to the high densities characteristic of neocortical sensory and association regions **(Collins *et al.*, 2010)**. In contrast to HM, RM densities displayed negative relationships with cortical atrophy, HM, and white matter activated microglia densities. In fact,

larger densities of RM were related to regions with less atrophy, which often corresponded to smaller densities of NFTs and HM. These relationships are exemplified in V1. Furthermore, densities of RM were positively related to neuron densities. These observations suggest that there may have been fewer pathologic triggers to convert RM to HM in regions of less atrophy, resulting in fewer HM to do potential harm or contribute to neuropathologic change and neurodegeneration in PPA-AD.

Conclusions

Consistent with our findings here, select studies have shown that neuron densities **(Freeman *et al.*, 2008; Eriksson *et al.*, 2009; Herculano-Houzel, 2009)** and microglia densities **(Serrano-Pozo *et al.*, 2011b)** do not correlate with postmortem or antemortem measurements of cortical thickness. Therefore, vasculature, components of cells (i.e., synapses, dendrites, and somas), or other cellular populations may in some combination make more significant contributions to cortical atrophy than NeuN-positive neurons or HLA-DR-positive microglia.

The current investigation showed that by the end stage of disease, microglial phenotypes are distinguishable by morphology and that these phenotypes may have differential involvement in neurodegeneration based on their associations with neurons and AD neuropathology in PPA-AD. Only NFTs were associated with more HM and white matter activated microglia, suggesting that the microglial response may be more sensitive to NFTs compared to APs and other neurodegenerative processes. Upon activation, the activated microglia might have mediated deleterious inflammation that worsened the disease process in the gray and white matter in PPA-AD. Therefore, the smaller densities of neurons associated with larger densities of NFTs and activated microglia could mean that multiple pathologic and inflammatory markers drive neurodegeneration in PPA-AD.

—GENERAL CONCLUSIONS—

While we can and do measure structural and functional changes in the brains of patients suffering from neurodegenerative disease such as AD, we often do not have a precise understanding of what causes the cortical abnormalities and steady decline. In amnestic AD, NFTs have been found to be the leading neuropathologic correlate of cortical atrophy and clinical deficits **(Dallaire-Théroux *et al.*, 2017)**. In addition, significant neurodegeneration and neuroinflammation accompany the AD neuropathology in amnestic AD, with the latter possibly exacerbating neurodegenerative processes **(McGeer and McGeer, 2001; Solito and Sastre, 2012)**. Given that AD causes non-amnestic clinical disorders **(Galton *et al.*, 2000; Kramer and Miller, 2000; Alladi *et al.*, 2007; Warren *et al.*, 2012)**, could NFTs also be the primary neuropathologic determinant of cortical atrophy in the atypical variants of AD? Is neuroinflammation associated with AD neuropathology and neurodegeneration and therefore an important component of the disease severity in non-amnestic presentations of AD? The current dissertation sought to address these questions using multidisciplinary approaches in several studies focused on PPA-AD, the aphasic variant of AD.

Each of the three studies was designed to contribute new knowledge to the neuropathologic and cellular determinants of cortical atrophy in a unique clinical population diagnosed with PPA. To that end, all postmortem and antemortem experiments were carried out in 5 PPA-AD participants that had acquired an MRI scan within 2.5 years of death, strengthening our understanding of how postmortem markers related to MRI-based atrophy. For the investigation of white matter activated microglia (Study 2), an additional 5 PPA-TDP participants were examined and compared to the PPA-AD group to better understand if an inflammatory marker displayed similar distributions and relationships with cortical atrophy across pathologic subtypes of PPA.

Another strength of the studies comprising this dissertation was that all of the comprehensive quantitation was performed in bilateral samples of anatomically matching regions that included the cognitive domains of language, memory, and vision.

Given previous findings in PPA-AD **(Gefen *et al.*, 2012; Josephs *et al.*, 2013)** and that AD neuropathology appears to be molecularly and morphologically identical in the brains across the clinical AD spectrum, we hypothesized that NFTs would be strongly related to the asymmetric pattern of cortical atrophy concentrated to the language regions of PPA-AD. Considering that neurons are space-occupying cells responsible for cognitive deficits, in addition to previous neuronal findings from DAT-AD **(Brun and Englund, 1981; Coleman and Flood, 1987; Gomez-Isla *et al.*, 1997; Braak and Braak, 1998)**, the investigation of neuron distributions in PPA-AD was expected to reveal smaller densities in left language regions with high atrophy and greater densities of neuropathology. With the growing evidence that activated microglia can mediate inflammatory, neurotoxic processes **(Mosser and Edwards, 2008; Perry *et al.*, 2010; Song and Colonna, 2018)**, we also anticipated that activated microglia would be related to greater AD neuropathology and fewer neurons, insinuating that activated microglia could be contributing to neurodegenerative processes and cortical atrophy.

The first study included in this dissertation described the neuropathologic basis of *in vivo* cortical atrophy in PPA-AD. Two major findings were reported: 1) NFTs, not APs, accumulated with the hemispheric asymmetry and language region selectivity expected for the PPA-AD clinical profile. Furthermore, NFTs—as well as APs—were significantly greater in left language regions compared to the left memory related entorhinal cortex. Therefore, we provided the first quantitative evidence for NFTs not following the Braak staging characteristic of amnestic AD; 2) only NFTs were significantly related to *in vivo* cortical atrophy in PPA-AD, demonstrating that NFTs could be the primary neuropathologic determinant of atrophy across the clinical AD

spectrum. These important neuropathologic findings in PPA-AD need to be replicated in a larger cohort, and the same analyses should be expanded to other clinical AD variants to validate the significance of NFT neurotoxicity. In an effort to identify the anatomical origins of AD neuropathology in PPA and examine selective vulnerability, it would be interesting to study the patterns of AD neuropathology at earlier stages of the disease course in PPA. In a similar way, other tau and amyloid-β markers could be pursued to examine earlier conformations of NFTs and APs to understand the evolution and propagation of neuropathology as it relates to neurodegenerative processes in the human brain. APs and NFTs are the pathologic hallmarks of AD, but it is not clear which is the initial trigger and more valid drug target. Investigating the genetic risk factors and molecular precursors to AD (e.g., tau and amyloid-β oligomers) in PPA-AD could produce new promising drug candidates and bolster the growing body of work that shows that the tau associated with NFTs could be an important neuropathologic target for earlier interventions that seek to prevent, slow, or cure AD.

The second study evaluated the microglial activation in the white matter of PPA participants to provide insight into how a marker for neuroinflammation was related to regions of high and low cortical atrophy across pathologic subtypes of PPA. In addition to finding that larger densities of activated microglia were present in the cortical white matter compared to gray matter, white matter activated microglia showed a predilection to language regions of peak cortical atrophy in the combined group of PPA participants. More specifically, white matter activated microglia in atrophied regions of the language-dominant hemisphere were significantly greater in atrophied language regions in comparison to their non-atrophied contralateral homologues and non-atrophied regions in the same hemisphere. We also found that the PPA-TDP cohort tended to show more activated microglia compared to the PPA-AD cohort. The prominent microglial activation in white matter of atrophic regions suggests that not only may they be a response to

neurodegeneration, but activated microglia could be exacerbating the disease process through local secretions of inflammatory molecules. It is not currently known what pathologic changes in white matter microglia are responding to or possibly worsening. It is also unclear if one type of proteinopathy can trigger more microglial activation compared to others, thereby potentially altering the course of disease progression. These uncertainties can be addressed in new experiments that identify the status of axons, myelin, and oligodendrocytes in addition to other markers for microglial activation in pathologic subtypes of PPA.

The third and final study returned to investigate the gray matter in PPA-AD to determine how cell densities were related to the AD neuropathology, white matter microglial activation, and *in vivo* cortical atrophy measured in the same regions from the first two studies. The quantified cells included neurons and two microglial phenotypes, RM and HM, with the latter representing the appearance of classic activated microglia that are closely associated with neuropathology and neuroinflammation. We reported for the first time in PPA-AD that microglial phenotypes may have differential involvement in neurodegeneration in PPA-AD. Whereas HM accumulated more in regions with fewer neurons, RM accumulated greater densities in the least atrophic regions with more neurons. Consistent with this dissociation was the fact that HM and RM were inversely related to each other. Since only NFTs were associated with more HM and white matter activated microglia, the microglial response may have been more sensitive to NFTs and the neurotoxic effects they exert compared to APs and other neuropathology. Additionally, not only were densities of HM, white matter activated microglia, and NFTs positively related to each other, each were also negatively associated with neuron densities in PPA-AD. Therefore, while reacting to neuropathologic changes, the activated microglia of the gray and white matter might have also mediated deleterious inflammation that worsened the disease process in PPA-AD.

The cellular substrates of cortical atrophy remain elusive in PPA-AD. When we performed

a small preliminary analysis of neuronal soma surface area in 3/5 PPA-AD cases, we found a reduction in the mean soma size of layer III pyramidal neurons when quantified in a highly atrophic language region (left aIPL) in comparison to its less atrophied contralateral homologue. This early finding in PPA-AD needs validation in a larger analysis, but is consistent with many lines of evidence that show neurons undergo structural changes in the face of neurodegenerative disease **(Coleman and Flood, 1987; DeKosky and Scheff, 1990; Englund and Brun, 1990; Terry *et al.*, 1991; Sjöbeck *et al.*, 2005; Scheff and Price, 2006)**. As neurons bear the increasing burden of intrinsic (NFTs) and extrinsic (APs) neuropathology, it is hypothesized but rarely shown that components of the neurons may slowly shrink or disappear before the entire neuron dies, if at all, by end stage of disease. Therefore, synapse and dendritic loss likely occur, disrupting normal cell signaling that probably constitutes the most prominent neural basis of cognitive dysfunction. However, the extent of axonal loss, cell shrinkage, and overall neuronal health are not yet known in PPA despite potentially being contributory determinants of clinical deficits as well. Identifying these neuronal changes, and how neighboring glial changes influence these alterations remain central questions to the study of the cellular basis of cortical atrophy.

In addition to investigating more forms of cellular changes with new postmortem markers, it will be important to investigate the utility of different MRI-based measurements of cortical atrophy in future studies. The analyses included in this dissertation reported on cortical thickness atrophy in PPA-AD, but the neurobiological basis of cortical surface area and volume remain poorly understood in PPA and other clinical disorders. As described earlier, most of the cortex is organized into cortical layers and columns that appear to have differential vulnerabilities to AD neuropathologic accumulation and neurodegeneration **(Hirano and Zimmerman, 1962; Pearson *et al.*, 1985; Lewis *et al.*, 1987; Arnold *et al.*, 1991; Braak and Braak, 1991; Chance *et al.*, 2011)**. Therefore, determining which MRI measurement of atrophy best captures the selective

neuronal loss and NFT/AP accumulation will provide an important window into disease progression and help validate structural MRI as a valuable biomarker for AD and its variants.

As the current 'ground truth' for pathologic diagnoses, postmortem examinations are needed to validate neuroimaging approaches currently used to characterize pathologic changes in living patients such as PPA. For instance, PET imaging serves potential diagnostic utility in AD given the design of radioligands that tag markers specifically associated with AD neuropathology such as tau, amyloid, and more recently microglia-mediated neuroinflammation. There is promising early evidence that these radiotracers will play an important role in *in vivo* diagnostic evaluation of clinical and research participants with amnestic or non-amnestic presentations of AD, including PPA **(Martersteck *et al.*, 2016; Xia *et al.*, 2017; Dani *et al.*, 2018; Edison *et al.*, 2018; Josephs *et al.*, 2018; Nasrallah *et al.*, 2018a; Whitwell *et al.*, 2018)**. However, it is not clear if the radiotracers used in the PET studies always bind to the selective pathologic marker they were designed to target. To remedy this uncertainty, quantitative postmortem examinations can corroborate the *in vivo* patterns of pathology produced by these PET scans, especially in atypical AD such as PPA. Therefore, the histopathologic findings collected from this PPA-AD cohort will be important to replicate in new PPA-AD cases with PET scans close to death to confirm how these pathologic events are related.

It will also be important to unravel how the same AD neuropathology gives rise to a spectrum of clinical disorders. One of the most fundamental questions that needs to be addressed in future investigations is what confers the differential susceptibility that leads to the clinical AD variants. While the current PPA-AD cohort had no known genetic risk factors, 3 participants had a personal and/or family history of learning disability. Additionally, 2 participants had a family history of either AD or Parkinson's disease. This raises the question of whether there are unidentified genetic and epigenetic effects that can explain why some anatomical regions, layers,

and cell types are prone to AD neuropathology and degeneration. In addition to neuroinflammation, could comorbidities such as vascular disease and non-AD proteinopathies (e.g., TDP-43 and Lewy bodies) play important roles in the disease origin, propagation, and severity? These are just some of the outstanding questions that still need to be answered in PPA-AD and the greater clinical AD spectrum.

These findings in PPA-AD would not have been possible without using quantitative approaches in large regional analyses rarely conducted in bilateral samples of human brains that had undergone MRI scans close to death. This experimental design facilitated the broad assessment of neuropathology, neuroinflammation, neurons, and MRI-based cortical atrophy in anatomically correspondent regions. The resulting relationships established between the antecedents of *in vivo* atrophy provided new insights into the histopathologic basis of PPA-AD, reflecting the feasibility and merit of this line of research.

FINAL REMARKS

These studies on PPA-AD were designed to elucidate the histopathologic correlates of MRI-based cortical atrophy to help pinpoint the most detrimental aspects of AD. This body of work produced several noteworthy findings: 1) new quantitative evidence for NFTs propagating in a unique staging pattern in PPA-AD that diverges from what is typically observed in DAT-AD, 2) the severity and distribution of NFTs suggested that NFTs are important determinants of *in vivo* cortical atrophy and microglial activation in PPA-AD, and 3) NFTs, in conjunction with a neuroinflammatory response mediated by activated microglia, may have contributed to smaller neuron densities leading to the impaired cognition characteristic of the PPA-AD clinical profile.

Taken together, these main results supported the hypothesis that neuropathologic changes, especially NFTs, are associated with inflammatory, structural, and clinical features in PPA-AD. However, the neuroinflammatory and cellular substrates of atrophy remain less clear in PPA-AD,

warranting future research to address this matter. It will be important to confirm the findings presented here in a larger PPA-AD cohort with shorter time intervals between final MRI scan and death. PPA-AD should be compared to reference groups that include other clinical AD variants and age-matched healthy control groups to establish the relative neuropathologic change, glial activation, and neuronal changes. In regions critical to language function, future studies should also identify which neuropathologic and cellular markers are the best predictors of the language impairments characteristic of PPA and its clinical subtypes.

Expanding upon the findings presented in this dissertation poses several benefits to PPA and neurodegenerative research as a whole. Firstly, many neurobiological determinants of neurodegeneration and cognitive impairment still await discovery in PPA-AD and related disorders. Secondly, discerning which postmortem markers have a potential link with pathogenic mutations may advance our understanding of their underlying molecular etiology and guide therapeutic strategies and drug development. Finally, and related to the previous point, these investigations have potential clinical and diagnostic impact. Establishing the histopathologic basis of MRI and clinical phenotypes like PPA-AD will help identify and validate new *in vivo* biomarkers for disease such as amyloid or tau PET imaging. These non-invasive biomarkers can then be used to screen living patients for clinical practice and trial design to properly test disease-modifying therapies in AD.

—REFERENCES—

Agosta F, Galantucci S, Canu E, Cappa SF, Magnani G, Franceschi M, Falini A, Comi G, Filippi M. Disruption of structural connectivity along the dorsal and ventral language pathways in patients with nonfluent and semantic variant primary progressive aphasia: A DT MRI study and a literature review. Brain and Language 2013; 127(2): 157-66.

Alladi S, Xuereb J, Bak T, Nestor P, Knibb J, Patterson K, Hodges JR. Focal cortical presentations of Alzheimer's disease. Brain 2007; 130(Pt 10): 2636-45.

Alonso AC, Zaidi T, Grundke-Iqbal I, Iqbal K. Role of abnormally phosphorylated tau in the breakdown of microtubules in Alzheimer disease. Proceedings of the National Academy of Sciences of the United States of America 1994; 91(12): 5562-6.

Amunts K, Zilles K. Architectonic Mapping of the Human Brain beyond Brodmann. Neuron 2015; 88(6): 1086-107.

Arendt T. Synaptic degeneration in Alzheimer's disease. Acta neuropathologica 2009; 118(1): 167-79.

Arendt T, Brückner MK, Gertz HJ, Marcova L. Cortical distribution of neurofibrillary tangles in Alzheimer's disease matches the pattern of neurons that retain their capacity of plastic remodelling in the adult brain. Neuroscience 1998; 83(4): 991-1002.

Arendt T, Morawski M, Gärtner U, Fröhlich N, Schulze F, Wohmann N, Jäger C, Eisenlöffel C, Gertz H-J, Mueller W, Brauer K. Inhomogeneous distribution of Alzheimer pathology along the isocortical relief. Are cortical convolutions an Achilles heel of evolution? Brain Pathology 2016.

Armstrong MJ, Litvan I, Lang AE, Bak TH, Bhatia KP, Borroni B, Boxer AL, Dickson DW, Grossman M, Hallett M, Josephs KA, Kertesz A, Lee SE, Miller BL, Reich SG, Riley DE, Tolosa E, Troster AI, Vidailhet M, Weiner WJ. Criteria for the diagnosis of corticobasal degeneration. Neurology 2013; 80(5): 496-503.

Armstrong RA. White matter pathology in sporadic frontotemporal lobar degeneration with TDP-43 proteinopathy. Clinical neuropathology 2017; 36 (2017)(2): 66-72.

Arnold SE, Hyman BT, Flory J, Damasio AR, Van Hoesen GW. The topographical and neuroanatomical distribution of neurofibrillary tangles and neuritic plaques in the cerebral cortex of patients with Alzheimer's disease. Cerebral cortex (New York, NY : 1991) 1991; 1(1): 103-16.

Arriagada PV, Growdon JH, Hedley-Whyte ET, Hyman BT. Neurofibrillary tangles but not senile plaques parallel duration and severity of Alzheimer's disease. Neurology 1992; 42(3): 631-.

Asai H, Ikezu S, Tsunoda S, Medalla M, Luebke J, Haydar T, Wolozin B, Butovsky O, Kügler S, Ikezu T. Depletion of microglia and inhibition of exosome synthesis halt tau propagation. Nature Neuroscience 2015; 18(11): 1584-93.

Azevedo FAC, Carvalho LRB, Grinberg LT, Farfel JM, Ferretti REL, Leite REP, Filho WJ, Lent R, Herculano-Houzel S. Equal numbers of neuronal and nonneuronal cells make the human brain an isometrically scaled-up primate brain. The Journal of Comparative Neurology 2009; 513(5): 532-41.

Bachstetter AD, Van Eldik LJ, Schmitt FA, Neltner JH, Ighodaro ET, Webster SJ, Patel E, Abner EL, Kryscio RJ, Nelson PT. Disease-related microglia heterogeneity in the hippocampus of Alzheimer's disease, dementia with Lewy bodies, and hippocampal sclerosis of aging. Acta Neuropathologica Communications 2015; 3(1): 32.

Ballatore C, Lee VMY, Trojanowski JQ. Tau-mediated neurodegeneration in Alzheimer's disease and related disorders. Nature Reviews Neuroscience 2007; 8(9): 663-72.

Barger SW, Harmon AD. Microglial activation by Alzheimer amyloid precursor protein and modulation by apolipoprotein E. Nature 1997; 388(6645): 878-81.

Bierer LM, Hof PR, Purohit DP, Carlin L, Schmeidler J, Davis KL, Perl DP. Neocortical neurofibrillary tangles correlate with dementia severity in Alzheimer's disease. Archives of Neurology 1995; 52(1): 81-8.

Bigio EH. Making the diagnosis of frontotemporal lobar degeneration. Arch Pathol Lab Med 2013; 137(3): 314-25.

Binder LI, Frankfurter A, Rebhun LI. The distribution of tau in the mammalian central nervous system. The Journal of Cell Biology 1985; 101(4): 1371-8.

Block ML, Hong J-S. Microglia and inflammation-mediated neurodegeneration: multiple triggers with a common mechanism. Progress in neurobiology 2005; 76(2): 77-98.

Block ML, Zecca L, Hong J-S. Microglia-mediated neurotoxicity: uncovering the molecular mechanisms. Nature Reviews Neuroscience 2007; 8(1): 57-69.

Bloom GS. Amyloid-β and Tau: The Trigger and Bullet in Alzheimer Disease Pathogenesis. JAMA Neurology 2014; 71(4): 505-8.

Bobinski M, Wegiel J, Wisniewski HM, Tarnawski M, Reisberg B, de Leon MJ, Miller DC. Neurofibrillary pathology--correlation with hippocampal formation atrophy in Alzheimer disease. Neurobiology of Aging 1996; 17(6): 909-19.

Bonakdarpour B, Rogalski EJ, Wang A, Sridhar J, Mesulam MM, Hurley RS. Functional Connectivity is Reduced in Early-stage Primary Progressive Aphasia When Atrophy is not Prominent. Alzheimer disease and associated disorders 2017; 31(2): 101-6.

Boon BDC, Hoozemans JJM, Lopuhaä B, Eigenhuis KN, Scheltens P, Kamphorst W, Rozemuller AJM, Bouwman FH. Neuroinflammation is increased in the parietal cortex of atypical Alzheimer's disease. Journal of Neuroinflammation 2018; 15(1): 170.

Bossù P, Salani F, Alberici A, Archetti S, Bellelli G, Galimberti D, Scarpini E, Spalletta G, Caltagirone C, Padovani A, Borroni B. Loss of function mutations in the progranulin gene are related to pro-inflammatory cytokine dysregulation in frontotemporal lobar degeneration patients. Journal of Neuroinflammation 2011; 8(1): 65.

Böttcher C, Schlickeiser S, Sneeboer MAM, Kunkel D, Knop A, Paza E, Fidzinski P, Kraus L, Snijders GJL, Kahn RS, Schulz AR, Mei HE, Psy NBB, Hol EM, Siegmund B, Glauben R, Spruth EJ, de Witte LD, Priller J. Human microglia regional heterogeneity and phenotypes determined by multiplexed single-cell mass cytometry. Nature Neuroscience 2019; 22(1): 78-90.

Braak H, Braak E. Neuropathological stageing of Alzheimer-related changes. Acta neuropathologica 1991; 82(4): 239-59.

Braak H, Braak E. Staging of Alzheimer's disease-related neurofibrillary changes. 1995; 16(3): 271-8- discussion 8-84.

Braak H, Braak E. Evolution of the neuropathology of Alzheimer's disease. Acta neurologica Scandinavica Supplementum 1996; 165: 3-12.

Braak H, Braak E. Evolution of neuronal changes in the course of Alzheimer's disease. Journal of neural transmission Supplementum 1998; 53: 127-40.

Braak H, Del Tredici K, Schultz C, Braak E. Vulnerability of Select Neuronal Types to Alzheimer's Disease. Annals of the New York Academy of Sciences 2000; 924(1): 53-61.

Brambati SM, Amici S, Racine CA, Neuhaus J, Miller Z, Ogar J, Dronkers N, Miller BL, Rosen H, Gorno-Tempini ML. Longitudinal gray matter contraction in three variants of primary progressive aphasia: A tenser-based morphometry study. NeuroImage: Clinical 2015; 8: 345-55.

Brettschneider J, Tredici KD, Lee VMY, Trojanowski JQ. Spreading of pathology in neurodegenerative diseases: a focus on human studies. Nature Reviews Neuroscience 2015; 16(2): 109-20.

Broe M, Hodges JR, Schofield E, Shepherd CE, Kril JJ, Halliday GM. Staging disease severity in pathologically confirmed cases of frontotemporal dementia. Neurology 2003; 60(6): 1005-11.

Broe M, Kril J, Halliday GM. Astrocytic degeneration relates to the severity of disease in frontotemporal dementia. Brain 2004; 127(Pt 10): 2214-20.

Brun A, Englund E. Regional pattern of degeneration in Alzheimer's disease: neuronal loss and histopathological grading. Histopathology 1981; 5(5): 549-64.

Burton EJ, Barber R, Mukaetova-Ladinska EB, Robson J, Perry RH, Jaros E, Kalaria RN, O'Brien JT. Medial temporal lobe atrophy on MRI differentiates Alzheimer's disease from dementia with Lewy bodies and vascular cognitive impairment: a prospective study with pathological verification of diagnosis. Brain 2009; 132(Pt 1): 195-203.

Burton EJ, Ladinska EBM, Perry RH, Jaros E, Barber R, O'Brien JT. Quantitative neurodegenerative pathology does not explain the degree of hippocampal atrophy on MRI in degenerative dementia. International Journal of Geriatric Psychiatry 2012; 27(12): 1267-74.

Busciglio J, Lorenzo A, Yeh J, Yankner BA. beta-amyloid fibrils induce tau phosphorylation and loss of microtubule binding. Neuron 1995; 14(4): 879-88.

Cairns NJ, Bigio EH, Mackenzie IRA, Neumann M, Lee VMY, Hatanpaa KJ, White CL, Schneider JA, Grinberg LT, Halliday G, Duyckaerts C, Lowe JS, Holm IE, Tolnay M, Okamoto K, Yokoo H, Murayama S, Woulfe J, Munoz DG, Dickson DW, Ince PG, Trojanowski JQ, Mann DMA. Neuropathologic diagnostic and nosologic criteria for frontotemporal lobar degeneration: consensus of the Consortium for Frontotemporal Lobar Degeneration. Acta neuropathologica 2007; 114(1): 5-22.

Caso F, Agosta F, Filippi M. Insights into White Matter Damage in Alzheimer's Disease: From Postmortem to in vivo Diffusion Tensor MRI Studies. Neurodegenerative Diseases 2015.

Catani M, Piccirilli M, Cherubini A, Tarducci R, Sciarma T, Gobbi G, Pelliccioli G, Petrillo SM, Senin U, Mecocci P. Axonal injury within language network in primary progressive aphasia. Annals of Neurology 2003; 53(2): 242-7.

Chance SA, Clover L, Cousijn H, Currah L, Pettingill R, Esiri MM. Microanatomical correlates of cognitive ability and decline: normal ageing, MCI, and Alzheimer's disease. Cerebral Cortex 2011; 21(8): 1870-8.

Cohen TJ, Lee VMY, Trojanowski JQ. TDP-43 functions and pathogenic mechanisms implicated in TDP-43 proteinopathies. Trends in Molecular Medicine 2011; 17(11): 659-67.

Coleman PD, Flood DG. Neuron numbers and dendritic extent in normal aging and Alzheimer's disease. Neurobiology of Aging 1987; 8(6): 521-45.

Collins CE, Airey DC, Young NA, Leitch DB, Kaas JH. Neuron densities vary across and within cortical areas in primates. Proceedings of the National Academy of Sciences 2010.

Collins-Praino LE, Francis YI, Griffith EY, Wiegman AF, Urbach J, Lawton A, Honig LS, Cortes E, Vonsattel JPG, Canoll PD, Goldman JE, Brickman AM. Soluble amyloid beta levels are elevated in the white matter of Alzheimer's patients, independent of cortical plaque severity. Acta Neuropathologica Communications 2014; 2(1): 137.

Crutch SJ, Schott JM, Rabinovici GD, Murray M, Snowden JS, van der Flier WM, Dickerson BC, Vandenberghe R, Ahmed S, Bak TH, Boeve BF, Butler C, Cappa SF, Ceccaldi M, de Souza LC, Dubois B, Felician O, Galasko D, Graff-Radford J, Graff-Radford NR, Hof PR,

Krolak-Salmon P, Lehmann M, Magnin E, Mendez MF, Nestor PJ, Onyike CU, Pelak VS, Pijnenburg Y, Primativo S, Rossor MN, Ryan NS, Scheltens P, Shakespeare TJ, Suárez González A, Tang-Wai DF, Yong KXX, Carrillo M, Fox NC. Consensus classification of posterior cortical atrophy. Alzheimer's & Dementia 2017; 13(8): 870-84.

Csernansky JG, Hamstra J, Wang L, McKeel D, Price JL, Gado M, Morris JC. Correlations between antemortem hippocampal volume and postmortem neuropathology in AD subjects. Alzheimer disease and associated disorders 2004; 18(4): 190-5.

D'Anna L, Mesulam MM, Thiebaut de Schotten M, Dell'Acqua F, Murphy D, Wieneke C, Martersteck A, Cobia D, Rogalski E, Catani M. Frontotemporal networks and behavioral symptoms in primary progressive aphasia. Neurology 2016; 86(15): 1393-9.

da Silva RP, Gordon S. Phagocytosis stimulates alternative glycosylation of macrosialin (mouse CD68), a macrophage-specific endosomal protein. The Biochemical journal 1999; 338 (Pt 3)(Pt 3): 687-94.

Dale AM, Fischl B, Sereno MI. Cortical Surface-Based Analysis. NeuroImage 1999; 9(2): 179-94.

Dallaire-Théroux C, Callahan BL, Potvin O, Saikali S, Duchesne S. Radiological-Pathological Correlation in Alzheimer's Disease: Systematic Review of Antemortem Magnetic Resonance Imaging Findings. J Alzheimers Dis 2017; 57(2): 575-601.

Dani M, Wood M, Mizoguchi R, Fan Z, Walker Z, Morgan R, Hinz R, Biju M, Kuruvilla T, Brooks DJ, Edison P. Microglial activation correlates in vivo with both tau and amyloid in Alzheimer's disease. Brain 2018; 173(Pt 6): 44.

de Calignon A, Polydoro M, Suárez-Calvet M, William C, Adamowicz DH, Kopeikina KJ, Pitstick R, Sahara N, Ashe KH, Carlson GA, Spires-Jones TL, Hyman BT. Propagation of Tau Pathology in a Model of Early Alzheimer's Disease. Neuron 2012; 73(4): 685-97.

De Tribolet N, Hamou MF, Mach JP, Carrel S, Schreyer M. Demonstration of HLA-DR antigens in normal human brain. 1984; 47(4): 417-8.

DeKosky ST, Scheff SW. Synapse loss in frontal cortex biopsies in Alzheimer's disease: Correlation with cognitive severity. Annals of Neurology 1990; 27(5): 457-64.

del C Alonso A, Grundke-Iqbal I, Iqbal K. Alzheimer's disease hyperphosphorylated tau sequesters normal tau into tangles of filaments and disassembles microtubules. Nature Medicine 1996; 2(7): 783-7.

Del Rio-Hortega P. Are the glia with very few processes homologous with Schwann cells? by Pío del Río-Hortega. 1922; 2012.

Deramecourt V, Lebert F, Debachy B, Mackowiak-Cordoliani MA, Bombois S, Kerdraon O, Buee L, Maurage CA, Pasquier F. Prediction of pathology in primary progressive language and speech disorders. Neurology 2009; 74(1): 42-9.

Desikan RS, Ségonne F, Fischl B, Quinn BT, Dickerson BC, Blacker D, Buckner RL, Dale AM, Maguire RP, Hyman BT, Albert MS, Killiany RJ. An automated labeling system for subdividing the human cerebral cortex on MRI scans into gyral based regions of interest. NeuroImage 2006; 31(3): 968-80.

Edison P, Donat CK, Sastre M. In vivo Imaging of Glial Activation in Alzheimer's Disease. Frontiers in neurology 2018; 9: 625.

Englund E, Brun A. White matter changes in dementia of Alzheimer's type: the difference in vulnerability between cell compartments. Histopathology 1990; 16(5): 433-9.

Eriksson SH, Free SL, Thom M, Symms MR, Martinian L, Duncan JS, Sisodiya SM. Quantitative grey matter histological measures do not correlate with grey matter probability values from in vivo MRI in the temporal lobe. Journal of Neuroscience Methods 2009; 181(1): 111-8.

Erten-Lyons D, Dodge HH, Woltjer R, Silbert LC, Howieson DB, Kramer P, Kaye JA. Neuropathologic basis of age-associated brain atrophy. JAMA Neurology 2013; 70(5): 616-22.

Fan Z, Brooks DJ, Okello A, Edison P. An early and late peak in microglial activation in Alzheimer's disease trajectory. Brain 2017; 124: aww349.

Femminella GD, Ninan S, Atkinson R, Fan Z, Brooks DJ, Edison P. Does Microglial Activation Influence Hippocampal Volume and Neuronal Function in Alzheimer's Disease and Parkinson's Disease Dementia? JAD 2016; 51(4): 1275-89.

Fischl B, Dale AM. Measuring the thickness of the human cerebral cortex from magnetic resonance images. Proceedings of the National Academy of Sciences of the United States of America 2000; 97(20): 11050-5.

Fischl B, van der Kouwe A, Destrieux C, Halgren E, Ségonne F, Salat DH, Busa E, Seidman LJ, Goldstein J, Kennedy D, Caviness V, Makris N, Rosen B, Dale AM. Automatically parcellating the human cerebral cortex. Cerebral cortex (New York, NY : 1991) 2004; 14(1): 11-22.

Forman MS, Farmer J, Johnson JK, Clark CM, Arnold SE, Coslett HB, Chatterjee A, Hurtig HI, Karlawish JH, Rosen HJ, Van Deerlin V, Lee VMY, Miller BL, Trojanowski JQ, Grossman M. Frontotemporal dementia: Clinicopathological correlations. Annals of Neurology 2006; 59(6): 952-62.

Freeman SH, Kandel R, Cruz L, Rozkalne A, Newell K, Frosch MP, Hedley-Whyte ET, Locascio JJ, Lipsitz LA, Hyman BT. Preservation of neuronal number despite age-related cortical brain atrophy in elderly subjects without Alzheimer disease. Journal of neuropathology and experimental neurology 2008; 67(12): 1205-12.

Frings L, Yew B, Flanagan E, Lam BYK, Hüll M, Huppertz H-J, Hodges JR, Hornberger M. Longitudinal Grey and White Matter Changes in Frontotemporal Dementia and Alzheimer's Disease. PLoS ONE 2014; 9(3): e90814.

Frisoni GB, Fox NC, Jack CR, Scheltens P, Thompson PM. The clinical use of structural MRI in Alzheimer disease. Nature Reviews Neurology 2010; 6(2): 67-77.

Frisoni GB, Pievani M, Testa C, Sabattoli F, Bresciani L, Bonetti M, Beltramello A, Hayashi KM, Toga AW, Thompson PM. The topography of grey matter involvement in early and late onset Alzheimer's disease. Brain 2007; 130(3): 720-30.

Galantucci S, Tartaglia MC, Wilson SM, Henry ML, Filippi M, Agosta F, Dronkers NF, Henry RG, Ogar JM, Miller BL, Gorno-Tempini ML. White matter damage in primary progressive aphasias: a diffusion tensor tractography study. Brain 2011; 134(Pt 10): 3011-29.

Galton CJ, Patterson K, Xuereb JH, Hodges JR. Atypical and typical presentations of Alzheimer's disease: a clinical, neuropsychological, neuroimaging and pathological study of 13 cases. Brain 2000; 123 Pt 3: 484-98.

Gefen T, Gasho K, Rademaker A, Lalehzari M, Weintraub S, Rogalski E, Wieneke C, Bigio E, Geula C, Mesulam MM. Clinically concordant variations of Alzheimer pathology in aphasic versus amnestic dementia. Brain 2012; 135(Pt 5): 1554-65.

Gehrmann J, Banati RB, Kreutzberg GW. Microglia in the immune surveillance of the brain: human microglia constitutively express HLA-DR molecules. 1993; 48(2): 189-98.

Genovese CR, Lazar NA, Nichols T. Thresholding of Statistical Maps in Functional Neuroimaging Using the False Discovery Rate. NeuroImage 2002; 15(4): 870-8.

Geula C, Nagykery N, Nicholas A, Wu C-K. Cholinergic Neuronal and Axonal Abnormalities Are Present Early in Aging and in Alzheimer Disease. Journal of neuropathology and experimental neurology 2008; 67(4): 309-18.

Ghosh S, Wu MD, Shaftel SS, Kyrkanides S, LaFerla FM, Olschowka JA, O'Banion MK. Sustained Interleukin-1 Overexpression Exacerbates Tau Pathology Despite Reduced Amyloid Burden in an Alzheimer's Mouse Model. The Journal of neuroscience : the official journal of the Society for Neuroscience 2013; 33(11): 5053-64.

Giannakopoulos P, Herrmann FR, Bussière T, Bouras C, Kövari E, Perl DP, Morrison JH, Gold G, Hof PR. Tangle and neuron numbers, but not amyloid load, predict cognitive status in Alzheimer's disease. Neurology 2003; 60(9): 1495-500.

Glenner GG, Wong CW. Alzheimer's disease: initial report of the purification and characterization of a novel cerebrovascular amyloid protein. Biochem Biophys Res Commun 1984; 120(3): 885-90.

Gomez-Isla T, Hollister R, West H, Mui S, Growdon JH, Petersen RC, Parisi JE, Hyman BT. Neuronal loss correlates with but exceeds neurofibrillary tangles in Alzheimer's disease. Annals of Neurology 1997; 41(1): 17-24.

Gomez-Isla T, Price JL, McKeel DW, Morris JC, growdon JH, Hyman BT. Profound loss of layer II entorhinal cortex neurons occurs in very mild Alzheimer's disease. The Journal of neuroscience : the official journal of the Society for Neuroscience 1996; 16(14): 4491-500.

Gomez-Nicola D, Fransen NL, Suzzi S, Perry VH. Regulation of Microglial Proliferation during Chronic Neurodegeneration. The Journal of neuroscience : the official journal of the Society for Neuroscience 2013; 33(6): 2481-93.

Gorno-Tempini ML, Hillis AE, Weintraub S, Kertesz A, Mendez M, Cappa SF, Ogar JM, Rohrer JD, Black S, Boeve BF, Manes F, Dronkers NF, Vandenberghe R, Rascovsky K, Patterson K, Miller BL, Knopman DS, Hodges JR, Mesulam MM, Grossman M. Classification of primary progressive aphasia and its variants. Neurology; 2011 2011/03/15; 2011. p. 1006-14.

Gorno-Tempini ML, Miller BL. Primary Progressive Aphasia as a model to study the neurobiology of language. Brain and Language 2013; 127(2): 105.

Grinberg LT, Rub U, Ferretti REL, Nitrini R, Farfel JM, Polichiso L, Gierga K, Filho WJ, Heinsen H. The dorsal raphe nucleus shows phospho-tau neurofibrillary changes before the transentorhinal region in Alzheimer's disease. A precocious onset? Neuropathology and Applied Neurobiology 2009; 35(4): 406-16.

Grossman M. Primary progressive aphasia: clinicopathological correlations. Nature Reviews Neurology 2010; 6(2): 88-97.

Grossman M. Biomarkers in the primary progressive aphasias. Aphasiology 2014; 28(8-9): 922-40.

Grudzien A, Shaw P, Weintraub S, Bigio E, Mash DC, Mesulam MM. Locus coeruleus neurofibrillary degeneration in aging, mild cognitive impairment and early Alzheimer's disease. Neurobiology of Aging 2007; 28(3): 327-35.

Han P, Shi J. A Theoretical Analysis of the Synergy of Amyloid and Tau in Alzheimer's Disease. J Alzheimers Dis 2016; 52(4): 1461-70.

Hardy JA, Higgins GA. Alzheimers-Disease - the Amyloid Cascade Hypothesis. Science 1992; 256(5054): 184-5.

Harris JM, Gall C, Thompson JC, Richardson AMT, Neary D, du Plessis D, Pal P, Mann DMA, Snowden JS, Jones M. Classification and pathology of primary progressive aphasia. neurologyorg 2013.

Herculano-Houzel S. The human brain in numbers: a linearly scaled-up primate brain. Frontiers in Human Neuroscience 2009; 3: 31.

Hirano A, Zimmerman HM. Alzheimer's neurofibrillary changes. A topographic study. Archives of Neurology 1962; 7: 227-42.

Hodges JR, Davies RR, Xuereb JH, Casey B, Broe M, Bak TH, Kril JJ, Halliday GM. Clinicopathological correlates in frontotemporal dementia. Annals of Neurology 2004; 56(3): 399-406.

Hof PR, Archin N, Osmand AP, Dougherty JH, Wells C, Bouras C, Morrison JH. Posterior cortical atrophy in Alzheimer's disease: analysis of a new case and re-evaluation of a historical report. Acta neuropathologica 1993; 86(3): 215-23.

Hof PR, Bouras C, Constantinidis J, Morrison JH. Balint's syndrome in Alzheimer's disease: specific disruption of the occipito-parietal visual pathway. Brain Research 1989; 493(2): 368-75.

Hopperton KE, Mohammad D, Trépanier MO, Giuliano V, Bazinet RP. Markers of microglia in post-mortem brain samples from patients with Alzheimer's disease: a systematic review. Molecular psychiatry 2018; 23(2): 177-98.

Hutton C, Draganski B, Ashburner J, Weiskopf N. A comparison between voxel-based cortical thickness and voxel-based morphometry in normal aging. NeuroImage 2009; 48(2): 371-80.

Hyman BT, Phelps CH, Beach TG, Bigio EH, Cairns NJ, Carrillo MC, Dickson DW, Duyckaerts C, Frosch MP, Masliah E, Mirra SS, Nelson PT, Schneider JA, Thal DR, Thies B, Trojanowski JQ, Vinters HV, Montine TJ. National Institute on Aging–Alzheimer's Association guidelines for the neuropathologic assessment of Alzheimer's disease. Alzheimer's & Dementia 2012; 8(1): 1-13.

Iqbal K, Liu F, Gong C-X. Tau and neurodegenerative disease: the story so far. Nature Reviews Neurology 2015; 12(1): 15-27.

Itagaki S, McGeer PL, Akiyama H, Zhu S, Selkoe D. Relationship of microglia and astrocytes to amyloid deposits of Alzheimer disease. Journal of Neuroimmunology 1989; 24(3): 173-82.

Jack CR, Dickson DW, Parisi JE, Xu YC, Cha RH, O'Brien PC, Edland SD, Smith GE, Boeve BF, Tangalos EG, Kokmen E, Petersen RC. Antemortem MRI findings correlate with hippocampal neuropathology in typical aging and dementia. Neurology 2002; 58(5): 750-7.

Jack CR, Knopman DS, Jagust WJ, Shaw LM, Aisen PS, Weiner MW, Petersen RC, Trojanowski JQ. Hypothetical model of dynamic biomarkers of the Alzheimer's pathological cascade. The Lancet Neurology 2010; 9(1): 119-28.

Jack Jr CR, Knopman DS, Jagust WJ, Petersen RC, Weiner MW, Aisen PS, Shaw LM, Vemuri P, Wiste HJ, Weigand SD, Lesnick TG, Pankratz VS, Donohue MC, Trojanowski JQ. Tracking pathophysiological processes in Alzheimer's disease: an updated hypothetical model of dynamic biomarkers. The Lancet Neurology 2013; 12(2): 207-16.

Jagust WJ, Zheng L, Harvey DJ, Mack WJ, Vinters HV, Weiner MW, Ellis WG, Zarow C, Mungas D, Reed BR, Kramer JH, Schuff N, DeCarli C, Chui HC. Neuropathological basis of magnetic resonance images in aging and dementia. Annals of Neurology 2008; 63(1): 72-80.

Johnson JK, Head E, Kim R, Starr A, Cotman CW. Clinical and Pathological Evidence for a Frontal Variant of Alzheimer Disease. Archives of Neurology 1999; 56(10): 1233-9.

Josephs KA, Dickson DW, Murray ME, Senjem ML, Parisi JE, Petersen RC, Jack CR, Whitwell JL. Quantitative neurofibrillary tangle density and brain volumetric MRI analyses in Alzheimer's disease presenting as logopenic progressive aphasia. Brain and Language 2013; 127(2): 127-34.

Josephs KA, Martin PR, Botha H, Schwarz CG, Duffy JR, Clark HM, Machulda MM, Graff-Radford J, Weigand SD, Senjem ML, Utianski RL, Drubach DA, Boeve BF, Jones DT, Knopman DS, Petersen RC, Jack CR, Lowe VJ, Whitwell JL. [18F]AV-1451 tau-PET and primary progressive aphasia. Annals of Neurology 2018; 83(3): 599-611.

Josephs KA, Whitwell JL, Ahmed Z, Shiung MM, Weigand SD, Knopman DS, Boeve BF, Parisi JE, Petersen RC, Dickson DW, Jack CR. Beta-amyloid burden is not associated with rates of brain atrophy. Annals of Neurology 2008; 63(2): 204-12.

Kang J, Lemaire H-G, Unterbeck A, Salbaum JM, Masters CL, Grzeschik K-H, Multhaup G, Beyreuther K, Müller-Hill B. The precursor of Alzheimer's disease amyloid A4 protein resembles a cell-surface receptor. Nature 1987; 325(6106): 733-6.

Kaur B, Himali JJ, Seshadri S, Beiser AS, Au R, McKee AC, Auerbach S, Wolf PA, DeCarli CS. Association between neuropathology and brain volume in the Framingham Heart Study. Alzheimer disease and associated disorders 2014; 28(3): 219-25.

Kersaitis C, Halliday GM, Kril JJ. Regional and cellular pathology in frontotemporal dementia: relationship to stage of disease in cases with and without Pick bodies. Acta neuropathologica 2004; 108(6): 515-23.

Kertesz A, McMonagle P, Blair M, Davidson W, Munoz DG. The evolution and pathology of frontotemporal dementia. Brain 2005; 128(Pt 9): 1996-2005.

Kim G, Ahmadian SS, Peterson M, Parton Z, Memon R, Weintraub S, Rademaker A, Bigio E, Mesulam MM, Geula C. Asymmetric pathology in primary progressive aphasia with progranulin mutations and TDP inclusions. Neurology 2016; 86(7): 627-36.

Kim G, Bolbolan K, Gefen T, Weintraub S, Bigio EH, Rogalski E, Mesulam M-M, Geula C. Atrophy and microglial distribution in primary progressive aphasia with TDP-43. Annals of Neurology 2018; 83(pt 8): 1184.

Knibb JA, Xuereb JH, Patterson K, Hodges JR. Clinical and pathological characterization of progressive aphasia. Annals of Neurology 2006; 59(1): 156-65.

Knopman DS, Roberts RO. Estimating the Number of Persons with Frontotemporal Lobar Degeneration in the US Population. Journal of Molecular Neuroscience 2011; 45(3): 330-5.

Kosik KS, Joachim CL, Selkoe DJ. Microtubule-associated protein tau (tau) is a major antigenic component of paired helical filaments in Alzheimer disease. Proceedings of the National Academy of Sciences of the United States of America 1986; 83(11): 4044-8.

Koss DJ, Jones G, Cranston A, Gardner H, Kanaan NM, Platt B. Soluble pre-fibrillar tau and β-amyloid species emerge in early human Alzheimer's disease and track disease progression and cognitive decline. Acta neuropathologica 2016; 132(6): 875-95.

Kramer JH, Miller BL. Alzheimer's Disease and Its Focal Variants. 2000; 20(04): 447-54.

Kreisl WC. Discerning the relationship between microglial activation and Alzheimer's disease. Brain 2017; 140(7): 1825-8.

Kreutzberg GW. Microglia: a sensor for pathological events in the CNS. Trends in Neurosciences 1996; 19(8): 312-8.

Kril JJ, Hodges J, Halliday G. Relationship between hippocampal volume and CA1 neuron loss in brains of humans with and without Alzheimer's disease. Neuroscience Letters 2004; 361(1-3): 9-12.

Lall D, Baloh RH. Microglia and C9orf72 in neuroinflammation and ALS and frontotemporal dementia. The Journal of Clinical Investigation 2017; 127(9): 3250-8.

Lam BYK, Halliday GM, Irish M, Hodges JR, Piguet O. Longitudinal white matter changes in frontotemporal dementia subtypes. Human Brain Mapping 2014; 35(7): 3547-57.

Lambert MP, Barlow AK, Chromy BA, Edwards C, Freed R, Liosatos M, Morgan TE, Rozovsky I, Trommer B, Viola KL, Wals P, Zhang C, Finch CE, Krafft GA, Klein WL. Diffusible, nonfibrillar ligands derived from Abeta1-42 are potent central nervous system neurotoxins. Proceedings of the National Academy of Sciences of the United States of America 1998; 95(11): 6448-53.

Lant SB, Robinson AC, Thompson JC, Rollinson S, Pickering-Brown S, Snowden JS, Davidson YS, Gerhard A, Mann DMA. Patterns of microglial cell activation in frontotemporal lobar degeneration. Neuropathology and Applied Neurobiology 2014; 40(6): 686-96.

Lee EB, Porta S, Michael Baer G, Xu Y, Suh E, Kwong LK, Elman L, Grossman M, Lee VMY, Irwin DJ, Van Deerlin VM, Trojanowski JQ. Expansion of the classification of FTLD-TDP: distinct pathology associated with rapidly progressive frontotemporal degeneration. Acta neuropathologica 2017; 134(1): 65-78.

Lewis DA, Campbell MJ, Terry RD, Morrison JH. Laminar and regional distributions of neurofibrillary tangles and neuritic plaques in Alzheimer's disease: a quantitative study of

visual and auditory cortices. The Journal of neuroscience : the official journal of the Society for Neuroscience 1987; 7(6): 1799-808.

Li Y, Liu L, Barger SW, Griffin WST. Interleukin-1 mediates pathological effects of microglia on tau phosphorylation and on synaptophysin synthesis in cortical neurons through a p38-MAPK pathway. Journal of Neuroscience 2003; 23(5): 1605-11.

Liu L, Drouet V, Wu JW, Witter MP, Small SA, Clelland C, Duff K. Trans-synaptic spread of tau pathology in vivo. PLoS ONE 2012; 7(2): e31302.

Lorenzo A, Yankner BA. Beta-amyloid neurotoxicity requires fibril formation and is inhibited by congo red. Proceedings of the National Academy of Sciences of the United States of America 1994; 91(25): 12243-7.

Mackenzie IR, Neumann M. Reappraisal of TDP-43 pathology in FTLD-U subtypes. Acta neuropathologica 2017; 134(1): 79-96.

Mackenzie IRA, Neumann M, Baborie A, Sampathu DM, du Plessis D, Jaros E, Perry RH, Trojanowski JQ, Mann DMA, Lee VMY. A harmonized classification system for FTLD-TDP pathology. Acta neuropathologica 2011; 122(1): 111-3.

Mahoney CJ, Malone IB, Ridgway GR, Buckley AH, Downey LE, Golden HL, Ryan NS, Ourselin S, Schott JM, Rossor MN, Fox NC, Warren JD. White matter tract signatures of the progressive aphasias. Neurobiology of Aging 2013; 34(6): 1687-99.

Maphis N, Xu G, Kokiko-Cochran ON, Jiang S, Cardona A, Ransohoff RM, Lamb BT, Bhaskar K. Reactive microglia drive tau pathology and contribute to the spreading of pathological tau in the brain. Brain 2015; 138(6): 1738-55.

Martens LH, Zhang J, Barmada SJ, Zhou P, Kamiya S, Sun B, Min S-W, Gan L, Finkbeiner S, Huang EJ, Farese RV. Progranulin deficiency promotes neuroinflammation and neuron loss following toxin-induced injury. The Journal of Clinical Investigation 2012; 122(11): 3955-9.

Martersteck A, Murphy C, Rademaker A, Wieneke C, Weintraub S, Chen K, Mesulam MM, Rogalski E. Is in vivo amyloid distribution asymmetric in primary progressive aphasia? Annals of Neurology 2016; 79(3): 496-501.

Masliah E, Crews L, Hansen L. Synaptic remodeling during aging and in Alzheimer's disease. J Alzheimers Dis 2006; 9(3 Suppl): 91-9.

Masliah E, Honer WG, Mallory M, Voigt M, Kushner P, Hansen L, Terry R. Topographical distribution of synaptic-associated proteins in the neuritic plaques of Alzheimer's disease hippocampus. Acta neuropathologica 1994; 87(2): 135-42.

Masliah E, Terry RD, Mallory M, Alford M, Hansen LA. Diffuse plaques do not accentuate synapse loss in Alzheimer's disease. The American journal of pathology 1990; 137(6): 1293-7.

Mattiace LA, Davies P, Dickson DW. Detection of HLA-DR on microglia in the human brain is a function of both clinical and technical factors. The American journal of pathology 1990; 136(5): 1101-14.

McGeer PL, Itagaki S, McGeer EG. Expression of the histocompatibility glycoprotein HLA-DR in neurological disease. Acta neuropathologica 1988; 76(6): 550-7.

McGeer PL, Itagaki S, Tago H, McGeer EG. Reactive microglia in patients with senile dementia of the Alzheimer type are positive for the histocompatibility glycoprotein HLA-DR. Neuroscience Letters 1987.

McGeer PL, McGeer EG. Inflammation, autotoxicity and Alzheimer disease. Neurobiology of Aging 2001; 22(6): 799-809.

McKhann GM, Knopman DS, Chertkow H. The diagnosis of dementia due to Alzheimer's disease: Recommendations from the National Institute on Aging-Alzheimer's Association workgroups on diagnostic guidelines for Alzheimer's disease. Alzheimer's & Dementia 2011; 7(263-269).

Mesulam M. The cholinergic lesion of Alzheimer's disease: pivotal factor or side show? Learn Mem 2004; 11(1): 43-9.

Mesulam M, Weintraub S, Parrish T, Gitelman D. Primary progressive aphasia: reversed asymmetry of atrophy and right hemisphere language dominance. Neurology 2005; 64(3): 556-7.

Mesulam M, Wicklund A, Johnson N, Rogalski E, Léger GC, Rademaker A, Weintraub S, Bigio EH. Alzheimer and frontotemporal pathology in subsets of primary progressive aphasia. Annals of Neurology 2008; 63(6): 709-19.

Mesulam MM. Slowly progressive aphasia without generalized dementia. Annals of Neurology 1982; 11(6): 592-8.

Mesulam MM. Neuroplasticity Failure Review in Alzheimer's Disease: Bridging the Gap between Plaques and Tangles. Neuron 1999; 24(3): 521-9.

Mesulam MM. Primary progressive aphasia. Annals of Neurology 2001; 49(4): 425-32.

Mesulam MM. Primary Progressive Aphasia — A Language-Based Dementia. New England Journal of Medicine 2003; 349(16): 1535-42.

Mesulam MM, Rogalski EJ, Wieneke C, Hurley RS, Geula C, Bigio EH, Thompson CK, Weintraub S. Primary progressive aphasia and the evolving neurology of the language network. Nature Reviews Neurology 2014a; 10(10): 554-69.

Mesulam MM, Weintraub S, Rogalski EJ, Wieneke C, Geula C, Bigio EH. Asymmetry and heterogeneity of Alzheimer's and frontotemporal pathology in primary progressive aphasia. Brain 2014b; 137(4): 1176-92.

Meyer M, Liem F, Hirsiger S, Jancke L, Hanggi J. Cortical Surface Area and Cortical Thickness Demonstrate Differential Structural Asymmetry in Auditory-Related Areas of the Human Cortex. Cerebral Cortex 2013; 24(10): 2541-52.

Migliaccio R, Agosta F, Possin KL, Rabinovici GD, Miller BL, Gorno-Tempini ML. White matter atrophy in Alzheimer's disease variants. Alzheimer's & Dementia 2012; 8(5): S78-S87.e2.

Miller ZA, Rankin KP, Graff-Radford NR, Takada LT, Sturm VE, Cleveland CM, Criswell LA, Jaeger PA, Stan T, Heggeli KA, Hsu SC, Karydas A, Khan BK, Grinberg LT, Gorno-Tempini ML, Boxer AL, Rosen HJ, Kramer JH, Coppola G, Geschwind DH, Rademakers R, Seeley WW, Wyss-Coray T, Miller BL. TDP-43 frontotemporal lobar degeneration and autoimmune disease. Journal of neurology, neurosurgery, and psychiatry 2013; 84(9): 956-62.

Miller ZA, Sturm VE, Camsari GB, Karydas A, Yokoyama JS, Grinberg LT, Boxer AL, Rosen HJ, Rankin KP, Gorno-Tempini ML, Coppola G, Geschwind DH, Rademakers R, Seeley WW, Graff-Radford NR, Miller BL. Increased prevalence of autoimmune disease within C9 and FTD/MND cohorts: Completing the picture. Neurol Neuroimmunol Neuroinflamm 2016; 3(6): e301.

Möller C, Vrenken H, Jiskoot L, Versteeg A, Barkhof F, Scheltens P, van der Flier WM. Different patterns of gray matter atrophy in early- and late-onset Alzheimer's disease. Neurobiology of Aging 2013; 34(8): 2014-22.

Montine TJ, Phelps CH, Beach TG, Bigio EH, Cairns NJ, Dickson DW, Duyckaerts C, Frosch MP, Masliah E, Mirra SS, Nelson PT, Schneider JA, Thal DR, Trojanowski JQ, Vinters HV, Hyman BT, National Institute on A, Alzheimer's A. National Institute on Aging-Alzheimer's Association guidelines for the neuropathologic assessment of Alzheimer's disease: a practical approach. Acta neuropathologica: Springer-Verlag; 2012. p. 1-11.

Moossy J, Zubenko GS, Martinez AJ, Rao GR. Bilateral symmetry of morphologic lesions in Alzheimer's disease. Archives of Neurology 1988; 45(3): 251-4.

Morrison JH, Hof PR. Life and death of neurons in the aging brain. Science 1997; 278(5337): 412-9.

Mosser DM, Edwards JP. Exploring the full spectrum of macrophage activation. Nature reviews Immunology 2008; 8(12): 958-69.

Mountcastle VB. Modality and topographic properties of single neurons of cat's somatic sensory cortex. Journal of neurophysiology 1957; 20(4): 408-34.

Mountcastle VB. The columnar organization of the neocortex. Brain 1997; 120 (Pt 4): 701-22.

Nasrallah IM, Chen YJ, Hsieh M-K, Phillips JS, Ternes K, Stockbower GE, Sheline Y, McMillan CT, Grossman M, Wolk DA. 18F-Flortaucipir PET/MRI Correlations in Nonamnestic and Amnestic Variants of Alzheimer Disease. Journal of nuclear medicine : official publication, Society of Nuclear Medicine 2018a; 59(2): 299-306.

Nasrallah IM, Chen YJ, Hsieh M-K, Phillips JS, Ternes K, Stockbower GE, Sheline Y, McMillan CT, Grossman M, Wolk DA. 18F-Flortaucipir PET/MRI Correlations in Nonamnestic and Amnestic Variants of Alzheimer Disease. Journal of nuclear medicine : official publication, Society of Nuclear Medicine 2018b; 59(2): 299-306.

Neumann M, Kwong LK, Truax AC, Vanmassenhove B, Kretzschmar HA, Van Deerlin VM, Clark CM, Grossman M, Miller BL, Trojanowski JQ, Lee VMY. TDP-43-positive white matter pathology in frontotemporal lobar degeneration with ubiquitin-positive inclusions. Journal of neuropathology and experimental neurology 2007; 66(3): 177-83.

Neumann M, Sampathu DM, Kwong LK, Truax AC, Micsenyi MC, Chou TT, Bruce J, Schuck T, Grossman M, Clark CM, McCluskey LF, Miller BL, Masliah E, Mackenzie IR, Feldman H, Feiden W, Kretzschmar HA, Trojanowski JQ, Lee VMY. Ubiquitinated TDP-43 in frontotemporal lobar degeneration and amyotrophic lateral sclerosis. Science 2006; 314(5796): 130-3.

Ohm DT, Kim G, Gefen T, Rademaker A, Weintraub S, Bigio EH, Mesulam MM, Rogalski E, Geula C. Prominent microglial activation in cortical white matter is selectively associated with cortical atrophy in primary progressive aphasia. Neuropathology and Applied Neurobiology 2018; 11(Pt 3): 592.

Ossenkoppele R, Cohn-Sheehy BI, La Joie R, Vogel JW, Möller C, Lehmann M, van Berckel BNM, Seeley WW, Pijnenburg YA, Gorno-Tempini ML, Kramer JH, Barkhof F, Rosen HJ, van der Flier WM, Jagust WJ, Miller BL, Scheltens P, Rabinovici GD. Atrophy patterns in early clinical stages across distinct phenotypes of Alzheimer's disease. Human Brain Mapping 2015a; 36(11): 4421-37.

Ossenkoppele R, Pijnenburg YAL, Perry DC, Cohn-Sheehy BI, Scheltens NME, Vogel JW, Kramer JH, van der Vlies AE, Joie RL, Rosen HJ, van der Flier WM, Grinberg LT, Rozemuller AJ, Huang EJ, van Berckel BNM, Miller BL, Barkhof F, Jagust WJ, Scheltens P, Seeley WW, Rabinovici GD. The behavioural/dysexecutive variant of Alzheimer's disease: clinical, neuroimaging and pathological features. Brain 2015b: awv191.

Ossenkoppele R, Schonhaut DR, Schöll M, Lockhart SN, Ayakta N, Baker SL, O'Neil JP, Janabi M, Lazaris A, Cantwell A, Vogel J, Santos M, Miller ZA, Bettcher BM, Vossel KA, Kramer JH, Gorno-Tempini ML, Miller BL, Jagust WJ, Rabinovici GD. Tau PET patterns mirror clinical and neuroanatomical variability in Alzheimer's disease. Brain 2016; 139(5): 1551-67.

Parvizi J, Van Hoesen GW, Damasio A. The selective vulnerability of brainstem nuclei to Alzheimer's disease. Annals of Neurology 2001; 49(1): 53-66.

Pearson RC, Esiri MM, Hiorns RW, Wilcock GK, Powell TP. Anatomical correlates of the distribution of the pathological changes in the neocortex in Alzheimer disease. Proceedings of the National Academy of Sciences of the United States of America 1985; 82(13): 4531-4.

Penfield W. Microglia and the Process of Phagocytosis in Gliomas. The American journal of pathology 1925; 1(1): 77-90.15.

Perry VH, Nicoll JAR, Holmes C. Microglia in neurodegenerative disease. Nature Reviews Neurology 2010; 6(4): 193-201.

Phillips JS, Da Re F, Dratch L, Xie SX, Irwin DJ, McMillan CT, Vaishnavi SN, Ferrarese C, Lee EB, Shaw LM, Trojanowski JQ, Wolk DA, Grossman M. Neocortical origin and progression of gray matter atrophy in nonamnestic Alzheimer's disease. Neurobiology of Aging 2017; 63: 75-87.

Powers JP, McMillan CT, Brun CC, Yushkevich PA, Zhang H, Gee JC, Grossman M. White matter disease correlates with lexical retrieval deficits in primary progressive aphasia. Frontiers in neurology 2013; 4: 212.

Rogalski E, Cobia D, Harrison TM, Wieneke C, Weintraub S, Mesulam MM. Progression of language decline and cortical atrophy in subtypes of primary progressive aphasia. Neurology 2011a; 76(21): 1804-10.

Rogalski E, Cobia D, Martersteck A, Rademaker A, Wieneke C, Weintraub S, Mesulam MM. Asymmetry of cortical decline in subtypes of primary progressive aphasia. Neurology 2014; 83(13): 1184-91.

Rogalski E, Rogalski E, Cobia D, Cobia D, Harrison TM, Harrison TM, Wieneke C, Wieneke C, Thompson CK, Thompson CK, Weintraub S, Weintraub S, Mesulam MM, Mesulam MM. Anatomy of language impairments in primary progressive aphasia. Journal of Neuroscience 2011b; 31(9): 3344-50.

Rogalski E, Sridhar J, Rader B, Martersteck A, Chen K, Cobia D, Thompson CK, Weintraub S, Bigio EH, Mesulam MM. Aphasic variant of Alzheimer disease: Clinical, anatomic, and genetic features. Neurology 2016; 87(13): 1337-43.

Rogalski E, Weintraub S, Mesulam MM. Are there susceptibility factors for primary progressive aphasia? Brain and Language 2013; 127(2): 135-8.

Rogalski EJ, Sridhar J, Martersteck A, Rader B, Cobia D, Arora AK, Fought AJ, Bigio EH, Weintraub S, Mesulam M-M, Rademaker A. Clinical and cortical decline in the aphasic variant of Alzheimer's disease. Alzheimer's & Dementia: The Journal of the Alzheimer's Association 2019.

Rogers J, Luber-Narod J, Styren SD, Civin WH. Expression of immune system-associated antigens by cells of the human central nervous system: Relationship to the pathology of Alzheimer's disease. Neurobiology of Aging 1988; 9: 339-49.

Rohrer JD, Rossor MN, Warren JD. Alzheimer's pathology in primary progressive aphasia. Neurobiology of Aging 2012; 33(4): 744-52.

Rub U, Del Tredici K, Schultz C, Thal DR, Braak E, Braak H. The evolution of Alzheimer's disease-related cytoskeletal pathology in the human raphe nuclei. Neuropathology and Applied Neurobiology 2000; 26(6): 553-67.

Sachdev PS, Zhuang L, Braidy N, Wen W. Is Alzheimer's a disease of the white matter? Current Opinion in Psychiatry 2013; 26(3): 244-51.

Salter MW, Stevens B. Microglia emerge as central players in brain disease. Nature Medicine 2017; 23(9): 1018-27.

Sassin I, Schultz C, Thal DR, Rub U, Arai K, Braak E, Braak H. Evolution of Alzheimer's disease-related cytoskeletal changes in the basal nucleus of Meynert. Acta neuropathologica 2000; 100(3): 259-69.

Scheff SW, Price DA. Alzheimer's disease-related alterations in synaptic density: neocortex and hippocampus. J Alzheimers Dis 2006; 9(3 Suppl): 101-15.

Schmitz C, Hof PR. Design-based stereology in neuroscience. Neuroscience 2005; 130(4): 813-31.

Schmitz TW, Nathan Spreng R, Initiative AasDN. Basal forebrain degeneration precedes and predicts the cortical spread of Alzheimer's pathology. Nature communications 2016; 7: 13249.

Schofield E, Kersaitis C, Shepherd CE, Kril JJ, Halliday GM. Severity of gliosis in Pick's disease and frontotemporal lobar degeneration: tau-positive glia differentiate these disorders. Brain 2003; 126(Pt 4): 827-40.

Ségonne F, Pacheco J, Fischl B. Geometrically accurate topology-correction of cortical surfaces using nonseparating loops. IEEE transactions on medical imaging 2007; 26(4): 518-29.

Serrano-Pozo A, Frosch MP, Masliah E, Hyman BT. Neuropathological Alterations in Alzheimer Disease. Cold Spring Harbor Perspectives in Medicine: 2011a; 1(1).

Serrano-Pozo A, Gomez-Isla T, Growdon JH, Frosch MP, Hyman BT. A phenotypic change but not proliferation underlies glial responses in Alzheimer disease. The American journal of pathology 2013a; 182(6): 2332-44.

Serrano-Pozo A, Mielke ML, Gomez-Isla T, Betensky RA, Growdon JH, Frosch MP, Hyman BT. Reactive Glia not only Associates with Plaques but also Parallels Tangles in Alzheimer's Disease. 2011b; 179(3): 1373-84.

Serrano-Pozo A, Muzikansky A, Gomez-Isla T, Growdon JH, Betensky RA, Frosch MP, Hyman BT. Differential relationships of reactive astrocytes and microglia to fibrillar amyloid deposits in Alzheimer disease. Journal of neuropathology and experimental neurology 2013b; 72(6): 462-71.

Sierra A, de Castro F, del Río-Hortega J, Rafael Iglesias-Rozas J, Garrosa M, Kettenmann H. The "Big-Bang" for modern glial biology: Translation and comments on Pío del Río-Hortega 1919 series of papers on microglia. Glia 2016; 64(11): 1801-40.

Silbert LC, Quinn JF, Moore MM, Corbridge E, Ball MJ, Murdoch G, Sexton G, Kaye JA. Changes in premorbid brain volume predict Alzheimer's disease pathology. Neurology 2003; 61(4): 487-92.

Singh S, Metz I, Amor S, van der Valk P, Stadelmann C, Brück W. Microglial nodules in early multiple sclerosis white matter are associated with degenerating axons. Acta neuropathologica 2013; 125(4): 595-608.

Sjöbeck M, Englund E. Glial levels determine severity of white matter disease in Alzheimer's disease: a neuropathological study of glial changes. Neuropathology and Applied Neurobiology 2003; 29(2): 159-69.

Sjöbeck M, Haglund M, Englund E. Decreasing myelin density reflected increasing white matter pathology in Alzheimer's disease—a neuropathological study. International Journal of Geriatric Psychiatry 2005; 20(10): 919-26.

Small SA, Duff K. Linking Aβ and Tau in Late-Onset Alzheimer's Disease: A Dual Pathway Hypothesis. Neuron 2008; 60(4): 534-42.

Solito E, Sastre M. Microglia function in Alzheimer's disease. Frontiers in pharmacology 2012; 3: 14.

Song WM, Colonna M. The identity and function of microglia in neurodegeneration. Nat Immunol 2018; 19(10): 1048-58.

Strain JF, Smith RX, Beaumont H, Roe CM, Gordon BA, Mishra S, Adeyemo B, Christensen JJ, Su Y, Morris JC, Benzinger TLS, Ances BM. Loss of white matter integrity reflects tau accumulation in Alzheimer disease defined regions. Neurology 2018; 91(4): e313-e8.

Streit WJ, Xue Q-S. Life and death of microglia. Journal of neuroimmune pharmacology : the official journal of the Society on NeuroImmune Pharmacology 2009; 4(4): 371-9.

Streit WJ, Xue Q-S, Tischer J, Bechmann I. Microglial pathology. Acta Neuropathologica Communications 2014; 2(1): 142.

Stricker NH, Schweinsburg BC, Delano-Wood L, Wierenga CE, Bangen KJ, Haaland KY, Frank LR, Salmon DP, Bondi MW. Decreased white matter integrity in late-myelinating fiber pathways in Alzheimer's disease supports retrogenesis. NeuroImage 2009; 45(1): 10-6.

Styren SD, Civin WH, Rogers J. Molecular, cellular, and pathologic characterization of HLA-DR immunoreactivity in normal elderly and Alzheimer's disease brain. Experimental neurology 1990; 110(1): 93-104.

Svahn AJ, Becker TS, Graeber MB. Emergent Properties of Microglia. Brain Pathology 2014; 24(6): 665-70.

Taipa R, Brochado P, Robinson A, Reis I, Costa P, Mann DM, Melo Pires M, Sousa N. Patterns of Microglial Cell Activation in Alzheimer Disease and Frontotemporal Lobar Degeneration. Neuro-degenerative diseases 2017a; 17(4-5): 145-54.

Taipa R, Ferreira V, Brochado P, Robinson A, Reis I, Marques F, Mann DM, Melo-Pires M, Sousa N. Inflammatory pathology markers (activated microglia and reactive astrocytes) in early and late onset Alzheimer disease: a post mortemstudy. Neuropathology and Applied Neurobiology 2017b; 44(3): 298-313.

Terry RD, Masliah E, Salmon DP, Butters N, DeTeresa R, Hill R, Hansen LA, Katzman R. Physical basis of cognitive alterations in Alzheimer's disease: synapse loss is the major correlate of cognitive impairment. Annals of Neurology 1991; 30(4): 572-80.

Thal DR, Rüb U, Orantes M, Braak H. Phases of A beta-deposition in the human brain and its relevance for the development of AD. Neurology 2002; 58(12): 1791-800.

Thompson PM, Hayashi KM, de Zubicaray G, Janke AL, Rose SE, Semple J, Herman D, Hong MS, Dittmer SS, Doddrell DM, Toga AW. Dynamics of gray matter loss in Alzheimer's disease. Journal of Neuroscience 2003; 23(3): 994-1005.

Uchihara T. Pretangles and neurofibrillary changes: similarities and differences between AD and CBD based on molecular and morphological evolution. Neuropathology 2014; 34(6): 571-7.

Urbanc B, Cruz L, Le R, Sanders J, Ashe KH, Duff K, Stanley HE, Irizarry MC, Hyman BT. Neurotoxic effects of thioflavin S-positive amyloid deposits in transgenic mice and Alzheimer's disease. Proceedings of the National Academy of Sciences of the United States of America 2002; 99(22): 13990-5.

Uylings HBM, de Brabander JM. Neuronal Changes in Normal Human Aging and Alzheimer's Disease. Brain and Cognition 2002; 49(3): 268-76.

Vassar R, Bennett BD, Babu-Khan S, Kahn S, Mendiaz EA, Denis P, Teplow DB, Ross S, Amarante P, Loeloff R, Luo Y, Fisher S, Fuller J, Edenson S, Lile J, Jarosinski MA, Biere AL, Curran E, Burgess T, Louis JC, Collins F, Treanor J, Rogers G, Citron M. Beta-secretase cleavage of Alzheimer's amyloid precursor protein by the transmembrane aspartic protease BACE. Science 1999; 286(5440): 735-41.

Vemuri P, Whitwell JL, Kantarci K, Josephs KA, Parisi JE, Shiung MS, Knopman DS, Boeve BF, Petersen RC, Dickson DW, Jack Jr CR. Antemortem MRI based STructural Abnormality iNDex (STAND)-scores correlate with postmortem Braak neurofibrillary tangle stage. NeuroImage 2008; 42(2): 559-67.

Warren JD, Fletcher PD, Golden HL. The paradox of syndromic diversity in Alzheimer disease. Nature Reviews Neurology 2012; 8(8): 451-64.

Weingarten MD, Lockwood AH, Hwo SY, Kirschner MW. A protein factor essential for microtubule assembly. Proceedings of the National Academy of Sciences of the United States of America 1975; 72(5): 1858-62.

Whitwell JL, Dickson DW, Murray ME, Weigand SD, Tosakulwong N, Senjem ML, Knopman DS, Boeve BF, Parisi JE, Petersen RC, Jack CR, Josephs KA. Neuroimaging correlates of pathologically defined subtypes of Alzheimer's disease: a case-control study. The Lancet Neurology 2012; 11(10): 868-77.

Whitwell JL, Graff-Radford J, Tosakulwong N, Weigand SD, Machulda M, Senjem ML, Spychalla AJ, Vemuri P, Jones DT, Drubach DA, Knopman DS, Boeve BF, Ertekin-Taner N, Petersen RC, Lowe VJ, Jack Jr CR, Josephs KA. Imaging correlations of tau, amyloid, metabolism, and atrophy in typical and atypical Alzheimer's disease. Alzheimer's & Dementia 2018.

Whitwell JL, Josephs KA, Murray ME, Kantarci K, Przybelski SA, Weigand SD, Vemuri P, Senjem ML, Parisi JE, Knopman DS, Boeve BF, Petersen RC, Dickson DW, Jack CR. MRI correlates of neurofibrillary tangle pathology at autopsy: A voxel-based morphometry study. Neurology 2008; 71(10): 743-9.

Winkler AM, Kochunov P, Blangero J, Almasy L, Zilles K, Fox PT, Duggirala R, Glahn DC. Cortical thickness or grey matter volume? The importance of selecting the phenotype for imaging genetics studies. NeuroImage 2010; 53(3): 1135-46.

Wolf HK, Buslei R, Schmidt-Kastner R, Schmidt-Kastner PK, Pietsch T, Wiestler OD, Blümcke I. NeuN: a useful neuronal marker for diagnostic histopathology. The Journal of Histochemistry and Cytochemistry 1996.

Xia C, Makaretz SJ, Caso C, McGinnis S, Gomperts SN, Sepulcre J, Gomez-Isla T, Hyman BT, Schultz A, Vasdev N, Johnson KA, Dickerson BC. Association of In Vivo [18F]AV-1451 Tau PET Imaging Results With Cortical Atrophy and Symptoms in Typical and Atypical Alzheimer Disease. JAMA Neurology 2017; 74(4): 427.

Xiang Z, Haroutunian V, Ho L, Purohit D, Pasinetti GM. Microglia activation in the brain as inflammatory biomarker of Alzheimer's disease neuropathology and clinical dementia. Disease markers 2006; 22(1-2): 95-102.

Younkin SG. The role of A beta 42 in Alzheimer's disease. J Physiol Paris 1998; 92(3-4): 289-92.

Yousef A, Robinson JL, Irwin DJ, Byrne MD, Kwong LK, Lee EB, Xu Y, Xie SX, Rennert L, Suh E, Van Deerlin VM, Grossman M, Lee VMY, Trojanowski JQ. Neuron loss and degeneration in the progression of TDP-43 in frontotemporal lobar degeneration. Acta Neuropathologica Communications 2017; 5(1): e0141836.

Zarow C, Vinters HV, Ellis WG, Weiner MW, Mungas D, White L, Chui HC. Correlates of hippocampal neuron number in Alzheimer's disease and ischemic vascular dementia. Annals of Neurology 2005; 57(6): 896-903.

—VITA—

Daniel T Ohm

300 E Superior St., Tarry Building 8th Floor, Chicago, IL 60611
631-707-1953
danielohm2012@u.northwestern.edu

EDUCATION

2012 – present	Predoctoral Student Northwestern University Interdepartmental Neuroscience Program, Northwestern University, Chicago, IL
2004 – 2008	B.S., Biology; B.A., Psychology Syracuse University, Syracuse, NY Honors: Cum laude

RESEARCH FUNDING

2016 – 2019	**F31-Diversity Individual NRSA** (NS095652) NIH National Institute of Neurological Disorders and Stroke Title: Concordance between cortical atrophy and histopathology in PPA with AD pathology
2014 – 2016	**T32 Institutional NRSA** (AG20506) NIH Mechanisms of Aging & Dementia Training Grant Title: Concordance Between Cortical Atrophy, Histopathology, and Function in Primary Progressive Aphasia with Alzheimer's Pathology PI: John Disterhoft, PhD

RESEARCH EXPERIENCE

2012 – present	*Neuroscience PhD Candidate* **Mesulam Center for Cognitive Neurology and Alzheimer's Disease Center (MCCNAD), Northwestern University, Chicago, IL** Co-PIs / Thesis Committee: E. Rogalski, PhD; C. Geula, PhD / M.-M. Mesulam, PhD; R. Vassar, PhD • Led a multidisciplinary collaboration across labs at the MCCNAD to determine the histopathologic and cellular basis of *in vivo* cortical atrophy in an Alzheimer variant known as primary progressive aphasia • Acquired expertise in design-based stereology, quantitative MRI, and immunohistochemistry
2008 – 2012	*Research Associate* **Neurobiology of Aging Laboratory, Mount Sinai School of Medicine, New York, NY** PI: John Morrison, PhD • Quantified changes to dendrites and spines in ovariectomized monkey models to show that standard hormone therapies given to women after menopause are unlikely capable of supporting synaptic plasticity and cognitive enhancement • Developed expertise in single-cell fluorescent dye filling and confocal microscopy
2007 – 2008	*Research Associate* **Center for Psychiatric Neuroimaging, SUNY Upstate Medical University, Syracuse, NY** PI: Wendy Kates, PhD • Analyzed longitudinal MRI data to show that a reduction in temporal lobe cortical folding correlated with prodromal symptoms associated with future psychiatric impairment in velo-cardio-facial syndrome

PEER-REVIEWED PUBLICATIONS

1. Mesulam, M., Lalehzari, N., Rahmani, F., **Ohm, D.T.**, Shahidehpour, R., Kim, G., Gefen, T., Weintraub, S., Bigio, E., Geula, C. (2019) Cortical cholinergic denervation in primary progressive aphasia with Alzheimer pathology. *Neurology.*

2. **Ohm, D.T.**, Kim, G., Gefen, T., Rademaker, A., Weintraub, S., Bigio, E., Mesulam, M., Rogalski, E. and Geula, C. (2018) Prominent microglial activation in cortical white matter is selectively associated with cortical atrophy in primary progressive aphasia. *Neuropathology and Applied Neurobiology*, 11(Pt 3), 592.

3. Cook, A, Sridhar, J, **Ohm, D**, Rademaker, A, Mesulam, M, Weintraub, S, Rogalski, E. (2017) Rates of Cortical Atrophy in Adults 80 Years and Older With Superior vs Average Episodic Memory. *JAMA*, *317*(13), 1373.

4. Young, M. E., **Ohm, D. T.**, Dumitriu, D., Rapp, P. R., & Morrison, J. H. (2014). Differential effects of aging on dendritic spines in visual cortex and prefrontal cortex of the rhesus monkey. *Neuroscience*, *274*, 33–43.

5. Young, M. E., **Ohm, D. T.**, Janssen, W. G. M., Gee, N. A., Lasley, B. L., & Morrison, J. H. (2013). Continuously delivered ovarian steroids do not alter dendritic spine density or morphology in macaque dorsolateral prefrontal cortical neurons. *Neuroscience*, 219-225.

6. **Ohm, D. T.**, Bloss, E. B., Janssen, W. G., Dietz, K. C., Wadsworth, S., Lou, W., Gee, N. A., Lasley, B., Rapp, P. R., Morrison, J. H. (2012). Clinically relevant hormone treatments fail to induce spinogenesis in prefrontal cortex of aged female rhesus monkeys. *The Journal of Neuroscience*, *32*(34), 11700–11705.

7. Bloss, E. B., Janssen, W. G., **Ohm, D. T.**, Yuk, F. J., Wadsworth, S., Saardi, K. M., McEwen, B. S., Morrison, J. H. (2011). Evidence for reduced experience-dependent dendritic spine plasticity in the aging prefrontal cortex. *The Journal of Neuroscience*, *31*(21), 7831–7839.

MANUSCRIPTS IN PREPARATION OR SUBMITTED FOR REVIEW

1. **Ohm, D.T.**, Kim, G., Gefen, T., Rademaker, A., Weintraub, S., Bigio, E., Mesulam, M., Rogalski, E. and Geula, C. (Under Review at *Brain*) Neuropathologic basis of *in vivo* cortical atrophy in the aphasic variant of Alzheimer's disease.

2. **Ohm, D.T.**, Rademaker, A., Weintraub, S., Bigio, E., Mesulam, M., Rogalski, E. and Geula, C. (In preparation) Relationships between neurofibrillary tangles, activated microglia, and neurons in primary progressive aphasia caused by Alzheimer's disease.

3. Gefen, T., Kim, G., Bolbolan, K., Geoly, A., **Ohm, D.T.**, Oboudiyat, C., Rademaker, F., Weintraub, S., Bigio, EH, Rogalski, E., Mesulam, MM, and Geula, C. (Under review at *Frontiers in Aging*) Activated microglia in cortical white matter across cognitive aging trajectories.

4. Rezvanian, A., **Ohm, D.T.**, Kukreja, L., Gefen, T., Abbassian, P., Weintraub, S., Rogalski, E., Mesulam, M.-M., Corrada, M., Kawas, C., and Geula, C. (In preparation) The oldest-old with preserved cognition and the full range of Alzheimer pathology.

PUBLISHED ABSTRACTS & CONFERENCE POSTERS

1. **Ohm D.T.**, Rademaker A., Weintraub, S., Bigio E., Rogalski E., Mesulam M.M., Geula C. (2018). Microglial subtypes differentially relate to neuron densities and *in vivo* cortical atrophy in primary progressive aphasia caused by Alzheimer's disease. *International Conference on Frontotemporal Dementias:* Chicago, IL.

2. **Ohm D.T.**, Kim G., Gefen, T., Rademaker A., Weintraub, S., Bigio E., Rogalski E., Mesulam M.M., Geula C. (2018). Neurofibrillary tangles predict *in vivo* cortical atrophy in primary progressive aphasia with Alzheimer's disease. *Alzheimer's Association International Conference:* Chicago, IL.

3. **Ohm D.T.**, Jamshidi P., Kim G., Bolbolan, K., Weintraub, S., Bigio E., Mesulam M.M., Geula C. (2018). Distribution of TDP-43 pathology in hippocampal synaptic relays suggests trans-synaptic propagation in primary progressive aphasia. *Society for Neuroscience:* San Diego, CA.

4. Dunlop, S., Lalehzari N., **Ohm D.T.**, Kim G., Weintraub S., Bigio E., Mesulam M-M. and Geula C. (2017) Vulnerability of the cholinergic basal forebrain to AD vs FTLD-TDP pathology in primary progressive aphasia. *Alzheimer's Association International Conference:* Chicago, IL.

5. **Ohm D.T.**, Kim G., Gefen T., Rademaker A., Weintraub S., Bigio E., Rogalski E., Mesulam M.M., Geula C. (2017). Prominent microglial activation in cortical white matter is selectively associated with cortical atrophy in primary progressive aphasia. *Alzheimer's Association International Conference:* London, England.

6. Lalehzari N., Rahmani F., **Ohm D.T.**, Kim G., Weintraub S., Bigio E., Mesulam M-M. and Geula C. (2017) Loss of basal forebrain cholinergic neurons in primary progressive aphasia with Alzheimer pathology. *Society for Neuroscience Annual Meeting*, Washington, DC.

7. Lalehzari N., **Ohm D.T.**, Kim G., Weintraub S., Bigio E., Mesulam M-M. and Geula C. (2016) Significant depletion of basal forebrain cholinergic system in primary progressive aphasia with Alzheimer pathology. *Society for Neuroscience Annual Meeting*, San Diego, CA.

8. Rezvanian, A., **Ohm, D.**, Kukreja, L., Gefen, T., Abbassian, P., Weintraub, S., Rogalski, E., Mesulam, M.-M., Corrada, M., Kawas, C., and Geula, C. (2016) The Oldest-Old with Preserved Cognition and the Full Range of Alzheimer Pathology. *Society for Neuroscience Annual Meeting*, San Diego, CA.

9. **Ohm D.T.**, Rademaker A., Bigio E., Mesulam M.M., Rogalski E., Geula C. (2016). Hypertrophic microglia are associated with more tangles and less neurons in primary progressive aphasia with Alzheimer pathology. *International Conference on Frontotemporal Dementias:* Munich, Germany.

10. **Ohm D.T.**, Kim G., Gefen, T., Parton, Z., Bigio E., Rogalski E., Mesulam M.M., Geula C. (2016). High densities of activated microglia are present in cortical white matter and correspond to regions of greatest atrophy in primary progressive aphasia. *Alzheimer's Association International Conference:* Toronto, Canada.

11. **Ohm D.T.**, Kim G., Martersteck A., Weintraub S., Bigio E., Mesulam M.M., Rogalski E., Geula C. (2015). Histopathologic markers are related to *in vivo* cortical atrophy in primary progressive aphasia with Alzheimer pathology. *Society for Neuroscience Annual Meeting:* Chicago, IL.

12. Cook, A.H., Martersteck, A., **Ohm, D.**, Rademaker, A., Mesulam, M.M., Weintraub, S., & Rogalski, E. (2015). Reduced cortical atrophy in cognitively successful elderly adults. *Journal of the International Neuropsychological Society, 21*(Supplement1):*79.*

13. **Ohm D.T.**, Kim G., Gefen T., Peterson M., Martersteck A., Weintraub S., Bigio E., Mesulam M.M., Rogalski E., Geula C. (2014). Clinical concordance between *in vivo* cortical atrophy and postmortem histopathology in primary progressive aphasia with Alzheimer pathology: A case report. *Society for Neuroscience Annual Meeting:* Washington, D.C.

14. Cook, A.H., Martersteck, A., **Ohm, D.**, Mesulam, M.M., Weintraub, S., & Rogalski, E. (2014). Maintenance of cortical thickness in SuperAgers: A key to preserved cognition in advanced age? *Journal of the International Neuropsychological Society, 20*(Supplement1):248-249.

15. Hauner K.K., **Ohm D.T.**, Gottfried J.A. (2013) Effects of Prediction and Control on the Perception of Aversive Olfactory Stimuli. AChemS XXXVAnnual Meeting; Huntington Beach, CA.

16. Morrison J.H., Hao J.D., Hara Y., Dumitriu D., Wang A.-J., Bailey M.E., Bloss E.B., **Ohm D.T.**, Janssen W.G., Yuk F., Puri R., Baxter M., Rapp P. (2013) Synaptic correlates of cognitive performance: Implications for aging and menopause. American Neuroendocrine Society 7th International Meeting on Steroids and Nervous System; Torino, Italy.

17. Yuk F., **Ohm D.**, Janssen W.G., Morrison J.H. (2012) Array tomographic synaptic analysis of dye-injected (Lucifer Yellow) filled neurons from behaviorally characterized neurons in nonhuman primate. Society for Neuroscience Annual Meeting; New Orleans, LA.

18. Bailey M.E., **Ohm D.T.**, Dumitriu D., Morrison J.H. (2012) The effects of aging on dendritic spine density and morphology in macaque dorsolateral prefrontal and primary visual cortices. Society for Neuroscience Annual Meeting; New Orleans, LA.

19. Bloss E.B., **Ohm D.T.**, Wadsworth S., Yuk F., Saardi K., Janssen W.G., McEwen B.S., and Morrison J.H. (2010) Interactive effects of stress and aging on structural plasticity in the prefrontal cortex. Society for Neuroscience Annual Meeting; San Diego, CA.

20. Bailey M.E., **Ohm D.T.**, Janssen W.G.M., Morrison J.H. (2010) Continuously delivered ovarian steroids are less effective than cyclic treatments at increasing morphological metrics of plasticity in macaque dorsolateral prefrontal cortical neurons. Society for Neuroscience Annual Meeting; San Diego, CA.

21. Wang A.-J., Yuk F., **Ohm D.**, Christoffel D. J., Janssen W. G. M., Morrison. J.H. (2010) N-methyl-D-aspartate receptor subunit 2B and phosphorylated 2B is preserved in aging female Rhesus monkey prefrontal cortex. Society for Neuroscience Annual Meeting; San Diego, CA.

LECTURES & CONFERENCE PRESENTATIONS

2019	*Invited speaker*. "Neurobiological basis of *in vivo* cortical atrophy in primary progressive aphasia caused by Alzheimer's Disease". Psychiatry Grand Rounds, Northwestern University, Chicago, IL
2018	*Invited speaker*. "Neurofibrillary tangles are associated with *in vivo* cortical atrophy in primary progressive aphasia with Alzheimer's disease". Alzheimer's Association International Conference: Professional Interest Area of Atypical Alzheimer's Disease and Associated Syndromes, Chicago, IL
2017	*Alumnus speaker*. "Prominent microglia activation in cortical white matter is selectively associated with cortical atrophy in primary progressive aphasia". *MAD T32 training grant retreat*, Northwestern University.
2016	*Predoctoral trainee*. "Hypertrophic microglia relate to *in vivo* cortical atrophy in primary progressive aphasia with Alzheimer pathology". *MAD T32 training grant retreat*, Northwestern University.
2015	*Predoctoral trainee*. "Concordance between histopathology and *in vivo* cortical atrophy in primary progressive aphasia with Alzheimer's pathology". *MAD T32 training grant retreat*, Northwestern University.
2014	*Predoctoral trainee*. "Concordance between cortical atrophy and histopathology in primary progressive aphasia with Alzheimer's pathology". *MAD T32 training grant retreat*, Northwestern University.
2014	*Predoctoral trainee*. "Clinical concordance between cortical atrophy and histopathology in primary progressive aphasia with Alzheimer pathology: a case report". *MAD T32 training grant retreat*, Northwestern University.

TEACHING & MENTORING EXPERIENCE

2017 – present	*Graduate Mentor.* Graduates Mentoring Undergraduates Program, Northwestern University, Chicago, IL
2013 – present	*Volunteer*. Brain Awareness Fair, Northwestern University Brain Awareness Outreach Program (NUBAO), Chicago, IL
2017	*Invited speaker*. "Human neuroanatomy & Alzheimer's Disease". NUBAO Neuroscience Seminar Series, Walter Payton High School, Chicago, IL
2016	*Volunteer*. Teacher's Workshop. Educational workshop for Chicago Public School science teachers, held in conjunction with NUBAO and Chicago SfN Chapter.
2015 – 2016	*Science Fair Judge*. Academy for Urban School Leadership, Chicago, IL
2013	*Teaching Assistant*. Undergraduate Biology and Physiology Laboratory (Bio 222), Northwestern University

HONORS & AWARDS

2016 – 2019	Ruth L. Kirschstein National Research Service Award (NRSA)

2018	Travel Scholarship to the 11th International Conference on Frontotemporal Dementias (ICFTD)
2018	Travel Award from Northwestern University Interdepartmental Neuroscience (NUIN) program
2018	Conference Travel Grant from The Graduate School at Northwestern University
2017	Travel Award from Northwestern University Interdepartmental Neuroscience (NUIN) program
2016	Travel Award to the 28th Alzheimer's Association International Conference (AAIC)
2016	NIH Training Fellowship to the University of Michigan fMRI Training Course
2016	Conference Travel Grant from The Graduate School at Northwestern University
2014 – 2016	NIH T32 Mechanisms of Aging & Dementia Training Grant
2008	Allport Senior Research Award, Syracuse University
2004 – 2008	Syracuse University Dean's List
2004 – 2008	Syracuse University Merit Scholarship
2004 – 2008	Syracuse University Chancellor's Scholarship
2004 – 2008	New York State Scholarship for Academic Excellence

PROFESSIONAL MEMBERSHIPS

2016 – present	*Student Member,* International Society to Advance Alzheimer's Research and Treatment (ISTAART), Alzheimer's Association
2014 – present	*Student Member,* Society for Neuroscience
2006 – 2008	*Student Member,* Tri-Beta Biology Honor Society
2006 – 2008	*Student Member,* Psi-Chi Psychology Honor Society
2005 – 2008	*Student Member,* National Society of Collegiate Scholars

ADVANCED TRAINING COURSES

2018	**Ready Set Go: Research Communication Training Program** Northwestern University, Chicago IL
2016	**Functional Magnetic Resonance Imaging Training Course** University of Michigan, Ann Arbor MI
2015	**Science Writing & Communication** Northwestern University, Evanston IL
2015	**Grantsmanship for the Research Professional Course** Northwestern University, Evanston IL
2015	**Introduction to Programming for Big Data Bootcamp** Northwestern University, Evanston IL
2014	**FreeSurfer Neuroimaging Workshop** Massachusetts General Hospital, Martinos Center for Biomedical Imaging, Boston MA

SOFTWARE SKILLS

- StereoInvestigator, FreeSurfer, SPSS, GraphPad Prism, Tableau, ImageJ/Fiji, Neurolucida, NeuronStudio